

# A multi-dimensional quasi-discrete model for the analysis of Diesel fuel droplet heating and evaporation

Sazhin, S. S. , Al Qubeissi, M. , Nasiri, R. , Gunko, V. M. ,  
Elwardany, A. E. , Lemoine, F. , Grisch, F. and Heikal, M. R.

**Author pre-print (accepted) deposited in CURVE January 2016**

**Original citation & hyperlink:**

Sazhin, S. S. , Al Qubeissi, M. , Nasiri, R. , Gunko, V. M. , Elwardany, A. E. , Lemoine, F. ,  
Grish, F. and Heikal, M. R. (2014) A multi-dimensional quasi-discrete model for the analysis  
of Diesel fuel droplet heating and evaporation. Fuel, volume 129 : 238-266

<http://dx.doi.org/10.1016/j.fuel.2014.03.028>

ISSN 0016-2361

DOI 10.1016/j.fuel.2014.03.028

**Copyright © and Moral Rights are retained by the author(s) and/ or other copyright owners. A copy can be downloaded for personal non-commercial research or study, without prior permission or charge. This item cannot be reproduced or quoted extensively from without first obtaining permission in writing from the copyright holder(s). The content must not be changed in any way or sold commercially in any format or medium without the formal permission of the copyright holders.**

**This document is the author's pre-print version, not incorporating any revisions agreed during the peer-review process. Some differences between the published version and this version may remain and you are advised to consult the published version if you wish to cite from it.**

**CURVE is the Institutional Repository for Coventry University**

<http://curve.coventry.ac.uk/open>

# A multi-dimensional quasi-discrete model for the analysis of Diesel fuel droplet heating and evaporation

S.S. Sazhin<sup>□\*</sup>, M. Al Qubeissi<sup>□</sup>, R. Nasiri<sup>□</sup>, V.M. Gunko<sup>•,□</sup>,  
A.E. Elwardany<sup>◇</sup>, F. Lemoine<sup>△,▽</sup>, F. Grisch<sup>▽</sup>, M.R. Heikal<sup>□</sup>

<sup>□</sup>*Sir Harry Ricardo Laboratories, Centre for Automotive Engineering,  
School of Computing, Engineering and Mathematics, Faculty of Science and Engineering,  
University of Brighton, Brighton, BN2 4GJ, UK*

<sup>•</sup>*Chuiko Institute of Surface Chemistry, 17 General Naumov Street, Kiev 03164, Ukraine*

<sup>◇</sup>*Clean Combustion Research Centre, Division of Physical Sciences and Engineering,  
King Abdullah University of Science and Technology (KAUST), Thuwal 23955-6900,  
Saudi Arabia*

<sup>△</sup>*Université de Lorraine, LEMTA, UMR 7563, Vandoeuvre-lès-Nancy, France*

<sup>▽</sup>*CNRS, LEMTA, UMR 7563, Vandoeuvre-lès-Nancy, France*

<sup>▽</sup>*INSA-Rouen, UMR-CNRS 6614, CORIA, BP 8, 76801 Saint Etienne du Rouvray  
Cedex, France*

---

## Abstract

A new multi-dimensional quasi-discrete model is suggested and tested for the analysis of heating and evaporation of Diesel fuel droplets. As in the original quasi-discrete model suggested earlier, the components of Diesel fuel with close thermodynamic and transport properties are grouped together to form quasi-components. In contrast to the original quasi-discrete model, the new model takes into account the contribution of not only alkanes, but also various other groups of hydrocarbons in Diesel fuels; quasi-components are formed within individual groups. Also, in contrast to the original quasi-discrete model, the contributions of individual components are not approximated by the distribution function of carbon numbers. The formation of quasi-components is based on taking into account the contributions of individual components without any approximations. Groups contributing small

---

\*Corresponding author. Tel. +44(0)1273642677; fax +44(0)1273642330; e-mail S.Sazhin@brighton.ac.uk

molar fractions to the composition of Diesel fuel (less than about 1.5%) are replaced with characteristic components. The actual Diesel fuel is simplified to form six groups: alkanes, cycloalkanes, bicycloalkanes, alkylbenzenes, indanes & tetralines, and naphthalenes, and 3 components  $C_{19}H_{34}$  (tricycloalkane),  $C_{13}H_{12}$  (diaromatic), and  $C_{14}H_{10}$  (phenanthrene). It is shown that the approximation of Diesel fuel by 15 quasi-components and components, leads to errors in estimated temperatures and evaporation times **in typical Diesel engine conditions** not exceeding about 3.7% and 2.5% respectively, which is acceptable for most engineering applications.

*Keywords:*

Droplets, heating, evaporation, Diesel fuel, multi-component fuel, discrete component model

---

## 1. Introduction

Diesel fuel droplet heating and evaporation is an important part of the processes leading to fuel combustion in Diesel engines [1]. Accurate modelling of these processes is essential for their understanding and ultimately improving engine design. The simplest model of Diesel fuel droplet heating and evaporation is based on a number of assumptions. These include the assumptions that Diesel fuel can be approximated by a single component (n-dodecane in most cases), temperature gradients inside droplets can be ignored, the droplet interface is stationary during the time step, and kinetic/molecular dynamic effects during heating and evaporation can be ignored [2].

Some of these assumptions were relaxed in several advanced models of droplet heating and evaporation, described in a number of papers including [3, 4, 5, 6]. As demonstrated in our recent publications [7, 8, 9], the most important of the above-mentioned assumptions is that Diesel fuel can be approximated by a single component. The early models, taking into account the effect of multiple components in Diesel engines, could be subdivided into two main families: those based on the analysis of individual components (Discrete Component Models (DCM))(e.g. [10, 11]), applicable in the case when a relatively small number of components needs to be taken into account, and those based on the probabilistic analysis of a large number of components (e.g. Continuous Thermodynamics approach [12]-[14] and the Distillation Curve Model [15]). In the second family of models, a number of additional

simplifying assumptions were used, including the assumption that species inside droplets mix infinitely quickly or do not mix at all. Models containing features of both these families were suggested in [16, 17].

A new approach to modelling the heating and evaporation of multi-component Diesel fuel droplets, suitable for the case when a large number of components is present in the droplets, was suggested in [7]. This approach is based on the introduction of hypothetical components with non-integer numbers of carbon atoms. These hypothetical components were called quasi-components. There are some similarities between the quasi-components introduced in [7] and the pseudo-components used in [17], but these quasi-components and pseudo-components were introduced in different ways. In contrast to the previously suggested models, designed for large numbers of components, the model suggested in [7] took into account the diffusion of liquid species and thermal diffusion, as in the classical Discrete Component Models, alongside recirculation inside droplets. This model was called the ‘quasi-discrete model’. In [8], this model was generalised to take into account the differences in liquid density, viscosity, specific heat capacity, and thermal conductivity for liquid components in Diesel and gasoline fuels.

Although the usefulness and efficiency of the quasi-discrete model was clearly demonstrated in [7, 8, 9], this model still has a number of serious limitations the most important of which is that it is based on the assumption that Diesel and gasoline fuels consist only of n-alkanes. At the same time, as will be shown later in this paper, the total molar fraction of alkanes (n-alkanes and iso-alkanes) is only about 40% of the overall composition of Diesel fuels (a similar conclusion could be drawn for gasoline fuel [18]). Hence, the contribution of other components apart from alkanes cannot be ignored.

In this paper, the model originally suggested in [7] is generalised to take into account the realistic composition of Diesel fuels. This composition is described in the following section. The model used in our analysis is introduced in Section 3. The new elements of the model are described alongside the previously developed elements to make the whole paper self-sufficient for practical application of the results. The solution algorithm is described in Section 4. The results of calculations are presented in Section 5. The main results of the paper are summarised in Section 6.

## 2. Composition of Diesel fuel

The commercial Diesel fuel selected in the present work conforms to standard European Union fuel (EN590). The detailed chemical species composition was obtained using comprehensive two-dimensional gas chromatography (GCXGC) which is a very convenient tool for the characterisation of petroleum-based fuels [19]-[21]. Molar fractions of various components in this fuel are presented in Table 1 [22]. The results presented in this table were simplified, taking into account that the properties of n-alkanes and iso-alkanes are rather close. Also, one can observe in Table 1 that the contributions of tricycloalkanes, diaromatics and phenanthrenes to Diesel fuel are rather small (less than about 1.6% for each of these components). This allows us to ignore the dependence of the properties of these components on the number of carbon atoms and replace these three groups with three components, tricycloalkane, diaromatic and phenanthrene, with particular arbitrary chosen values of carbon numbers. A simplified version of Table 1, in which n-alkanes and iso-alkanes are merged into one group of alkanes, and tricycloalkanes, diaromatics and phenanthrenes are excluded, is presented as Table 2. Transport and thermodynamic properties of the components included in Table 2 are summarised in Appendices 1-6. Transport and thermodynamic properties of three components, tricycloalkane, diaromatic and phenanthrene, are summarised in Appendix 7. Based on the results presented in Table 1, we assume that the molar fraction of tricycloalkanes is 1.5647%, while the molar fraction of diaromatics and phenanthrenes are equal to 1.2240% and 0.6577%, respectively.

Our analysis is based on the results presented in Table 2, in addition to the three discrete components: tricycloalkane, diaromatic and phenanthrene.

## 3. Model

### 3.1. Quasi-components

In the original quasi-discrete model [7, 8], the contribution of various n-alkanes is described by the distribution function  $f_m(n)$  [8]:

$$f_m(n) = C_m(n_0, n_f) \frac{(M(n) - \gamma)^{\alpha-1}}{\beta^\alpha \Gamma(\alpha)} \exp \left[ - \left( \frac{M(n) - \gamma}{\beta} \right) \right], \quad (1)$$

where  $n_0 \leq n \leq n_f$ , subscripts  $_0$  and  $_f$  stand for initial and final,  $\Gamma(\alpha)$  is the Gamma function,  $\alpha$  and  $\beta$  are parameters that determine the shape of the

distribution,  $\gamma$  determines the original shift,

$$C_m(n_0, n_f) = \left\{ \int_{n_0}^{n_f} \frac{(M(n) - \gamma)^{\alpha-1}}{\beta^\alpha \Gamma(\alpha)} \exp \left[ - \left( \frac{M(n) - \gamma}{\beta} \right) \right] dn \right\}^{-1}. \quad (2)$$

This choice of  $C_m$  assures that

$$\int_{n_0}^{n_f} f_m(n) dn = 1.$$

Assuming that the properties of hydrocarbons in a certain narrow range of  $n$  are close, the continuous distribution  $f_m(n)$  was replaced with a discrete one, consisting of  $N_f$  quasi-components with carbon numbers

$$\bar{n}_j = \frac{\int_{n_{j-1}}^{n_j} n f_m(n) dn}{\int_{n_{j-1}}^{n_j} f_m(n) dn}, \quad (3)$$

and the corresponding molar fractions

$$X_j = \int_{n_{j-1}}^{n_j} f_m(n) dn. \quad (4)$$

where  $j$  is an integer in the range  $1 \leq j \leq N_f$ . Note that

$$\sum_{j=1}^{j=N_f} X_j = 1. \quad (5)$$

The choice of  $n_j$  could be arbitrary. It was assumed that all  $n_j - n_{j-1}$  are equal, i.e. all quasi-components have the same range of values of  $n$ . For the case when  $N_f = 1$  this approach reduces the analysis of multi-component droplets to that of mono-component droplets. These new quasi-components were not the actual physical hydrocarbon components ( $\bar{n}_j$  are not integers in the general case). Hence this model was called a quasi-discrete model. These quasi-components were treated as actual components in the conventional Discrete Component Model (DCM), including taking into account the diffusion of liquid quasi-components in droplets, discussed later in this section. This model was expected to be particularly useful when  $N_f$  is much less than the number of actual species in the hydrocarbon mixture.

There are two main problems with the application of this approach to realistic Diesel fuels, the composition of which is shown in Table 2. Firstly, even if we restrict our analysis only to alkanes, it does not appear to be easy to approximate this distribution with a reasonably simple distribution function  $f_m(n)$ , given by Expression (1) (similar to the one used in [7, 8, 9]). Secondly, the contributions of the other five hydrocarbon groups apart from alkanes, presented in Table 2, cannot be ignored in any realistic model of Diesel fuels. In the model, suggested in this paper, both of these issues will be addressed.

In the new model, the focus is shifted from the analysis of the distribution function to the direct analysis of molar fractions of the components. These are described by the matrix  $X_{nm}$ , where  $n$  refers to the number of carbon atoms, and  $m$  refers to the groups (e.g. alkanes) or individual components (tricycloalkane, diaromatic and phenanthrene). The link between the values of  $m$  and the components is shown in Table 3.

| $m$ | Component            |
|-----|----------------------|
| 1   | alkanes              |
| 2   | cycloalkanes         |
| 3   | bicycloalkanes       |
| 4   | alkylbenzenes        |
| 5   | indanes & tetralines |
| 6   | naphthalenes         |
| 7   | tricycloalkane       |
| 8   | diaromatic           |
| 9   | phenanthrene         |

Table 3

For each  $m$  the values of  $\bar{n}_{jm}$  of quasi-components **can be** introduced as

$$\left. \begin{aligned} \bar{n}_{1m} &= \frac{\sum_{n=n_{1m}}^{n=n_{(\varphi_m+1)m}} (nX_{nm})}{\sum_{n=n_{1m}}^{n=n_{(\varphi_m+1)m}} X_{nm}}, \\ \bar{n}_{2m} &= \frac{\sum_{n=n_{(\varphi_m+2)m}}^{n=n_{(2\varphi_m+2)m}} (nX_{nm})}{\sum_{n=n_{(\varphi_m+2)m}}^{n=n_{(2\varphi_m+2)m}} X_{nm}}, \\ \bar{n}_{3m} &= \frac{\sum_{n=n_{(2\varphi_m+3)m}}^{n=n_{(3\varphi_m+3)m}} (nX_{nm})}{\sum_{n=n_{(2\varphi_m+3)m}}^{n=n_{(3\varphi_m+3)m}} X_{nm}}, \\ &\dots\dots\dots \\ \bar{n}_{\ell m} &= \frac{\sum_{n=n_{((\ell-1)\varphi_m+\ell)m}}^{n=n_{k_m}} (nX_{nm})}{\sum_{n=n_{((\ell-1)\varphi_m+\ell)m}}^{n=n_{k_m}} X_{nm}}, \end{aligned} \right\} \quad (6)$$

where  $n_{1m}=n_{m(\min)}$  is the minimal value of  $n$  for which  $X_{nm} \neq 0$ ,  $n_{k_m}=n_{m(\max)}$  is the maximal value of  $n$  for which  $X_{nm} \neq 0$  (see Table 2),  $\ell = \text{integer } ((k_m + \varphi_m)/(\varphi_m + 1))$ . Parameter  $\varphi_m$  is assumed to be integer;  $\varphi_m + 1$  is equal to the number of components to be included into quasi-components, except possibly the last one in the group.  $\varphi_m$  is assumed to be the same for all quasi-components within group  $m$ . If  $\varphi_m = 0$  then  $\ell = k_m$  and the number of quasi-components is equal to the number of actual components.  $\varphi_m$  and  $k_m$  depend on  $m$  in the general case.

**This approach to generation of quasi-components is based on the selection of the number of components in each quasi-component ( $\varphi_m + 1$ ) in most cases. An alternative approach to their generation is based on the selection of the number of quasi-components  $n_q$ . In this case the number of components in each quasi-component, except possibly the last one, ( $n_c$ ) is taken equal to the nearest integer of the ratio  $k_m/n_q$ . If  $k_m/n_q$  is not an integer then the number of components in the last quasi-component ( $n_{lc}$ ) is either greater than  $n_c$ , if  $(k_m/n_q) > n_c$ , or less than  $n_c$ , if  $(k_m/n_q) \leq n_c$ . We found the second approach to be more convenient for practical applications and it was used in our analysis. The values of  $\bar{n}_{im}$  were calculated using the same approach as in the case presented in Equation (6).**

As in the case of the original quasi-discrete model,  $\bar{n}_{im}$  are not integers in the general case. In the case when mass fractions of components/quasi-components with large carbon numbers are small then these components/quasi-components can be merged to form single quasi-components. Due to the ad-



ditional dimensions introduced by the subscript  $m$  in Equation (6), the new model is called the multi-dimensional quasi-discrete model.

The minimal number of  $\bar{n}_{im}$  for the groups shown in Table 2 is 6 (when  $\varphi_m = k_m - 1$  for all  $m$ ). Taking into account three additional components, not included in Table 2, the minimal number of quasi-components/components approximating Diesel fuel within the new model is 9. The multi-component model can be further simplified and approximated by the single-component model. The maximal number of these quasi-components/components, providing the most accurate approximation of Diesel fuel, is 98. In this paper we will investigate by how much the latter number can be reduced, provided that the errors introduced by this reduction are acceptable for practical engineering applications. Note that in the model considered in [7, 8] the minimal and maximal numbers of quasi-components for Diesel fuel were 1 and 20 respectively.

The molar fractions of these quasi-components/components are estimated as

$$\left. \begin{aligned} X_{1m} &= \sum_{n=n_{1m}}^{n=n_{(\varphi_m+1)m}} X_{nm}, \\ X_{2m} &= \sum_{n=n_{(\varphi_m+2)m}}^{n=n_{(2\varphi_m+2)m}} X_{nm}, \\ &\dots\dots\dots \\ X_{\ell m} &= \sum_{n=n_{((\ell-1)\varphi_m+\ell)m}}^{n=n_{k_m}} X_{nm}. \end{aligned} \right\} \quad (7)$$

Note that in the case when the maximal  $\ell = k_m$  was used, the new model reduces to the conventional Discrete Component Model (DCM), while the previously suggested quasi-discrete model does not have this property. In the case considered in [7, 8], Diesel fuel was approximated by 21 components (n-alkanes), but the maximal number of quasi-components was just 20.

Once the quasi-components have been introduced they are treated in the same way as in [7, 8], using transport and thermodynamic properties of the components summarised in Appendices 1-7. The mixtures are treated as ideal (Raoult's law is assumed to be valid). In this case, partial pressures of individual quasi-components/components are estimated as:

$$p_v(\bar{n}_{im}) = X_{lsim}(\bar{n}_{im})p^{\text{sat}}(\bar{n}_{im}), \quad (8)$$

where  $X_{lsim}$  are the molar fractions of liquid quasi-components at the surface of the droplet,  $p^{\text{sat}}(\bar{n}_{im})$  are calculated from the data presented in Appendices

1-7. In the case of discrete components, these pressures do not depend on  $n$  (they are functions of temperature only).

As in the case of [7, 8], the temperature gradient and quasi-components' diffusion inside droplets are taken into account based on the analytical solutions to the heat conduction and species diffusion equations inside droplets respectively. These are discussed in the following sections, mainly following [23].

### 3.2. Droplet heating

The process of heating mono- and multi-component droplets is described by the transient heat conduction equation for the temperature  $T \equiv T(t, R)$  in the liquid phase, assuming that all processes are spherically symmetric [24, 25]. An analytical solution to this equation, subject to the initial  $T(t = 0) = T_{d0}(R)$  and the boundary condition (assuming that the effects of evaporation can be ignored):

$$h(T_g - T_s) = k_{\text{eff}} \left. \frac{\partial T}{\partial R} \right|_{R=R_d-0}, \quad (9)$$

and assuming that the convection heat transfer coefficient  $h = \text{const}$ , can be presented as [27]:

$$\begin{aligned} T(R, t) = & \frac{1}{R} \sum_{n=1}^{\infty} \left\{ q_n \exp[-\kappa_R \lambda_n^2 t] - \frac{R_d^2 \sin \lambda_n}{\|v_n\|^2 \lambda_n^2} \mu_0(0) \exp[-\kappa_R \lambda_n^2 t] \right. \\ & \left. - \frac{R_d^2 \sin \lambda_n}{\|v_n\|^2 \lambda_n^2} \int_0^t \frac{d\mu_0(\tau)}{d\tau} \exp[-\kappa_R \lambda_n^2 (t - \tau)] d\tau \right\} \sin \left[ \lambda_n \left( \frac{R}{R_d} \right) \right] + T_g(t), \end{aligned} \quad (10)$$

where  $\lambda_n$  are solutions to the equation:

$$\lambda \cos \lambda + h_0 \sin \lambda = 0, \quad (11)$$

$$\|v_n\|^2 = \frac{R_d}{2} \left( 1 - \frac{\sin 2\lambda_n}{2\lambda_n} \right) = \frac{R_d}{2} \left( 1 + \frac{h_0}{h_0^2 + \lambda_n^2} \right),$$

$$q_n = \frac{1}{\|v_n\|^2} \int_0^{R_d} \tilde{T}_0(R) \sin \left[ \lambda_n \left( \frac{R}{R_d} \right) \right] dR, \quad \kappa_R = \frac{k_{\text{eff}}}{c_l \rho_l R_d^2}, \quad \mu_0(t) = \frac{h T_g(t) R_d}{k_{\text{eff}}},$$

$h_0 = (h R_d / k_{\text{eff}}) - 1$ ,  $\tilde{T}_0(R) = R T_{d0}(R)$ . The solution to Equation (11) gives a set of positive eigenvalues  $\lambda_n$  numbered in ascending order

( $n = 1, 2, \dots$ ). The trivial solution  $\lambda = 0$  is not considered.  $T_s = T_s(t)$  is the droplet's surface temperature,  $T_g = T_g(t)$  is the ambient gas temperature,  $h$  is linked with the Nusselt number  $\text{Nu}$  via the equation  $\text{Nu} = 2R_d h / k_g$ ,  $k_g$  is the gas thermal conductivity. We assume that fuel vapour is dilute and  $k_g$  is equal to the thermal conductivity of air. We are interested only in a solution which is continuously differentiable twice in the whole domain. This implies that  $T$  should be bounded for  $0 \leq R < R_d$ .

Solution (10) is valid for  $h_0 > -1$ , which is satisfied, remembering the physical background of the problem ( $h > 0$ ). The condition  $h = \text{const}$  is valid for sufficiently small time steps.

$k_{\text{eff}}$ ,  $c_l$ , and  $\rho_l$  in Expression (10) are the effective thermal conductivity, specific heat capacity, and density respectively of the liquid phase,  $R$  is the distance from the centre of the droplet,  $t$  is time.  $k_{\text{eff}}$  is linked with the liquid thermal conductivity  $k_l$  via the following equation:

$$k_{\text{eff}} = \chi k_l, \quad (12)$$

where the coefficient  $\chi$  can be approximated as [26]:

$$\chi = 1.86 + 0.86 \tanh [2.225 \log_{10} (\text{Pe}_{d(l)}/30)], \quad (13)$$

where  $\text{Pe}_{d(l)} = \text{Re}_{d(l)} \text{Pr}_l$  is the liquid Peclet number. Liquid fuel transport properties and the liquid velocity just below the droplet surface (see [26] for details) were used for calculating  $\text{Pe}_{d(l)}$ . The model based on Equations (12) and (13) is known as the Effective Thermal Conductivity (ETC) model.

The effect of droplet evaporation in analytical solution (10), is taken into account by replacing gas temperature with the so-called effective temperature defined as:

$$T_{\text{eff}} = T_g + \frac{\rho_l L \dot{R}_{de}}{h}, \quad (14)$$

where  $L$  is the latent heat of evaporation,  $\dot{R}_{de}$  is the change of droplet radius due to evaporation, which is taken from the previous time step and estimated based on Equation (31).  $R_d$  and all other thermodynamic and transport properties are assumed constant in the analytical solution, but are updated at the end of each time step

$\Delta t$ . The effects of non-constant droplet radius during the droplet heating process were discussed in [4, 5].

In the limit  $k_{\text{eff}} \rightarrow \infty$  the prediction of Expression (10) reduces to the one which follows from the model based on the assumption that  $k_{\text{eff}} = \infty$  [28] (Infinite Thermal Conductivity (ITC) model). The value of Nu for an isolated moving droplet is estimated based on the following equation [26]:

$$\text{Nu}_{\text{iso}} = 2 \frac{\ln(1 + B_T)}{B_T} \left( 1 + \frac{(1 + \text{Re}_d \text{Pr}_d)^{1/3} \max[1, \text{Re}_d^{0.077}] - 1}{2F(B_T)} \right), \quad (15)$$

where  $B_T = \frac{c_{pv}(T_g - T_s)}{L_{\text{eff}}}$  is the Spalding heat transfer number,  $F(B_T) = (1 + B_T)^{0.7 \frac{\ln(1+B_T)}{B_T}}$ ,  $L_{\text{eff}} = L + \frac{Q_L}{\dot{m}_d} = \sum_i \epsilon_i L_i + \frac{Q_L}{\sum_i \dot{m}_i}$ ,  $Q_L$  is the power spent on droplet heating,  $c_{pv}$  is the specific heat capacity of fuel vapour,  $\epsilon_i = \epsilon_i(t)$  are the evaporation rates of species  $i$ ,  $\dot{m}_i = \epsilon_i \dot{m}_d$  ( $\dot{m}_d = \sum_i \dot{m}_i$ ). The effects of the interaction between droplets are ignored (simplified models for these effects are discussed in [29, 11]).

### 3.3. Species diffusion in the liquid phase

The diffusion of species inside a spherical droplet is described by a well known species diffusion equation [3]. The analytical solution to this equation was obtained subject to the following boundary condition [10]:

$$\alpha(\epsilon_i - Y_{lis}) = -D_{\text{eff}} \left. \frac{\partial Y_{li}}{\partial R} \right|_{R=R_d-0}, \quad (16)$$

and the initial condition  $Y_{li}(t = 0) = Y_{li0}(R)$ , where  $Y_{lis} = Y_{lis}(t)$  are liquid components' mass fractions at the droplet's surface ( $i = 1, 2, 3, \dots$ ),

$$\alpha = \frac{|\dot{m}_d|}{4\pi\rho_l R_d^2}, \quad (17)$$

$\dot{m}_d$  is the droplet evaporation rate, the calculation of which is discussed in the next subsection (see Equation (24)). As in the case of the heat conduction equation, we are interested only in a solution which is continuously differentiable twice in the whole domain.

This implies that  $Y_{li}$  should be bounded for  $0 \leq R \leq R_d$ . This led to the following expression for  $Y_{li}$  [10]:

$$Y_{li} = \epsilon_i + \frac{1}{R} \left\{ \left[ \exp \left[ D_{\text{eff}} \left( \frac{\lambda_0}{R_d} \right)^2 t \right] [q_{i0} - Q_0 \epsilon_i] \sinh \left( \lambda_0 \frac{R}{R_d} \right) + \sum_{n=1}^{\infty} \left[ \exp \left[ -D_{\text{eff}} \left( \frac{\lambda_n}{R_d} \right)^2 t \right] [q_{in} - Q_n \epsilon_i] \sin \left( \lambda_n \frac{R}{R_d} \right) \right] \right\}, \quad (18)$$

where  $\lambda_0$  and  $\lambda_n$  ( $n \geq 1$ ) are solutions to the equations

$$\tanh \lambda_0 = -\frac{\lambda_0}{h_{0Y}} \quad \text{and} \quad \tan \lambda_n = -\frac{\lambda_n}{h_{0Y}} \quad (n \geq 1),$$

respectively,  $h_{0Y} = -\left(1 + \frac{\alpha R_d}{D_{\text{eff}}}\right)$ ,

$$Q_n = \begin{cases} -\frac{1}{||v_0||^2} \left( \frac{R_d}{\lambda_0} \right)^2 (1 + h_{0Y}) \sinh \lambda_0 & \text{when } n = 0 \\ \frac{1}{||v_n||^2} \left( \frac{R_d}{\lambda_n} \right)^2 (1 + h_{0Y}) \sin \lambda_n & \text{when } n \geq 1 \end{cases} \quad (19)$$

$$q_{in} = \frac{1}{||v_n||^2} \int_0^{R_d} R Y_{li0}(R) v_n(R) dR, \quad (20)$$

$n \geq 0$ ,

$$v_0(R) = \sinh \left( \lambda_0 \frac{R}{R_d} \right), \quad v_n(R) = \sin \left( \lambda_n \frac{R}{R_d} \right), \quad n \geq 1.$$

$D_{\text{eff}}$  is linked with the liquid diffusivity  $D_l$  via the following equation

$$D_{\text{eff}} = \chi_Y D_l, \quad (21)$$

where the coefficient  $\chi_Y$  can be approximated as:

$$\chi_Y = 1.86 + 0.86 \tanh \left[ 2.225 \log_{10} \left( \text{Re}_{d(l)} \text{Sc}_l / 30 \right) \right], \quad (22)$$

$\text{Sc}_l = \nu_l / D_l$  is the liquid Schmidt number,  $\nu_l$  is the liquid kinematic viscosity. As in the case of  $k_{\text{eff}}$ , liquid fuel transport properties and the liquid velocity just below the droplet surface were used for calculating  $\text{Re}_{d(l)}$ . The model based on Equations (21) and (22)

is known as the Effective Diffusivity (ED) model. The model, based on the assumption that species diffusivity is infinitely fast ( $D_{\text{eff}} = \infty$ ) is referred to as the Infinite Diffusivity (ID) model.  $D_l$  is assumed to be the same for all species. The combined ITC/ID model is sometimes known as a well-mixed model.

Assuming that species concentrations in the ambient gas are equal to zero, the values of  $\epsilon_i$  can be found from the following relationship [10]:

$$\epsilon_i = \frac{Y_{vis}}{\sum_i Y_{vis}}, \quad (23)$$

where the subscript  $_v$  indicates the vapour phase.

#### 3.4. Droplet evaporation

The evaporation rate of isolated stationary or moving mono-component droplets can be estimated as [26, 3]:

$$\dot{m}_d = -2\pi R_d D_v \rho_{\text{total}} B_M \text{Sh}_{\text{iso}}, \quad (24)$$

where  $D_v$  is the binary diffusion coefficient of vapour in air,  $B_M$  is the Spalding mass transfer number defined as:

$$B_M = \frac{\rho_{vs} - \rho_{v\infty}}{\rho_{gs}} = \frac{Y_{vs} - Y_{v\infty}}{1 - Y_{vs}}, \quad (25)$$

$Y_v$  is the vapour mass fraction,  $\text{Sh}_{\text{iso}}$  is the Sherwood number approximated for the isolated droplets as [3]:

$$\text{Sh}_{\text{iso}} = 2 \frac{\ln(1 + B_M)}{B_M} \left( 1 + \frac{(1 + \text{Re}_d \text{Sc}_d)^{1/3} \max[1, \text{Re}_d^{0.077}] - 1}{2F(B_M)} \right), \quad (26)$$

$\text{Sc}_d = \frac{\nu_{\text{air}}}{D_v}$  is the Schmidt number,  $F(B_M) = (1 + B_M)^{0.7 \frac{\ln(1+B_M)}{B_M}}$ .  $B_T$  and  $B_M$  are linked by the following equation [3, 26]:

$$B_T = (1 + B_M)^\varphi - 1, \quad (27)$$

where

$$\varphi = \left( \frac{c_{pv}}{c_{pa}} \right) \left( \frac{\text{Sh}^*}{\text{Nu}^*} \right) \frac{1}{\text{Le}}, \quad (28)$$

$Le = k_g / (c_{pa} \rho_{\text{total}} D_v) = Sc_d / Pr_d$  is the Lewis number,

$$Sh^* = 2 \left( 1 + \frac{(1 + Re_d Sc_d)^{1/3} \max[1, Re_d^{0.077}] - 1}{2F(B_M)} \right), \quad (29)$$

$$Nu^* = 2 \left( 1 + \frac{(1 + Re_d Pr_d)^{1/3} \max[1, Re_d^{0.077}] - 1}{2F(B_T)} \right). \quad (30)$$

The derivation of Equation (24) is essentially based on the assumption that  $\rho_{\text{total}}$  remains the same at all distances from the droplet surface. This assumption was relaxed in the recently developed model described in [31, 32]. As follows from Equation (28),  $\varphi$  is a function of  $B_T$ . Hence, the iteration process needs to be performed to calculate  $B_T$  from Equation (27). In our previous paper [30] it was shown that, in some practically important cases, Formula (28) can be simplified assuming that  $\frac{Sh^*}{Nu^*} = 1$ . In our case, the analysis is based on Formula (28).

In the case of multi-component droplets, the problem of modelling droplet evaporation is complicated by the fact that different species diffuse at different rates and the evaporation rate of one of the species is affected by the evaporation rate of other species. Our analysis of  $\dot{m}_d$  is based on Equation (24), assuming that the mixture of vapour species can be treated as a separate gas ( $Y_{vs} = \sum_i Y_{vis}$ ).

When calculating the value of  $\dot{R}_d$  we took into account both droplet evaporation and the change in droplet density during the time step (see Equation (20) in [23]):

$$\dot{R}_d = \dot{R}_{de} + \dot{R}_{ds}, \quad (31)$$

where  $\dot{R}_{de}$  and  $\dot{R}_{ds}$  are the rates of change of droplet radii due to evaporation and swelling defined as;

$$\dot{R}_{de} = \frac{\dot{m}_d}{4\pi R_d^2 \rho_l}, \quad \dot{R}_{ds} = \frac{R_d(\bar{T}_0)}{\Delta t} \left[ \left( \frac{\rho(\bar{T}_0)}{\rho(\bar{T}_1)} \right)^{1/3} - 1 \right],$$

$\bar{T}_0$  and  $\bar{T}_1$  are average droplet temperatures at the beginning  $t = t_0$  and the end of the time step  $t = t_1$ ,  $\Delta t = t_1 - t_0$ .

### 3.5. Liquid diffusion coefficient

In the original papers [7, 8], the diffusion coefficient of component  $j$  relative to all other components was estimated based on the simplified version of the Sanchez and Clifton formula [33]:  $D_{jm} = X_j D_{mj}^0 + X_m D_{jm}^0$ , where  $m$  refers to the mixture of all other components,  $D_{jm}^0$  and  $D_{mj}^0$  are diffusivities of dilute solute  $j$  in solvent  $m$  and dilute solute  $m$  in solvent  $j$  respectively, both are in  $\text{m}^2/\text{s}$ . Note that there are errors in the corresponding expressions for  $D_{jm}$  given in [10, 11]. At the same time it was shown in [34, 35] that a more accurate approximation for  $D_{jm}$  is given by the formula  $D_{jm} = (D_{mj}^0)^{X_j} (D_{jm}^0)^{X_m}$  (the authors are grateful to P. Kelley for drawing our attention to [34, 35]). In our case, the difference between these approximations is not important as the simplified model, based on the assumption that  $D_{mj}^0 = D_{jm}^0$ , is used in our analysis.

Among various approximations for  $D_{jm}^0$  and  $D_{mj}^0$  the Wilke-Chang approximation was chosen. Assuming that  $D_{jm}$  is the same for all species, we can write [36]:

$$D_{jm} \equiv D_l = \frac{7.4 \times 10^{-15} \sqrt{\overline{M}_v} T}{\mu_l V_v^{0.6}}, \quad (32)$$

where  $\overline{M}_v$  is the average molar mass defined as

$$\overline{M}_v = \left[ \sum_{m=1}^{m=9} \sum_{i=1}^{i=N_m} (Y_{im}/M_{im}) \right]^{-1}. \quad (33)$$

When deriving Expression (33) the contributions of tricycloalkanes, diaromatics and phenanthrenes are taken into account in addition to the groups of compounds presented in Table 2. For these three individual components  $N_m = 1$ .

Mass fractions  $Y_{im}$  are linked with the molar fractions  $X_{im}$  by the following formula

$$Y_{im} = \frac{X_{im} M_{im}}{\sum_{m=1}^{m=9} \sum_i M_{im} X_{im}}, \quad (34)$$

the summation is performed over all species including the ones not included in Table 2,  $V_v$  is defined as

$$V_v = (\sigma_v/1.18)^3, \quad (35)$$



$\sigma_v$  is the Lennard-Jones length (in Å). For individual components this length could be estimated based on the following formula [39]:

$$\sigma_v^3 = 0.17791 + 11.779 \left( \frac{T_c}{p_c} \right) - 0.049029 \left( \frac{T_c}{p_c} \right)^2, \quad (36)$$

where critical temperatures  $T_c$  and pressures  $p_c$  are in K and bar respectively. Our analysis, however, is based on a simpler formula [37]:

$$\sigma_v = 1.468 \overline{M}_v^{0.297}, \quad (37)$$

where  $\overline{M}_v$  is the molar mass (in kg/kmole). These values of  $\sigma_v$  appeared to be close to the experimentally observed values reported in [40].

The thermodynamic and transport properties of all quasi-components within individual groups were estimated based on the values of  $\overline{n}_{im}$  as in [7, 8, 9].

### 3.6. Vapour diffusion coefficient

As in our previous papers (e.g. [10, 7, 8]), we could assume that Diesel fuel vapour diffuses from the surface of the droplet, without changing its composition, with the average diffusion coefficient estimated from the Wilke and Lee formula [33]:

$$D_{va} = \frac{\left[ 3.03 - \left( 0.98 / M_{va}^{1/2} \right) \right] (10^{-7}) T^{3/2}}{p M_{va}^{1/2} \sigma_{va}^2 \Omega_D}, \quad (38)$$

where  $D_{va}$  is in  $\text{m}^2/\text{s}$ ,  $T$  is temperature in K,

$$M_{va} = 2 \left[ (1/\overline{M}_v) + (1/M_a) \right]^{-1},$$

$M_a$  is molar mass of air,  $p$  is pressure in bar,  $\sigma_{va} = (\sigma_v + \sigma_a)/2$ ,  $\sigma_v$  and  $\sigma_a$  are characteristic Lennard-Jones lengths for vapour and air respectively, measured in Angstrom (Å) (see Equation (37)),  $\Omega_D$  is the function of the normalised temperature  $T^* = k_B T / \varepsilon_{va}$ ,  $\varepsilon_{va} = \sqrt{\varepsilon_v \varepsilon_a}$ ,  $\varepsilon_v$  and  $\varepsilon_a$  are characteristic Lennard-Jones energies for vapour and air respectively,  $k_B$  is the Boltzmann constant.  $\Omega_D$  is estimated based on Equation (B6) in [41], assuming that  $\varepsilon_v$  is equal to that of n-dodecane and  $\varepsilon_v/k_B = 245$  K [38, 41]. The latter assumption is justified by the fact that  $\Omega_D$  is a relatively weak

function of  $\varepsilon_v$  and the values of  $\varepsilon_v$  for most components of Diesel fuel are not known to us.

**The approach based on Expression (38) could potentially take into account changes in  $D_{va}$  due to the change in composition of Diesel fuel during the evaporation process. At this stage, however, our analysis is based on the assumption that  $D_{va}$  remains equal to the dodecane/air diffusion coefficient and is estimated based on the following approximate formula [42]**

$$D_{va} = 5.27 \times 10^{-6} \left( \frac{T}{300} \right) \frac{1}{p} \frac{\text{m}^2}{\text{s}}, \quad (39)$$

**where  $T$  is in K, pressure  $p$  is in bars.**

All liquid properties are calculated for the average temperature inside droplets. All gas properties are calculated for the reference temperature  $T_r = (2/3)T_s + (1/3)T_g$ , where  $T_s$  and  $T_g$  are droplet surface and ambient gas temperatures, respectively. Enthalpy of evaporation and saturated vapour pressure are estimated at the surface temperature  $T_s$ .

### 3.7. Average values of properties

The average values of liquid density, specific heat capacity capacity, latent heat of evaporation and saturated vapour pressure taking into account the contributions of all individual groups were estimated using the following formulae [33, 23]:

$$\bar{\rho}_l = \left[ \sum_{i=1}^{i=N} (Y_i / \rho_{li}) \right]^{-1}, \quad (40)$$

$$\bar{c}_l = \sum_{i=1}^{i=N} (Y_i c_{li}), \quad (41)$$

$$\bar{L} = \sum_{i=1}^{i=N} \epsilon_i L_i, \quad (42)$$

$$\bar{p}_v = \sum_{i=1}^{i=N} X_i p_{vi}. \quad (43)$$

where the subscripts  $_{li}$  refer to the corresponding liquid quasi-components/components,  $N$  is the total number of quasi-components/components.

The values of  $\rho_{li}$ ,  $c_{li}$ ,  $L_i$  and  $p_{vi}$  for quasi-components were calculated based on the corresponding average carbon numbers. The values of  $Y_i$  are the values of the corresponding mass fractions averaged over the whole volume occupied by the droplets. The above average values were recalculated at each time step.

Various approximations for liquid mixture viscosity are discussed in Section 9-13 of [33]. All approximations suggested so far can be considered as further developments of the method of Grunberg and Nissan, originally suggested in 1949. According to this method the dynamic viscosity of the liquid mixture can be estimated from the following formula:

$$\ln \bar{\mu}_l = \sum_{i=1}^{i=N} X_i \ln \mu_{li} + \frac{1}{2} \sum_{i=1}^{i=N} \sum_{j=1}^{j=N} X_i X_j G_{ij}, \quad (44)$$

where  $G_{ij}$  is an interaction parameter which is the function of components, temperature and sometimes composition. The estimate of  $G_{ij}$  is not a trivial task (see [33] for details) especially in the case of such complex liquids as Diesel fuel. Our task, however, is simplified by the fact that the results of our analysis are a very weak function of viscosity. This allows us to ignore this term altogether and simplify Expression (44) to

$$\ln \bar{\mu}_l = \sum_{i=1}^{i=N} X_i \ln \mu_{li}. \quad (45)$$

Our analysis is based on Formula (45).

Finding a suitable approximation for the thermal conductivity of a complex liquid mixture, such as Diesel fuel, turned out to be no less difficult than for viscosity. When the ratios of thermal conductivity of quasi-components/components do not exceed two, the mixture conductivity can be estimated based upon the power law method as [33]:

$$\bar{k}_l = \left( \sum_{i=1}^{i=N} Y_i k_{li}^{-2} \right)^{-1/2}. \quad (46)$$

Formula (46) was successfully used in our previous paper [23], where we studied the process of heating and evaporation of biodiesel fuel droplets. For these droplets the ratios of thermal conductivities of components indeed do not exceed 2. In the case of Diesel fuel droplets, however, this ratio can

exceed an order of magnitude, and the application of Formula (46) for them cannot be justified.

Our analysis will be based on the values of average thermal conductivity of typical Diesel fuels as inferred from published data. These are assumed to be reasonably close to the values of thermal conductivity of Diesel fuel on which our analysis is focused. The details of the analysis of Diesel fuel thermal conductivity are presented in Appendix 8.

#### 4. Solution algorithm

These are the main steps of the numerical algorithm:

1. Assume the initial distribution of temperature and mass fractions of species inside the droplet or use the distributions obtained at the previous time step (in our case both initial distributions were assumed homogeneous; the initial molar fractions are given in Table 2). Recalculate the molar fractions of species into mass fractions of species.
2. Calculate the values of liquid thermal conductivity and effective thermal conductivity of the droplet using Equations (85) and (12).
3. Calculate species partial pressures and molar fractions in the gas phase using Equation (8).
4. Assuming that the concentration of vapour of all species in the ambient gas can be ignored, calculate the value of the Spalding mass transfer number, using Equation (25).
5. Calculate the values of liquid heat capacity and diffusivity of the mixture of vapour species in the air, using Equations (41) and (39) respectively, and species evaporation rates ( $\epsilon_i$ ) using Equation (23).
6. Calculate the value of the Spalding heat transfer number using the iteration process based on Equations (27)-(30).
7. Calculate the values of the Nusselt and Sherwood numbers for isolated droplets using Equations (15) and (26).
8. Calculate the values of  $Nu^*$  and  $Sh^*$  using Equations (29) and (30).
9. Calculate the rate of change of droplet radius using Equation (31).
10. Calculate the effective temperature, using Equation (14).
11. Calculate the distribution of temperature inside the droplet based on Equation (10), using 33 terms in the series.
12. Calculate the distribution of species inside the droplet based on Equation (18), using 33 terms in the series. Note that the chosen number of terms

affects the predicted distribution of species if this number is much less than 33. This effect is much weaker for the distribution of temperature in droplets.

13. Recalculate the droplet's radius at the end of the time step  $\Delta t$ . If this radius is negative then the time step is reduced and the calculations are repeated. If the ratio of this radius to the initial radius is less than an *a priori* chosen small number,  $\varepsilon_s = 10^{-6}$ , then the remaining part of the droplet is assumed to be evaporated with all liquid species transferred into the gas phase with a corresponding decrease in gas temperature. If this ratio is greater than  $10^{-6}$  then go to the next step.

14. Recalculate the distributions of temperature and species for the new droplet radius (e.g.  $T(R) = T(R R_{d2}/R_{d1}) = T(\tilde{R})$ , where  $R_{d1,2}$  are droplet radii at the beginning and the end of the time step,  $\tilde{R}$  is the new  $R$  used at the second time step,  $T$  are the values of temperature at the end of the first time step).

15. Return to Step 1 and repeat the calculations for the next time step.

## 5. Results

We assume that  $R_{d0} = 10 \mu\text{m}$ , which is compatible with Sauter Mean Diameters of Diesel fuel droplets reported in [48, 49] ( $17.7 \mu\text{m}$  [48] and  $18.3 \mu\text{m}$  [49]). As in [7] we assumed the following values for ambient air density and pressure (assuming that the ideal gas law is valid):

$$\rho_a = 11.9 \text{ kg/m}^3, \quad T_a = 880 \text{ K}, \quad p_a = 30 \text{ bar}.$$

Firstly, the results of calculations based on the Effective Thermal Conductivity (ETC) model and for stationary droplets will be presented (**in this case the ETC model reduces to a pure conduction model**). The plots of the droplet surface temperatures  $T_s$  and radii  $R_d$  versus time for various approximations of Diesel fuel composition are shown in Figs. 1-8. In Fig. 1 these plots are shown for 4 cases: the contributions of all 98 components are taken into account (indicated as (98)); the contributions of only 20 alkane components shown in Table 2 are taken into account (standard approximation used in the original quasi-discrete model [7, 8]) (indicated as (20A)); the contribution of all 98 components is approximated by 6 quasi-components (corresponding to 6 groups shown in Table 2) and 3 components (tricycloalkane, diaromatic and phenanthrene) without taking into account the diffusion between them so that their mass fractions remain equal to the

initial mass fractions and they behave like a single quasi-component (indicated as (S)); and the contributions of only 20 alkane components shown in Table 2 are taken into account and these are approximated by a single quasi-component with the average value of the carbon number ( $C_{14.763}H_{31.526}$ ; indicated as (SA)). In the cases when only the contribution of alkanes was taken into account, the mass fractions of the components were recalculated to ensure that the total mass fractions of all alkanes were equal to 1. **The same comment applies to the cases when other components are removed from the analysis.**

As follows from Fig. 1, the approximation of 98 actual components with a single quasi-component (**formed of 9 quasi-components/components; plots S**) leads to a noticeable under-estimation of the droplet surface temperature, and an under-estimation of the evaporation time by about 17%. In the case when Diesel fuel is approximated with 20 alkane components, the predicted droplet surface temperatures appeared to be higher and the evaporation time shorter by about 23% than in the case of approximation of Diesel fuel with 98 components. This means that the approximation of Diesel fuel with alkanes, a widely used assumption in the modelling of Diesel fuels (see [7, 8] and the references therein), leads to results which are less accurate, compared with the approximation of Diesel fuel by a single quasi-component. The approximation of Diesel fuel with a single alkane quasi-component ( $C_{14.763}H_{31.526}$ ) leads to under-prediction of the evaporation time by about 37% which is not acceptable even for qualitative analysis of the process. This leads us to question of the validity of the results of numerous papers where Diesel fuel was approximated with a single alkane component (e.g. [43]).

Note that in all cases shown in Fig. 1 the droplet surface temperatures keep increasing with time until the droplets evaporate. This is consistent with our earlier studies of this process (e.g. [42, 8]). This result questions the applicability of the assumption that the droplet surface temperature remains constant during the evaporation process which is widely used in simplified models of this process (see e.g. [44, 45]). The well known  $d^2$ -law is implicitly based on this assumption (see [3]).

The results of calculations of the droplet surface temperatures  $T_s$  and radii  $R_d$  versus time for more refined approximations of Diesel fuel, compared with the case shown in Fig. 1, are shown in Fig. 2. The following approximations were considered:

1. The contributions of all 98 components are taken into account as in the case shown in Fig. 1 (indicated as (98));
2. The contribution of alkanes is approximated by 19 quasi-components/components (QC/C, 18 components and 1 QC incorporating 2 components with the largest values of  $n$ ); the contribution of cycloalkanes is approximated by 17 QC/C (16 components and 1 QC incorporating 2 components with the largest values of  $n$ ); the contribution of bicycloalkanes is approximated by 8 QC; the contribution of alkylbenzenes is approximated by 16 QC/C (15 components and 1 QC incorporating 2 components with the largest values of  $n$ ); the contribution of indanes & tetralines is approximated by 12 QC/C (11 components and 1 QC incorporating 2 components with the largest values of  $n$ ); the contribution of naphthalenes is approximated by 10 QC/C (9 components and 1 QC incorporating 2 components with the largest values of  $n$ ); the contributions of tricycloalkanes, diaromatics and phenanthrenes are taken into account; this leads to the model based on 85 QC/C (indicated as (85));
3. The contribution of alkanes is approximated by 19 QC/C; the contribution of cycloalkanes is approximated by 9 QC; the contribution of bicycloalkanes is approximated by 8 QC; the contribution of alkylbenzenes is approximated by 8 QC; the contribution of indanes & tetralines is approximated by 6 QC; the contribution of naphthalenes is approximated by 5 QC; the contributions of tricycloalkane, diaromatic and phenanthrene are taken into account; this leads to the model based on 58 QC/C (indicated as (58));
4. The contribution of alkanes is approximated by 10 QC; the contribution of cycloalkanes is approximated by 9 QC; the contribution of bicycloalkanes is approximated by 5 QC; the contribution of alkylbenzenes is approximated by 8 QC; the contribution of indanes & tetralines is approximated by 3 QC; the contribution of naphthalenes is approximated by 2 QC; the contributions of tricycloalkane, diaromatic and phenanthrene are taken into account; this leads to the model based on 40 QC/C (indicated as (40));
5. The contributions of all 98 components are approximated with 9 single QC/C with average parameters, but diffusion between these QC/C is not allowed so that their mass fractions remain equal to the initial mass fractions and they behave like a single QC (indicated as (S)) as in Fig. 1).

The quasi-components in the above-mentioned approximations were selected as described in Section 3. Zoomed parts of Fig. 2 for droplet surface temperatures and radii are shown in Figs. 3 and 4 respectively.

As follows from Figs. 2-4, the values of  $T_s$  and  $R_d$  predicted by all approximations, except the one of a single quasi-component, are very close. The temperatures predicted based on Approximations 2-4 are slightly higher than the ones predicted by the model taking into account the contributions of all 98 components. The calculations, based on Approximations 2-4 predict slightly shorter evaporation times than the ones predicted by the model taking into account the contributions of all 98 components. Even in the case of Approximation 4 (40 QC/C) the predicted evaporation time is only about 1.5% shorter than the evaporation time predicted by the model, taking into account the contributions of all 98 components. This difference can be safely ignored in most practical engineering applications. The longer evaporation times predicted by the model taking into account the contributions of all 98 components, compared with the models based on other approximations of Diesel fuel, can be attributed to the fact that at the final stages of droplet evaporation, the speed of evaporation is controlled by the least volatile component. When Diesel fuel is approximated with QC/C, the least volatile of these quasi-components is never more volatile than the least volatile component of the Diesel fuel.

The results referring to the cases when the contributions of all 98 components are taken into account and the contribution of these 98 components is approximated with 9 single QC/C with average parameters, but diffusion between these QC/C is not allowed (Approximations 1 and 5), shown in Figs. 1-4, are reproduced in Figs. 5-8. The following additional approximations were considered for the plots shown in Figs. 5-8:

6. The contribution of alkanes is approximated by 5 QC; the contribution of cycloalkanes is approximated by 4 QC; the contribution of bicycloalkanes is approximated by 3 QC; the contribution of alkylbenzenes is approximated by 3 QC; the contribution of indanes & tetralines is approximated by 3 QC; the contribution of naphthalenes is approximated by 2 QC; the contributions of tricycloalkane, diaromatic and phenanthrene are taken into account; this leads to the model based on 23 QC/C (indicated as (23));

**7. The same as above but without diaromatic and phenanthrene; this leads to the model based on 21 QC/C (indicated as (21));**

8. The contribution of alkanes is approximated by 4 QC; the contribution of cycloalkanes is approximated by 3 QC; the contribution of bicycloalkanes is approximated by 2 QC; the contribution of alkylbenzenes is approximated by 3 QC; the contribution of indanes & tetralines is approximated by 2 QC;



the contribution of naphthalenes is approximated by 2 QC; the contribution of tricycloalkane is taken into account but not that of diaromatic and phenanthrene; this leads to the model based on 17 QC/C (indicated as (17));

9. The contribution of alkanes is approximated by 4 QC; the contribution of cycloalkanes is approximated by 3 QC; the contribution of bicycloalkanes is approximated by 1 QC; the contribution of alkylbenzenes is approximated by 3 QC; the contribution of indanes & tetralines is approximated by 2 QC; the contribution of naphthalenes is approximated by 1 QC; the contribution of tricycloalkane is taken into account but not that of diaromatic and phenanthrene; this leads to the model based on 15 QC/C (indicated as (15));

10. The contribution of alkanes is approximated by 4 QC; the contribution of cycloalkanes is approximated by 2 QC; the contribution of bicycloalkanes is approximated by 1 QC; the contribution of alkylbenzenes is approximated by 2 QC; the contribution of indanes & tetralines is approximated by 1 QC; the contribution of naphthalenes is approximated by 1 QC; the contribution of tricycloalkane is taken into account but not that of diaromatic and phenanthrene; this leads to the model based on 12 QC/C (indicated as (12));

11. The contributions of all six groups shown in Table 2 are approximated by single QCs and the contribution of tricycloalkane, diaromatic and phenanthrene are taken into account; this leads to the model based on 9 QC/C (indicated as (9)); in contrast to the single component approximation mentioned above, diffusions between QC/C are allowed in this case;

12. The contributions of all six groups shown in Table 2 are approximated by single QCs and the contribution of tricycloalkane is taken into account but not that of diaromatic and phenanthrene; this leads to the model based on 7 QC/C (indicated as (7));

13. Approximation 5 is further simplified by replacing the contributions of 9 QC/C with 7 QC/C excluding the contributions of diaromatic and phenanthrene; as in the case of Approximation 5, diffusion between QC/C is not allowed so that their mass fractions remain equal to the initial mass fractions and they behave like a single component (indicated as (S7)).

As in the cases shown in Figs. 2-4, the quasi-components/components (QC/C) in the above-mentioned approximations were selected rather arbitrarily.

As one can see from Figs. 5-8, the plots for surface temperatures and radii based on Approximations 13 and 5 are almost indistinguishable. Also, the

corresponding plots based on Approximations 11 and 12 are rather close. The same applies to the plots based on Approximations 6 and 7. This means that the contribution of diaromatic and phenanthrene can be safely ignored in the approximation of Diesel fuel when modelling the heating and evaporation of fuel droplets in realistic Diesel engine-like conditions. Both for droplet surface temperatures and radii, the accuracy of approximations improves as the number of QC/C increases. In the case of 15 QC/C the droplet evaporation time can be estimated with an error of about 2.5%. In the case of 21 QC/C, this error reduces to about 1.5%. This error is comparable with the one for the approximation of Diesel fuel with 40 QC/C. Thus when balancing simplicity with accuracy of the model we can recommend the approximation of Diesel fuel with 21 QC/C if errors less than about 2% can be tolerated. This number of QC/C can be reduced to 15 if errors less than about 3% can be tolerated.

The plots of the surface mass fractions  $Y_{lis}$  of 18 characteristic and/or dominant components, predicted based on the model, taking into account the contributions of all 98 components, for the same conditions as in Figs. 1-8, are shown in Figs. 9-10. These are the components shown in Fig. 9: alkanes  $C_{18}H_{38}$  (1),  $C_{25}H_{52}$  (2) and  $C_{27}H_{56}$  (3), cycloalkanes  $C_{20}H_{40}$  (4),  $C_{24}H_{48}$  (5),  $C_{26}H_{52}$  (6) and  $C_{27}H_{54}$  (7), alkylbenzene  $C_{10}H_{14}$  (8), and tricycloalkane  $C_{19}H_{34}$  (9). These are the components shown in Fig. 10: alkane  $C_{10}H_{22}$  (1), bicycloalkanes  $C_{11}H_{20}$  (2) and  $C_{25}H_{48}$  (3), alkylbenzenes  $C_{23}H_{40}$  (4) and  $C_{24}H_{42}$  (5), indane or tetraline  $C_{13}H_{18}$  (6), naphthalenes  $C_{10}H_8$  (7),  $C_{11}H_{10}$  (8) and  $C_{19}H_{26}$  (9). Note that the scales in Fig. 9 are about an order of magnitude larger compared with Fig. 10.

As can be seen from Figs. 9-10, the mass fractions of the lightest components, such as  $C_{10}H_{14}$ ,  $C_{10}H_{22}$ ,  $C_{11}H_{10}$ ,  $C_{10}H_8$  and  $C_{11}H_{20}$ , monotonically decrease with time, while the mass fraction of one of the heaviest components,  $C_{27}H_{54}$ , monotonically increases with time. The behaviour of the intermediate components appears to be more complex. Initially mass fractions of these components increase with time, but at the end of the evaporation period they start decreasing with time. At the very final stage of droplet evaporation only one, the least volatile component, remains in the liquid phase ( $C_{27}H_{54}$  in the case shown in Fig. 9). This behaviour of the surface mass fractions is consistent with that predicted by the simplified version of the quasi-discrete model described in [7, 8]. Note that strictly speaking the heaviest component in the mixture shown in Fig. 9 is  $C_{27}H_{56}$ . This component, however, turned out to be slightly more volatile than  $C_{27}H_{54}$ . Hence, a rather sharp increase in the

mass fraction of  $C_{27}H_{56}$  close to the end of the evaporation period is followed by an equally sharp decrease at the final stage of evaporation.

Plots similar to those shown in Figs. 9-10, but for 8 characteristic and/or dominant QC/C, as predicted by the model based on the approximation of Diesel fuel by 21 QC/C, are shown in Fig. 11. These are the QC/C presented in this figure: alkane  $C_{17.622}H_{37.244}$  (range  $C_{16}H_{34} - C_{19}H_{40}$ ) (1), alkane  $C_{20.869}H_{43.737}$  (range  $C_{20}H_{42} - C_{23}H_{48}$ ) (2), cycloalkane  $C_{25.644}H_{51.287}$  (range  $C_{25}H_{50} - C_{27}H_{54}$ ) (3), bicycloalkane  $C_{21.243}H_{40.485}$  (range  $C_{20}H_{38} - C_{25}H_{48}$ ) (4), alkylbenzene  $C_{10.207}H_{14.413}$  (range  $C_8H_{10} - C_{13}H_{20}$ ) (5), indane or tetraline  $C_{11.407}H_{14.814}$  (range  $C_{10}H_{12} - C_{13}H_{18}$ ) (6), naphthalene  $C_{11.533}H_{11.067}$  (range  $C_{10}H_8 - C_{15}H_{18}$ ) (7), tricycloalkane  $C_{19}H_{34}$  (8).

As can be seen from Fig. 11, the surface mass fractions of the lightest QC,  $C_{10.207}H_{14.413}$  and  $C_{11.407}H_{14.814}$ , monotonically decrease with time, while the surface mass fraction of the heaviest QC,  $C_{25.644}H_{51.287}$ , monotonically increases with time. The surface mass fractions of other QC/C initially increase and then decrease with time. This behaviour of the mass fractions is similar to that shown in Figs. 9-10 for individual components.

Plots similar to those shown in Fig. 11, but for 11 characteristic and/or dominant QC/C, as predicted by the model based on the approximation of Diesel fuel by 15 QC/C, are shown in Fig. 12. These are the QC/C presented in this figure: alkane  $C_{10.335}H_{22.670}$  (range  $C_8H_{18} - C_{12}H_{26}$ ) (1), alkane  $C_{19.380}H_{40.760}$  (range  $C_{20}H_{42} - C_{23}H_{48}$ ) (2), cycloalkane  $C_{12.562}H_{25.125}$  (range  $C_{10}H_{20} - C_{15}H_{30}$ ) (3), cycloalkane  $C_{18.297}H_{36.595}$  (range  $C_{16}H_{32} - C_{21}H_{42}$ ) (4), cycloalkane  $C_{22.977}H_{45.953}$  (range  $C_{22}H_{44} - C_{27}H_{54}$ ) (5), bicycloalkane  $C_{14.743}H_{27.487}$  (range  $C_{10}H_{18} - C_{25}H_{48}$ ) (6), alkylbenzene  $C_{10.207}H_{14.413}$  (range  $C_8H_{10} - C_{13}H_{20}$ ) (7), indane or tetraline  $C_{12.495}H_{16.990}$  (range  $C_{10}H_{12} - C_{16}H_{24}$ ) (8), indane or tetraline  $C_{18.615}H_{29.229}$  (range  $C_{17}H_{26} - C_{22}H_{36}$ ) (9), naphthalene  $C_{12.392}H_{12.783}$  (range  $C_{10}H_8 - C_{20}H_{28}$ ) (10), tricycloalkane  $C_{19}H_{34}$  (11).

As can be seen from Fig. 12, the surface mass fractions of the lightest QC,  $C_{10.335}H_{22.670}$ ,  $C_{10.207}H_{14.413}$ , and  $C_{12.495}H_{16.990}$ , monotonically decrease with time, while the surface mass fraction of the heaviest QC,  $C_{22.977}H_{45.953}$ , monotonically increases with time. The surface mass fractions of other QC/C initially increase and then decrease with time. This behaviour of the mass fractions is similar to that shown in Figs. 9-10 for individual components and Fig. 11 for QC/C in the model based on the approximation of Diesel fuel by 21 QC/C.

Plots of the mass fractions of alkylbenzene  $C_{10}H_{14}$  and tricycloalkane  $C_{19}H_{34}$  versus normalised distance from the droplet centre ( $R/R_d$ ) at four

instants of time as predicted by the model, taking into account the contributions of all 98 components, are shown in Fig. 13. These components were chosen as typical high-volatile and low-volatile components. As can be seen from this figure, the surface mass fraction of  $C_{10}H_{14}$  decreases, while the surface mass fraction of  $C_{19}H_{34}$  increases with time, in agreement with the results shown in Fig. 9. Also, these changes in the surface mass fractions of  $C_{10}H_{14}$  and  $C_{19}H_{34}$  lead to corresponding changes in mass fractions inside the droplets, leading to the formation of the spatial gradients of the corresponding mass fractions. This clearly demonstrates the limitation of the Infinite Diffusivity (ID) model and the model based on the approximation of Diesel fuel with a single quasi-component, which are widely used for the analysis of Diesel fuel droplet heating and evaporation.

Plots of temperature versus normalised distance from the droplet centre ( $R/R_d$ ) at four instants of time as predicted by the model, taking into account the contributions of all 98 components, are shown in Fig. 14. As can be seen from this figure, temperatures throughout the droplet increase with time, and the temperature gradients can be plainly seen at all instants of time. This clearly shows the limitations of the Infinite Thermal Conductivity (ITC) model, which is widely used for the analysis of droplet heating and evaporation (see [3] and the references therein). The droplet surface temperatures predicted by Fig. 14 are the same as those shown in Fig. 1, as expected.

Plots similar to those shown in Fig. 13, but for the mass fractions of alkylbenzene quasi-component  $C_{10.207}H_{14.413}$  (range  $C_8H_{10} - C_{13}H_{20}$ ) and tricycloalkane  $C_{19}H_{34}$ , predicted by the model based on the approximation of Diesel fuel by 15 QC/C, are presented in Fig. 15. The plots presented in Figs. 13 and 15 show the same trends, although the mass fraction of the quasi-component  $C_{10.207}H_{14.413}$  is clearly larger than that of alkylbenzene  $C_{10}H_{14}$ .

Plots similar to those shown in Fig. 14, but predicted by the model based on the approximation of Diesel fuel by 15 QC/C, are presented in Fig. 16. The trends of the plots shown in Figs. 14 and 16 are rather similar; the droplet surface temperatures inferred from Fig. 16 are the same as those inferred from Fig. 5 as expected.

We have found that the results, similar to those presented in Figs. 15 and 16 for alkylbenzene quasi-component  $C_{10.207}H_{14.413}$ , tricycloalkane  $C_{19}H_{34}$  and temperature, but for the model based on the approximation of Diesel fuel by 21 QC/C, do not show any qualitatively new features compared with those presented in Figs. 15 and 16. These plots are not presented.

The values of droplet surface temperatures  $T_s$  and radii  $R_d$  versus the number of QC/C, predicted by the ETC/ED model for stationary droplets at time instants  $t = 0.02$  ms,  $t = 0.5$  ms,  $t = 1$  ms,  $t = 2$  ms and  $t = 2.5$  are shown in Figs. 17-21. As follows from these figures, the predictions of the models based on the approximation of Diesel fuel by about or more than 21 QC/C are reasonably close to the prediction of the model taking into account the contribution of all 98 components. The values of droplet radii at these time instants show trends similar to those observed for the surface temperature. This is consistent with the results shown in Figs. 7 and 8 for the droplet evaporation time. This confirms the previous conclusion, inferred from Figs. 7 and 8, that a realistic Diesel fuel can be approximated by about 21 QC/C. Moreover, the number of these QC/C can be reduced to 15 if the errors of about 3.7% for the surface temperature and 2.5% for evaporation time can be tolerated. The errors in the estimates of  $T_s$  and  $R_d$  appear to be particularly large in the case when the number of QC/C is less than 15 at  $t = 2$  ms.

Note that in contrast to the case when Diesel fuel is approximated by alkanes only (see [7, 8, 9]), in our case we do not observe a clear reduction in errors with increasing numbers of QC/C. For example, in the case shown in Fig. 19, the value of the surface temperature predicted by the model based on the approximation of Diesel fuel with 58 QC/C is clearly less accurate than the value of this temperature predicted by the model based on the approximation of Diesel fuel with 21 QC/C. This can be attributed to the fact that mole fractions of components in realistic Diesel fuel cannot be approximated by a smooth function of the carbon numbers for various groups shown in Table 2. These errors are generally reasonably small (not more than about 26 K for surface temperatures and not more than about  $1.8 \mu\text{m}$  for droplet radii) when the number of QC/C is approaching or more than 21 for the cases shown in Figs. 17-21 and can be safely ignored in most practical engineering applications. These errors can increase at the very final stage of droplet evaporation, but are generally not important in engineering applications. These errors increase slightly when the number of QC/C approaches 15 (not more than 29.5 K for surface temperatures and not more than about  $2.5 \mu\text{m}$  for droplet radii),

but even in this case they can be tolerated in most engineering applications.

Plots similar to those shown in Fig. 5, but for a droplet moving with velocity 10 m/s, and based on the assumptions that Diesel fuel can be approximated by 98 and 15 QC/C and a single quasi-component, are presented in Fig. 22. In the same figure, the plots calculated using the multi-component model, based on the Infinite Thermal Conductivity/Infinite Diffusivity (ITC/ID) approach, are shown. Comparing Figs. 5 and 22, one can see that moving droplets are heated up faster than stationary droplets and reach higher temperatures. Note that at the final stages of evaporation of droplets for which Diesel fuel is approximated by 98 and 15 QC/C, temperatures can approach or even exceed the critical temperatures of some components. In this case the results become less reliable. As in the cases considered in [7, 8], there are noticeable differences in the predictions based on the ETC/ED and ITC/ID models, especially for temperatures at the initial stage of droplet heating. As mentioned in [2], accurate prediction of these temperatures is particularly important for the prediction of the auto-ignition timing in Diesel engines. This brings into question the reliability of the models for heating and evaporation of Diesel fuel droplets based on the ITC/ID approximations. These models are almost universally used for the analysis of these processes.

Plots similar to those shown in Fig. 22, but for droplet radii are presented in Fig. 23. Comparing Figs. 7 and 23 it can be seen that moving droplets evaporate about 3 times faster than stationary droplets. Similar to the case shown in Figs. 7 and 8, the model based on the approximation of Diesel fuel by a single quasi-component leads to under-prediction of the droplet evaporation time. For the case shown in Fig. 23 this under-prediction was estimated to be about 19% **for the ETC/ED model**. At the same time, the evaporation time is not very sensitive to the choice of ETC/ED or ITC/ID models. In the case when Diesel fuel is approximated by 98 components, the application of the ITC/ID model leads to under-estimation of the evaporation time by only about 3%. This is consistent with the results earlier reported in [41]. As in the case shown in Figs. 7 and 8, the approximation of Diesel fuel with 15 QC/C leads to under-estimation of the evaporation time by about 2.5% (see Fig. 23). This confirms our earlier conclusion, based on the analysis of stationary droplets, that 15 QC/C can reasonably accurately approximate realistic Diesel fuel for the analysis of heating and evaporation of droplets.

**To illustrate the computational efficiency of the new model, a diagram of CPU time, required for calculation of stationary droplet**

heating and evaporation with parameters specified earlier in the paper, versus the number of QC/C is shown in Fig. 24. Intel Xeon (core duo) E8400, 3 GHz and 3 GB RAM, was used. The time step was set as  $1 \mu\text{s}$ . As one can see from this figure, the model based on 15 QC/C requires almost 6 times less CPU time compared with the model taking into account the contribution of all 98 components. This clearly illustrates the efficiency of the new model.

## 6. Conclusions

A new multi-dimensional quasi-discrete model is suggested and tested for the analysis of heating and evaporation of Diesel fuel droplets. As in the original quasi-discrete model suggested earlier, the components of Diesel fuel with close thermodynamic and transport properties are grouped together to form quasi-components. In contrast to actual components, these quasi-components are allowed to have non-integer values of carbon atoms. This, however, does not prohibit their treatment as actual components, and the modelling of the diffusion of these quasi-components inside the droplets. In contrast to the original quasi-discrete model, the new model takes into account the contribution of various groups of hydrocarbons in Diesel fuels; quasi-components are formed within individual groups. Hence, the term ‘multi-dimensional’ is used to describe the new model. Also, in contrast to the original quasi-discrete model, the contribution of individual components is not approximated by the distribution function of carbon numbers. The formation of quasi-components is based on directly taking into account the contributions of individual components. Groups contributing small molar fractions to the composition of Diesel fuel (less than about 1.5%) are replaced by individual components.

The application of the new model is illustrated for one specific type of Diesel fuel, containing the following molar fractions of the groups of components: 13.6518% of n-alkanes, 26.4039% of iso-alkanes, 14.8795% of cycloalkanes, 7.6154% of bicycloalkanes, 1.5647% of tricycloalkanes, 16.1719% of alkylbenzenes, 9.1537% of indanes & tetralines, 8.6773% of naphthalenes, 1.2240% of diaromatics, and 0.6577% of phenanthrenes. Since the contributions of tricycloalkanes, diaromatics, and phenanthrenes are less than about 1.5%, they are replaced with individual components  $\text{C}_{19}\text{H}_{34}$  (tricycloalkane),  $\text{C}_{13}\text{H}_{12}$  (diaromatic), and  $\text{C}_{14}\text{H}_{10}$  (phenanthrene). The difference between

the thermodynamic and transport properties of n-alkanes and iso-alkanes is ignored and they are treated as alkanes. This led us to a simplified presentation of Diesel fuel with the following six groups: alkanes (molar fraction 40.0556%), cycloalkanes (molar fraction 14.8795%), bicycloalkanes (molar fraction 7.6154%), alkylbenzenes (molar fraction 16.1719%) indanes & tetralines (molar fraction 9.1537%), and naphthalenes (molar fraction 8.6773%), and 3 components,  $C_{19}H_{34}$  (molar fraction 1.5647%),  $C_{13}H_{12}$  (molar fraction 1.2240%), and  $C_{14}H_{10}$  (molar fraction 0.6577%).

The total number of components in the simplified approximation of Diesel fuel is equal to 98. Thermodynamic and transport properties of all these components are presented. Mixing rules are used for calculation of properties of the mixtures of the components, except for the thermal conductivity. The latter is based on the approximation of the results of experimental studies of typical Diesel fuels. Several further approximations of the above simplified approximation of Diesel fuel were considered. These include the approximation of Diesel fuel by a single quasi-component (mass fractions of all components inside the droplet do not change with time), the approximation of Diesel fuel by only alkanes, ignoring the contributions of all other components, the approximation of each of the above-mentioned six groups by single quasi-components with average values of carbon numbers (9 quasi-components and components altogether), and the approximation of each of the above-mentioned six groups by one or more quasi-components, leading to between 12 and 98 quasi-components and components. All these approximations were used for the analysis of heating and evaporation of a typical Diesel fuel droplet in Diesel engine-like conditions. It is pointed out that approximations of Diesel fuel with only alkanes leads to less accurate modelling results compared with the approximation of Diesel fuel by a single quasi-component. This questions the applicability of the previously developed quasi-discrete model based on the former approximation (see [7, 8, 9]). Also, it is pointed out that the approximations of Diesel fuel by less than about 15 quasi-components/components lead to unacceptably large errors (relative to the prediction of the model, taking into account the contributions of all 98 components) in predicting droplet temperatures and evaporation times and are not recommended for practical engineering applications. The approximation of Diesel fuel by 15 quasi-components/components, leads to errors in estimated temperature and evaporation times not exceeding about 1.6% and 2.5% respectively, which is acceptable for most engineering applications. **This model requires about 6 times less CPU time compared with**



the model taking into account the contributions of all 98 components.

## Acknowledgements

The authors are grateful to Paul Harris for useful discussions and INTERREG IVa (Project E3C3, Reference 4274) and EPSRC (UK) (Project EP/J006793/1) for their financial support of this project.

## Appendix 1

### Transport and thermodynamic properties of alkanes

All values of parameters in this and other appendices are given in SI units. All approximations for transport and thermodynamic properties, given in this and other appendices, are strictly only valid for the limited range of temperatures and carbon numbers stated. Two methods of extrapolating these values beyond this range are commonly used. Firstly, it can be assumed that the values at  $T < T_{\min}$  and  $n < n_{\min}$  are the same as the values at  $T = T_{\min}$  and  $n = n_{\min}$ , and the values at  $T > T_{\max}$  and  $n > n_{\max}$  are the same as the values at  $T = T_{\max}$  and  $n = n_{\max}$ . Secondly, the approximations can be used beyond the range of temperatures and carbon numbers for which they were originally obtained. In both cases, these extrapolations can lead to errors which are difficult to control, and their choice depends on the physical nature of the properties and the availability of experimental data beyond the range of temperatures for which they were obtained (see [46, 47]). The methods of extrapolation will be specified for specific properties of particular components. The values of properties at  $T > T_{\text{cr}}$  are assumed to be the same as those at  $T = T_{\text{cr}}$  (this approximation allows us to avoid rigorous analysis of the case when the droplet temperatures exceed the critical temperatures of the lightest components; the errors imposed by this approximation are expected to be small).

#### *Molecular structure, boiling and critical temperatures*

The chemical formula of alkanes is  $\text{C}_n\text{H}_{2n+2}$  ( $8 \leq n \leq 27$ ) and they incorporate n-alkanes and iso-alkanes, the chemical structures of which for

$n = 20$  and  $n = 16$  are shown in Fig. A1 (n-icosane and 3,6,9,10-methyldodecane). The difference in transport and thermodynamic properties of n-alkanes and iso-alkanes is ignored in our analysis. For example, the difference between the boiling temperatures of alkanes and iso-alkanes for  $n = 8 - 20$  does not exceed 4.5 K [46], which is less than about 1% of the value of this temperature.

Using data provided in [46], the dependence of critical and boiling temperatures on  $n$  was approximated by the following equations in the range  $5 \leq n \leq 25$  [7]:

$$T_{\text{cr(a)}}(n) = a_{ca} + b_{ca}n + c_{ca}n^2 + d_{ca}n^3, \quad (47)$$

$$T_{\text{b(a)}}(n) = a_{ba} + b_{ba}n + c_{ba}n^2 + d_{ba}n^3, \quad (48)$$

where the coefficients are presented in Table A1, (a) stands for alkanes.

|             |                |               |               |              |
|-------------|----------------|---------------|---------------|--------------|
| coefficient | $a_{ca}$       | $b_{ca}$      | $c_{ca}$      | $d_{ca}$     |
| value       | 242.3059898052 | 55.9186659144 | -2.1883720897 | 0.0353374481 |
| coefficient | $a_{ba}$       | $b_{ba}$      | $c_{ba}$      | $d_{ba}$     |
| value       | 118.3723701848 | 44.9138126355 | -1.4047483216 | 0.0201382787 |

Table A1

The range of applicability of these coefficients was extended to  $26 \leq n \leq 27$ , remembering that the molar fractions of alkanes with these  $n$  is less than 0.05%. The validity of this was checked by finding new correlations valid in the range  $8 \leq n \leq 27$ . The predictions of these new correlations turned out to be almost indistinguishable from those predicted by Correlations (47) and (48).

#### *Liquid density*

The temperature dependence of the density of liquid alkanes for  $8 \leq n \leq 27$  was approximated, using data reported in [46], as:

$$\rho_l(T) = 1000A_\rho B_\rho^{-\left(1 - \frac{T}{T_{\text{cr}}}\right)^{C_\rho}}, \quad (49)$$

where  $A_\rho$ ,  $B_\rho$  and  $C_\rho$  for individual values of  $n$  were approximated by the following expressions:

$$\begin{cases} A_\rho = 0.00006196104 n + 0.234362 \\ B_\rho = 0.00004715697 n^2 - 0.00237693 n + 0.2768741 \\ C_\rho = 0.000597039 n + 0.2816916 \end{cases} \quad (50)$$

$T_{\text{cr}} = T_{\text{cr(a)}}$  are critical temperatures (see Equation (47)).

Expression (49) is identical to the one used in [8], but with different values of the coefficients (these were obtained for  $5 \leq n \leq 25$ ). The maximal difference between the predictions of Expression (49) and the corresponding equation given in [8] is less than 0.5%.

Approximation (49) is assumed to be valid up to the critical temperatures of all components ( $T_{\text{cr}}$ ). Note that for some components  $T_{\text{cr}}$  in Expression (49) needs to be replaced with a temperature which is slightly less than the critical temperature. This effect is not taken into account in our analysis.

#### *Liquid viscosity*

Following [50], the temperature dependence of the dynamic viscosity of liquid alkanes for  $4 \leq n \leq 44$  was approximated as:

$$\mu_l(T) = 10^{-3} \left[ 10^{[100(0.01 T)^{b(n)}]} - 0.8 \right], \quad (51)$$

where

$$b(n) = -5.745 + 0.616 \ln(n) - 40.468 n^{-1.5}. \quad (52)$$

The temperature range of the applicability of Approximations (51) and (52) was not explicitly specified in [50], but the author of [8] demonstrated good agreement between the predictions of these approximations and experimental data in the range of temperatures from 10°C to 100°C. Also, it was demonstrated in [8] that the agreement between the values of liquid viscosity predicted by Approximations (51) and (52) and the results presented on the NIST website [51] is almost ideal. Note that the values of dynamic viscosity affect droplet heating and evaporation only via the corrections to the values of thermal conductivity and diffusivity in the Effective Thermal Conductivity and Effective Diffusivity (ETC/ED) models. In most practically important cases, the influence of viscosity on the final results is expected to be very weak. In our analysis it was assumed that Approximations (51) and (52) are valid up to the critical temperatures; no low temperature limits for their validity were imposed.

### *Liquid heat capacity*

Following [52], the temperature dependence of the heat capacity of liquid alkanes for  $2 \leq n \leq 26$  was approximated as:

$$c_l(T) = 1000 \left[ \frac{43.9 + 13.99(n-1) + 0.0543(n-1)T}{M(n)} \right], \quad (53)$$

where  $M(n) = 14n + 2$  is the molar mass of alkanes.

The temperature range of applicability of Approximation (53) was not clearly identified in [52] for all  $n$ , except to say that this approximation is not valid at temperatures close to the temperature of fusion. It was shown in [8] that the agreement between the values of the liquid heat capacity predicted by Approximation (53) and the experimental results for  $T = 300$  K [51] is almost ideal. In our analysis it is assumed that Approximation (53) is valid up to the immediate vicinity of the critical temperatures; no low temperature limit for its validity was imposed remembering that our analysis is focused on liquids. Bearing in mind that molar fractions of alkanes with  $n = 27$  are about 0.3% we assume that Equation (53) is valid in the whole range  $8 \leq n \leq 27$ .

### *Liquid thermal conductivity*

Although we were able to show that it is more accurate and reliable to base the estimate of the thermal conductivity of liquid Diesel fuel on experimental data rather than on correlations using the thermal conductivities of individual components, we believe that it would be appropriate to present the latter conductivities for all components. This approach opens the way for using more efficient correlations for the estimate of the thermal conductivity of the mixtures, should these correlations be suggested in the future.

Following [53], the temperature dependence of thermal conductivity of liquid alkanes for  $5 \leq n \leq 20$  can be approximated as:

$$k_l(T) = 10 \left[ A_k + B_k \left( 1 - \frac{T}{T_{cr}} \right)^{2/7} \right], \quad (54)$$

where  $T_{cr}$  are critical temperatures as in Approximation (49), the numerical values of  $A_k$  and  $B_k$  for individual values of  $n$  are given in [53]. These values were approximated by the following expressions [8]:

$$\begin{cases} A_k = 0.002911 n^2 - 0.071339 n - 1.319595 \\ B_k = -0.002498 n^2 + 0.058720 n + 0.710698. \end{cases} \quad (55)$$

Although Approximations (54) and (55) were derived for  $5 \leq n \leq 20$ , they can be used in the whole range  $8 \leq n \leq 27$ . Possible errors imposed by these approximations in the range  $21 \leq n \leq 27$  are expected to have a very small effect on the final results as the molar fractions of alkanes in this range of  $n$  are less than 1.5%. The range of applicability of Approximation (54) depends on the values of  $n$ . For  $n = 8$  this range was determined as 216-540 K; for  $n = 9$  – 243-588 K; for  $n = 10$  – 248-607 K; for  $n = 11$  – 230-625 K; for  $n = 12$  – 264-625 K; for  $n = 13$  – 268-642 K; for  $n = 14$  – 279-658 K; for  $n = 15$  – 283-671 K; for  $n = 16$  – 291-685 K; for  $n = 17$  – 327-732 K; for  $n = 18$  – 301-708 K; for  $n = 19$  – 305-718 K; and for  $n = 20$  – 310-729 K [53]. It is assumed that the temperature range for  $n > 20$  is the same as for  $n = 20$ . As shown in [8], the values of  $k_l$  predicted for  $T = 300$  K and  $T = 450$  K agree well with the data reported in [51].

The upper limits of the temperature ranges, shown above, are close to critical temperatures. If they are greater than the corresponding critical temperatures, then these limits can be imposed as the critical temperatures. The values of thermal conductivity at temperatures below the minimal temperatures can be assumed to be equal to those at the minimal temperatures.

#### *Saturated vapour pressure and enthalpy of evaporation*

The following approximation (Antoine equation) for the dependence of the saturation vapour pressure (in Pa) on  $n$  was used in our analysis [54]:

$$\log_{10} [0.001 \times p^{\text{sat}}(n)] = A(n) - \frac{B(n)}{T + C(n)}, \quad (56)$$

where

$$A(n) = 0.022n + 5.8474, \quad B(n) = 52.807n + 981.92,$$

$$C(n) = -5.0431n - 31.205,$$

$T$  is in K. The above approximations for  $A(n)$ ,  $B(n)$ ,  $C(n)$  were derived for  $8 < n < 27$ . They are valid in the temperature range 298-423 K for  $n = 8$ ; 315-449 K for  $n = 9$ ; 338-468 K for  $n = 10$ ; 356-499 K for  $n = 11$ ; 367-520 K for  $n = 12$ ; 384-540 K for  $n = 13$ ; 399-559 K for  $n = 14$ ; 413-577 K for  $n = 15$ ; 426-594 K for  $n = 16$ ; 438-610 K for  $n = 17$ ; 449-625 K for  $n = 18$ ; 462-639 K for  $n = 19$ ; 475/652 K for  $n = 20$ ; 393-630 K for  $n = 21$ ; 402-642 K for  $n = 22$ ; 411-653 K for  $n = 23$ ; 419-664 K for  $n = 24$ ; 427-675 K for  $n = 25$ ; 434-685 K for  $n = 26$ ; and 442-695 K for  $n = 27$ .

In our analysis, Approximation (56) was used up to the critical temperature. No low temperature limit for the applicability of this approximation was imposed. At low temperatures (close to room temperature), the values of pressure are expected to be small and realistic errors in its estimate are not expected to produce noticeable effects on the overall picture of droplet heating and evaporation. By the time the droplet surface temperatures reach values higher than the above-mentioned temperature ranges, their radii have become very small in most cases. In this case the errors in determination of the vapour pressure are also expected to produce a small effect on the overall picture of droplet heating and evaporation.

This approximation is consistent with one used earlier in [7, 8]; the approximation used in these papers was valid for  $n < 17$ .

Following [46] the values of specific enthalpy of evaporation for alkanes were approximated as

$$L = \frac{A(1 - T_r)^B}{M(n)} \times 10^6, \quad (57)$$

where the values of  $A$  for specific values of  $n$  provided by [46] were approximated as

$$A \equiv A_L = 0.0066 n^2 + 4.697 n + 20.258$$

for  $n \leq 20$  and

$$A \equiv A_H = -0.1143 n^2 + 7.853 n - 8.8344$$

for  $n > 20$ . The original values of  $B$  provided by [46] were used:  $B = 0.439$  for  $n = 8$ ,  $B = 0.377$  for  $n = 9$ ,  $B = 0.451$  for  $n = 10$ ,  $B = 0.413$  for  $n = 11$ ,  $B = 0.407$  for  $n = 12$ ,  $B = 0.416$  for  $n = 13$ ,  $B = 0.418$  for  $n = 14$ ,  $B = 0.419$  for  $n = 15$ ,  $B = 0.422$  for  $n = 16$ ,  $B = 0.433$  for  $n = 17$ ,  $B = 0.451$  for  $n = 18$ ,  $B = 0.448$  for  $n = 19$ ,  $B = 0.409$  for  $n = 20$  and  $B = 0.380$  for  $n \geq 21$ .

The accuracy of the above-mentioned approximations of  $A$  by  $A_L$  and  $A_H$  is illustrated in Fig. A2. As can be seen from this figure, the values provided by [46] are reasonably close to the values of  $A_L$  or  $A_H$ , which justifies the application of the latter in our analysis. Similar closeness between approximations and the values of  $A$  and  $B$  provided by [46] was observed for other hydrocarbons (the plots are not presented). In all cases, Approximation (57) is assumed to be valid up to the critical temperature in all cases [46]. No low temperature limit for the validity of this approximation was imposed.

## Appendix 2

### Transport and thermodynamic properties of cycloalkanes

#### *Molecular structure, boiling and critical temperatures*

The chemical formula of cycloalkanes is  $C_nH_{2n}$  ( $10 \leq n \leq 27$ ) and their typical chemical structure is shown in Fig. A1 (1-propyl-3-hexyl-cycloheptan)

Using data provided in [46], the dependence of critical and boiling temperatures on  $n$  was approximated by the following equations:

$$T_{cr(c)}(n) = a_{cc} + b_{cc}n + c_{cc}n^2 + d_{cc}n^3, \quad (58)$$

$$T_{b(c)}(n) = a_{bc} + b_{bc}n + c_{bc}n^2, \quad (59)$$

where the coefficients are presented in Table A2, (c) stands for cycloalkane.

| coefficient       | $a_{cc}$ | $b_{cc}$ | $c_{cc}$ | $d_{cc}$ |
|-------------------|----------|----------|----------|----------|
| value $n \leq 10$ | 667      | 0        | 0        | 0        |
| value $n > 10$    | 425.28   | 31.442   | -0.9002  | 0.0125   |
| coefficient       | $a_{bc}$ | $b_{bc}$ | $c_{bc}$ |          |
| value             | 176.51   | 32.312   | -0.4776  |          |

Table A2

Expressions similar to those given in (58) and (59) could be obtained using the analysis presented in [55]-[57].

#### *Liquid density*

The temperature dependence of the density of liquid cycloalkanes for  $5 \leq n \leq 25$  was approximated by Expression (49) with  $A_\rho$ ,  $B_\rho$  and  $C_\rho$  approximated as:

$$\begin{cases} A_\rho = 0.00003 n^2 - 0.0016 n + 0.278 \\ B_\rho = 0.00003 n^2 - 0.00237693 n + 0.2823 \\ C_\rho = 0.28571 \end{cases} \quad (60)$$

$T_{cr} = T_{cr(c)}$  are critical temperatures (see Eq. (58)).

For  $11 \leq n \leq 25$  the values of densities predicted by Eq. (49) with the coefficients defined by Eqs. (60) almost exactly coincide with those given in

[46]. For  $n \geq 26$  the deviation between these results could be up to 3%. This deviation is not important since the molar fractions of cycloalkanes for these  $n$  are expected to be less than 0.03% (see Table 2).

As in the case of alkanes, Approximation (49) is valid up to the immediate vicinity of the critical temperatures of all components ( $T_{\text{cr}}$ ).

#### *Liquid viscosity*

Following [58], the temperature dependence of the dynamic viscosity of liquid cycloalkanes for  $10 \leq n \leq 94$  was approximated by Approximation (51) with  $b(n)$  defined as:

$$b(n) = -9.001 + 2.350 \log_{10}(14n).$$

As in the case of alkanes, in our analysis it is assumed that Approximation (51) with  $b(n)$ , defined by the above expression, is valid up to the critical temperatures; no low temperature limits for its validity were imposed.

#### *Liquid heat capacity*

Following [59, 60], the temperature dependence of the heat capacity of liquid cycloalkanes for  $10 \leq n \leq 27$  was approximated as:

$$c_l(T) = \frac{R_u}{M(n)} \left[ a_c + b_c \left( \frac{T}{100} \right) + c_c \left( \frac{T}{100} \right)^2 \right], \quad (61)$$

where  $R_u = 8315 \text{ J/kmole}$  is the universal gas constant,  $M(n)$  is the molar mass in  $\text{kg/kmole}$ ,

$$a_c = 33.75209 + 2.7345 (n - 10),$$

$$b_c = -5.21095283 + 0.122732 (n - 10) \text{ K}^{-1},$$

$$c_c = 2.78089 - 0.123482 (n - 10) \text{ K}^{-2}.$$

The temperature range of applicability of Equation (61) is between melting and boiling temperatures.



### *Liquid thermal conductivity*

The temperature dependence of thermal conductivities of liquid cycloalkanes for  $10 \leq n \leq 27$  can be estimated from the following expression (derived from the combination of the boiling-point method and Riedel formula) [46]:

$$k_l(T) = \frac{2.64 \times 10^{-3}}{\sqrt{M_n}} \times \frac{3 + 20(1 - T_r)^{2/3}}{3 + 20(1 - T_{br})^{2/3}}, \quad (62)$$

where  $M_n = 14n$  is the molar mass,  $T_r = T/T_{cr}$ ,  $T_{br} = T_b/T_{cr}$ . The approximations of  $T_{cr}$  and  $T_b$  are given by Expressions (58) and (59).

Expression (62) is valid up to the boiling temperatures.

### *Saturated vapour pressure and enthalpy of evaporation*

Following [54], the saturated vapour pressure is approximated by the Antoine equation (56) with

$$A(n) = 0.0201n + 5.8268, \quad B(n) = 47.34n + 1115.2, \quad C(n) = -5.4145n - 23.03.$$

Equation (56) with the above values of coefficients for cycloalkanes is valid in the range 340-484 K for  $n = 10$ ; 359-508 K for  $n = 11$ ; 376-530 K for  $n = 12$ ; 393-551 K for  $n = 13$ ; 367-399 K for  $n = 14$ ; 423-589 K for  $n = 15$ ; 429-606 K for  $n = 16$ ; 450-622 K for  $n = 17$ ; 458-637 K for  $n = 18$ ; 474-651 K for  $n = 19$ ; 486-665 K for  $n = 20$ ; 496-677 K for  $n = 21$ ; 507-689 K for  $n = 22$ ; 414-664 K for  $n = 23$ ; 422-675 K for  $n = 24$ ; and 430-686 K for  $n = 25$ .

As in the case of alkanes, the above approximations for  $A(n)$ ,  $B(n)$ ,  $C(n)$  were used outside the range of temperatures for which they were obtained, up to the critical temperatures and below the above-mentioned minimal temperatures.

As in the case of alkanes, following [46] the values of  $L$  for cycloalkanes were estimated by Expression (57). The values of  $A$  for individual  $n$  provided by [46] were approximated as

$$A = -0.0085 n^3 + 0.4134 n^2 - 2.556 n + 56.345, \quad B = 0.38$$

for  $n \neq 16$ . As in [46],  $A = 101.3122$  and  $B = 0.49$  for  $n = 16$ .

As in the case of alkanes, Expression (57) for cycloalkanes is assumed to be valid up to the critical temperatures.

## Appendix 3

### Transport and thermodynamic properties of bicycloalkanes

#### *Molecular structure, boiling and critical temperatures*

The chemical formula of bicycloalkanes is  $C_nH_{2n-2}$  ( $10 \leq n \leq 25$ ) and their typical chemical structures are shown in Fig. A1 (diethylbicycloheptan and ethylcycloheptan-cyclononane).

Using data provided in [46] for  $10 \leq n \leq 25$ , the dependence of critical and boiling temperatures on  $n$  was approximated by the following equations:

$$T_{\text{cr(b)}}(n) = 134.85 \ln(n) + 395.85, \quad (63)$$

for  $13 \leq n \leq 24$ ,

$$T_{\text{b(b)}}(n) = 217.41 \ln(n) - 32.662, \quad (64)$$

for  $10 \leq n \leq 25$ .

$T_{\text{cr(b)}}(10) = 703.60$  K,  $T_{\text{cr(b)}}(11) = 752.51$  K,  $T_{\text{cr(b)}}(12) = 762.49$  K. (b) stands for bicycloalkanes.

Following [46], in the correlations shown later in this appendix  $T_{\text{cr(b)}}(10)$  is replaced with the parameter  $T_{\text{c(b)}}(10) = 702.25$  K. Since  $T_{\text{cr(b)}}(25)$  for bicycloalkanes is not available for us, we used  $T_{\text{cr(b)}}(25) = 833.34$  K for 1,1 dicyclohexyltridecane instead of  $T_{\text{cr(b)}}(25)$  for bicycloalkanes in these correlations.

#### *Liquid density*

Using data supplied in [67], the temperature dependence of the density of liquid bicycloalkanes for  $10 \leq n \leq 25$  was approximated by Expression (49) with  $C_\rho = 0.28571$  and  $A_\rho$  and  $B_\rho$  approximated by the following expressions.

For  $11 \leq n \leq 12$ :

$$\begin{cases} A_\rho = -0.0034 n + 0.3231, \\ B_\rho = -0.0031 n + 0.3022. \end{cases}$$

For  $13 \leq n \leq 18$ :

$$\begin{cases} A_\rho = 0.0002 n^2 - 0.0072 n + 0.3529, \\ B_\rho = -0.0003 n^2 - 0.0278 n + 0.4966. \end{cases}$$

For  $19 \leq n \leq 25$ :

$$\begin{cases} A_\rho = 5 \times 10^{-5} n^2 - 0.0032 n + 0.3168, \\ B_\rho = 0.0004 n^2 - 0.0179 n + 0.4965. \end{cases}$$

Remembering that the molar fraction of bicycloalkanes for  $n = 10$  is less than 0.7% we assumed that  $\rho_{l(b)}(T)(n = 10) = \rho_{l(b)}(T)(n = 11)$ .

As in the case of previously considered components, Approximation (49) for bicycloalkanes is assumed to be valid up to the immediate vicinity of the critical temperature, and no low temperature limit was imposed.

#### *Liquid viscosity*

Following [58], the temperature dependence of the dynamic viscosity of liquid bicycloalkanes for  $10 \leq n \leq 94$  is approximated by Expression (51) with  $b(n)$  defined as:

$$b(n) = -9.513 + 2.248 \log_{10}(14n - 2).$$

As in the case of previously considered components, in our analysis it is assumed that Approximation (51) with  $b(n)$ , defined by the above expression, is valid up to the critical temperatures; no low temperature limits for its validity were imposed.

#### *Liquid heat capacity*

Following [59, 60], the temperature dependence of the heat capacity of liquid bicycloalkanes for  $10 \leq n \leq 25$  was approximated by Expression (61) with the coefficients defined as:

$$\begin{aligned} a_c &= 19.2782 + 2.7345 (n - 11), \\ b_c &= 4.722955 + 0.122732 (n - 11) \text{ K}^{-1}, \\ c_c &= 0.08912 + 0.123482 (n - 11) \text{ K}^{-2}. \end{aligned}$$

As in the case of previously considered components, the temperature range of applicability of these approximations is between melting and boiling temperatures.

#### *Liquid thermal conductivity*

Following [47], the temperature dependence of thermal conductivity of liquid bicycloalkanes for  $10 \leq n \leq 25$  was estimated by Expression (62) with  $M_n = 14n - 2$ . As in the case of previously considered components, Expression (62) for bicycloalkanes is valid up to the boiling temperatures.

*Saturated vapour pressure and enthalpy of evaporation*

Following [46, 47], the saturated vapour pressure for bicycloalkanes for  $10 \leq n \leq 25$  is approximated by the following formula:

$$\ln(p_{vb}/p_{cb}) = f^0 + \omega_b f^1, \quad (65)$$

where

$$f^0 = 5.92714 - \frac{6.09648}{T_r} - 1.28862 \ln T_r + 0.169347 T_r^6,$$

$$f^1 = 15.2518 - \frac{15.6875}{T_r} - 13.4721 \ln T_r + 0.43577 T_r^6,$$

$T_r = T/T_{\text{cr(b)}}$ ,  $T_{\text{cr(b)}}$  is the critical temperature estimated from (63),  $p_{cb}$  is the critical pressure of bicycloalkanes estimated as

$$p_{cb} = 10^5 (0.0711 n^2 - 3.8116 n + 60.998) \text{ Pa},$$

$$\omega \equiv \omega_b = -0.001 n^2 + 0.0679 n - 0.3039.$$

As in the case of previously considered components, Expression (65) is assumed to be valid up to the critical temperatures.

As in the case of alkanes and cycloalkanes, the values of  $L$  for bicycloalkanes could be estimated by Expression (57) with the values of  $A$  provided in [46] approximated as

$$A = -0.1405 n^2 + 8.1341 n - 3.2083,$$

and  $B = 0.434$  for  $n = 10$  and  $B = 0.38$  otherwise.

In contrast to previously considered hydrocarbons, however, we have found that a more accurate approximation for  $L$  for bicycloalkanes is given by the following expression (cf. [47, 33]):

$$L = \begin{cases} -\frac{R_u T_{\text{cr(b)}}}{M(n)} \Phi_1(T_r, \omega_b) & \text{when } T_r < 0.6 \\ \frac{R_u}{M(n)} T_{\text{cr(b)}} \Phi_2(T_r, \omega_b) & \text{when } T_r \geq 0.6, \end{cases} \quad (66)$$

where the units of  $R_u$  and  $M(n)$  are the same as in Equations (61),

$$\Phi_1 = [(-6.09648 - 15.6875\omega_b) + (1.28862 + 13.4721\omega_b) T_r - 6(0.169347 + 0.43577\omega_b) T_r^7],$$

$$\Phi_2 = 7.08 (1 - T_r)^{0.354} + 10.95 \omega_b (1 - T_r)^{0.456},$$

$T_r = T/T_{\text{cr(b)}}$ ,  $\omega_b$  was defined earlier.

Approximation (66) was compared with the data provided in [46] for  $\text{C}_{10}\text{H}_{18}$ ,  $\text{C}_{11}\text{H}_{20}$ ,  $\text{C}_{12}\text{H}_{22}$  and  $\text{C}_{25}\text{H}_{48}$ . The maximal deviation between the results predicted by (66) and data provided by [46] did not exceed about 5%.

Equation (66) was used in our analysis. As in the case of alkanes and cycloalkanes, this expression is valid up to the critical temperatures.

## Appendix 4

### Transport and thermodynamic properties of alkylbenzenes

#### *Molecular structure, boiling and critical temperatures*

The chemical formula of alkylbenzenes is  $\text{C}_n\text{H}_{2n-6}$  ( $8 \leq n \leq 24$ ) and their chemical structures are shown in Fig. A1 (1,4-dipropylbenzene and 1,4-dipentylbenzene).

Using data provided in [46, 55, 56, 57, 61, 62, 63, 64, 65, 53], the dependence of critical and boiling temperatures on  $n$  was approximated by the following equations:

$$T_{\text{cr(ab)}}(n) = a_{cab} + b_{cab}n + c_{cab}n^2, \quad (67)$$

$$T_{\text{b(ab)}}(n) = a_{bab} + b_{bab}n + c_{bab}n^2, \quad (68)$$

where the coefficients are presented in Table A3, (ab) stands for alkylbenzenes.

|             |           |           |           |
|-------------|-----------|-----------|-----------|
| coefficient | $a_{cab}$ | $b_{cab}$ | $c_{cab}$ |
| value       | 427.89    | 27.408    | -0.4388   |
| coefficient | $a_{bab}$ | $b_{bab}$ | $c_{bab}$ |
| value       | 171.6     | 33.426    | -0.5252   |

Table A3

### *Liquid density*

Using data supplied in [46], the temperature dependence of the density of liquid alkylbenzenes for  $5 \leq n \leq 25$  was approximated as:

$$\rho_{l(ab)}(T) = A_{\rho ab} + B_{\rho ab}T + C_{\rho ab}T^2 + D_{\rho ab}T^3, \quad (69)$$

where  $A_{\rho ab}$ ,  $B_{\rho ab}$ ,  $C_{\rho ab}$  and  $D_{\rho ab}$  for individual values of  $n$  were approximated by the following expressions.

For  $n = 8$  and  $n = 9$ :

$$\begin{cases} A_{\rho ab} = -32.04 \times n + 1422.6 \\ B_{\rho ab} = 0.1831 \times n - 2.824 \\ C_{\rho ab} = -0.0005 \times n + 0.0056 \\ D_{\rho ab} = 6 \times 10^{-7} \times n - 7 \times 10^{-6}; \end{cases} \quad (70)$$

for  $n = 11 - 20$ :

$$\begin{cases} A_{\rho ab} = -0.0477 \times n^2 - 0.4141 \times n + 1082.6 \\ B_{\rho ab} = 0.0004 \times n^2 - 0.0062 \times n - 0.7017 \\ C_{\rho ab} = D_{\rho ab} = 0. \end{cases} \quad (71)$$

It is assumed that  $\rho(n = 10) = 0.5(\rho(n = 9) + \rho(n = 11))$  and  $\rho(n > 20) = \rho(n = 20)$ . The latter assumption is justified by the fact that molar fraction of components with  $n > 20$  is about or less than 0.2%.

Approximations (69)–(71) are assumed to be valid up to the immediate vicinity of the critical temperatures. Their predictions agree with experimental data provided in [66].

### *Liquid viscosity*

Following [58], the temperature dependence of the dynamic viscosity of liquid alkylbenzenes is approximated by Expression (51) with  $b(n)$  defined as:

$$b(n) = -9.692 + 2.261 \log_{10}(14n - 6).$$

As in the case of alkanes, cycloalkanes and bicycloalkanes, in our analysis it is assumed that Approximation (51) with  $b(n)$ , defined by the above expression, is valid up to the critical temperatures; no low temperature limits for its validity were imposed.

### *Liquid heat capacity*

Following [59, 60], the temperature dependence of the heat capacity of liquid alkylbenzenes for  $8 \leq n \leq 24$  was approximated by Expression (61) with the coefficients defined as:

$$\begin{aligned}a_c &= 15.1109 + 2.7345 (n - 7), \\b_c &= 0.68109 + 0.122732 (n - 7) \text{ K}^{-1}, \\c_c &= 1.96346 - 0.123482 (n - 7) \text{ K}^{-2}.\end{aligned}$$

The temperature range of applicability of these approximations is between melting and boiling temperatures.

### *Liquid thermal conductivity*

Following [46, 47], the temperature dependence of thermal conductivity of liquid alkylbenzenes for  $8 \leq n \leq 24$  can be estimated by Expression (62) with  $M_n = 14n - 6$ . As in the case of cycloalkanes and bicycloalkanes, Expression (62) for alkylbenzenes is valid up to the boiling temperatures.

### *Saturated vapour pressure and enthalpy of evaporation*

Following [54], the saturated vapour pressure for alkylbenzenes is approximated by the Antoine equation (56) with

$$\begin{aligned}A(n) &= 0.0007 n^2 - 0.0064 n + 6.0715, \quad B(n) = 51.811 n + 1049.1, \\C(n) &= 0.1215 n^2 - 9.6892n + 11.161.\end{aligned}$$

The temperature ranges of applicability of Equation (56) for alkylbenzenes are the following: 306-420 K for  $n = 8$ ; 323-455 K for  $n = 9$ ; 343-486 K for  $n = 10$ ; 361-510 K for  $n = 11$ ; 378-531 K for  $n = 12$ ; 394-553 K for  $n = 13$ ; 406-571 K for  $n = 14$ ; 421-590 K for  $n = 15$ ; 438-606 K for  $n = 16$ ; 450-622 K for  $n = 17$ ; 458-636 K for  $n = 18$ ; 473-651 K for  $n = 19$ ; 485-665 K for  $n = 20$ ; 495-677 K for  $n = 21$ ; 505-688 K for  $n = 22$ ; 414-664 K for  $n = 23$ ; and 423-675 K for  $n = 24$ .

As in the case of alkanes and cycloalkanes, the above approximations for  $A(n)$ ,  $B(n)$ ,  $C(n)$  are used up to the critical temperatures. In most cases, the upper limits of applicability of these approximations, as established in [54], are close to the critical temperatures. Temperatures between the above-mentioned upper limits of applicability of these expressions and the critical

temperatures might be observed only at the very final stage of droplet evaporation and the errors in the estimates of vapour pressure in this case are expected to produce negligibly small effects on the evaporation process.

As in the case of alkanes and cycloalkanes, values of  $L$  for alkylbenzenes were estimated by Expression (57) [46]. The values of  $A$  and  $B$  provided in [46] were approximated as

$$A = 0.0007124 n^5 - 0.05315 n^4 + 1.4963 n^3 - 19.83 n^2 + 128.65 n - 276.8,$$

$$B = -0.007 n^2 + 0.1172 n - 0.0989 \text{ when } 8 \leq n \leq 10,$$

$$B = -0.0062 n^2 + 0.1829 n - 0.9093 \text{ when } 11 \leq n \leq 14,$$

$$B = -0.0013315 n^3 + 0.0634 n^2 - 0.9842 n + 5.3794 \text{ when } 15 \leq n \leq 19,$$

$$B = 0.38 \text{ when } n \geq 20.$$

As in the case of alkanes and cycloalkanes, Expression (57) for alkylbenzenes is assumed to be valid up to the critical temperatures.

## Appendix 5

### Transport and thermodynamic properties of indanes & tetralines

#### *Molecular structure, boiling and critical temperatures*

The chemical formula of indanes and tetralines is  $C_nH_{2n-8}$  ( $10 \leq n \leq 22$ ) and their chemical structures are shown in Fig. A1 (penty lindane, as an example of indanes, and 1-propyl-(1,2,3,4-tetrahydronaphthalene), as an example of tetralines). Indanes and tetralines differ by the numbers of carbon atoms in the second ring. When this number is equal to 5 we have indanes; when this number is equal to 6 we have tetralines. Their properties are very close and will not be distinguished in this appendix.

Using data provided in [46], the dependence of critical and boiling temperatures on  $n$  was approximated by the following equations:

$$T_{\text{cr(i)}}(n) = a_{ci} + b_{ci}n + c_{ci}n^2, \quad (72)$$

$$T_{\text{b(i)}}(n) = a_{bi} + b_{bi}n + c_{bi}n^2, \quad (73)$$

where the coefficients are presented in Table A4, (i) stands for indanes & tetralines.



|                    |          |          |          |
|--------------------|----------|----------|----------|
| coefficient        | $a_{ci}$ | $b_{ci}$ | $c_{ci}$ |
| value ( $n = 10$ ) | 720.15   | 0        | 0        |
| value ( $n > 10$ ) | 555.59   | 17.898   | -0.2486  |
| coefficient        | $a_{bi}$ | $b_{bi}$ | $c_{bi}$ |
| value              | 249.21   | 25.894   | -0.3319  |

Table A4

*Liquid density*

Following [46], the temperature dependence of the density of liquid indanes and tetralines for  $10 \leq n \leq 22$  was approximated by Expression (49) with  $A_\rho$ ,  $B_\rho$  and  $C_\rho$  approximated by the following expressions.

For  $10 \leq n \leq 16$ :

$$\begin{cases} A_{\rho i} = 0.0002 \times n^2 - 0.0079 \times n + 0.3622, \\ B_{\rho i} = -710^{-5} \times n^3 + 0.0031 \times n^2 - 0.0438 \times n + 0.4608, \\ C_{\rho i} = 0.2677 \text{ for } n = 10; \quad C_{\rho i} = 0.28571 \text{ for } 11 \leq n \leq 16; \end{cases} \quad (74)$$

for  $17 \leq n \leq 20$ :

$$\begin{cases} A_{\rho i} = 0.0002 \times n^2 - 0.0079 \times n + 0.3622, \\ B_{\rho i} = 6 \times 10^{-5} \times n^2 - 0.0025 \times n + 0.2908, \\ C_{\rho i} = 0.28571. \end{cases} \quad (75)$$

It is assumed that  $\rho(n > 20) = \rho(n = 20)$ . This is justified by the fact that molar fractions of these components are less than 0.2%.

Eqs. (74) and (75) are valid in the range of temperatures 237.4 – 720.15 K for  $n = 10$ ; 232.3 – 722 K for  $n = 11$ ; 243.6 – 735 K for  $n = 12$ ; 254.8 – 745 K for  $n = 13$ ; 266.1 – 756 K for  $n = 14$ ; 277.4 – 767 K for  $n = 15$ ; 288.6 – 777 K for  $n = 16$ ; 299.9 – 788 K for  $n = 17$ ; 311.2 – 797 K for  $n = 18$ ; 322.5 – 805 K for  $n = 19$ ; and 333.7 – 814 K for  $n \geq 20$ .

As in the case of previously considered components, Approximations (74)–(75) are assumed to be valid up to the immediate vicinity of the critical temperatures.

### *Liquid viscosity*

Following [58], the temperature dependence of the dynamic viscosity of liquid indanes & tetralines for  $10 \leq n \leq 94$  is approximated by Expression (51) with  $b(n)$  defined as:

$$b(n) = -9.411 + 2.217 \log_{10}(14n - 8).$$

As in the case of previously considered components, in our analysis it is assumed that Approximation (51) with  $b(n)$ , defined by the above expression, is valid up to the critical temperatures; no low temperature limits for its validity were imposed.

### *Liquid heat capacity*

Following [59, 60], the temperature dependence of the heat capacity of liquid indanes & tetralines for  $10 \leq n \leq 22$  was approximated by Expression (61) with the coefficients defined as:

$$\begin{aligned} a_c &= 14.136 + 2.7345 (n - 11), \\ b_c &= 6.43698 + 0.122732 (n - 11) \text{ K}^{-1}, \\ c_c &= 14.136 - 0.123482 (n - 11) \text{ K}^{-2}. \end{aligned}$$

As in the case of previously considered components, the temperature range of applicability of these approximations is between melting and boiling temperatures.

### *Liquid thermal conductivity*

Following [46, 47], the temperature dependence of thermal conductivity of liquid indanes & tetralines for  $10 \leq n \leq 22$  can be approximated by Expression (62) with  $M_n = 14n - 8$ . As in the case of previously considered components, Expression (62) for indanes & tetralines is valid up to the boiling temperatures.

### *Saturated vapour pressure and enthalpy of evaporation*

Following [46, 47], the saturated vapour pressure for indanes & tetralines is approximated by Expression (65) in which  $f^0$  and  $f^1$  were defined earlier,  $T_r = T/T_{\text{cr(i)}}$ ,  $T_{\text{cr(i)}}$  is the critical temperature estimated from (72) (cf. Expression (65) for bicycloalkanes),  $p_{ci}$  is the critical pressure estimated as

$$p_{ci} = 10^5 (0.0693 n^2 - 3.8821 n + 63.771) \text{ Pa},$$

$\omega_i$  (the acentric factor) is estimated as

$$\omega_i = 0.617 \ln(n) - 1.11.$$

As in the case of previously considered components, Expression (65) for indanes & tetralines is assumed to be valid up to the critical temperatures.

As in the case of alkanes, cycloalkanes and alkylbenzenes, the values of  $L$  for indanes & tetralines were estimated by Expression (57). The values of  $A$  provided in [46] were approximated as

$$A = -0.0793 n^2 + 6.3293 n + 5.7796.$$

The following values of  $B$  provided by [46] were used:  $B = 0.303$  when  $n \leq 10$  and  $B = 0.38$  when  $n > 10$ .

As in the case of alkanes, cycloalkanes and alkylbenzenes, Expression (57) for indanes & tetralines is assumed to be valid up to the critical temperatures.

## Appendix 6

### Transport and thermodynamic properties of naphthalenes

#### *Molecular structure, boiling and critical temperatures*

The chemical formula of naphthalenes is  $C_nH_{2n-12}$  ( $10 \leq n \leq 20$ ) and their typical chemical structure is shown in Fig. A1 (1-propylnaphthalene).

Using data provided in [46], the dependence of critical and boiling temperatures on  $n$  was approximated by the following equations:

$$T_{cr(n)}(n) = a_{cn} + b_{cn}n, \quad (76)$$

$$T_{b(n)}(n) = a_{bn} + b_{bn}n, \quad (77)$$

where the coefficients are presented in Table A5, (n) stands for naphthalenes.

|             |          |          |
|-------------|----------|----------|
| coefficient | $a_{cn}$ | $b_{cn}$ |
| value       | 655.14   | 9.7878   |
| coefficient | $a_{bn}$ | $b_{bn}$ |
| value       | 350.37   | 15.218   |

Table A5

### *Liquid density*

Using data supplied in [66, 67], the temperature dependence of the density of liquid naphthalenes for  $10 \leq n \leq 20$  was approximated as:

$$\rho_{l(n)}(T) = A_{\rho n} + B_{\rho n}T, \quad (78)$$

where  $A_{\rho n}$  and  $B_{\rho n}$  for individual values of  $n$  were approximated by the following expressions:

$$\begin{cases} A_{\rho n} = 1.45 n^2 - 55.715 n + 1671.9 \\ B_{\rho n} = 0.0087 n - 0.8084. \end{cases} \quad (79)$$

As in the case of previously considered components, Approximation (78) is assumed to be valid up to the immediate vicinity of the critical temperature, and no low temperature limit was imposed.

### *Liquid viscosity*

Following [58], the temperature dependence of the dynamic viscosity of liquid naphthalenes for  $10 \leq n \leq 94$  is approximated by Expression (51) with  $b(n)$  defined as:

$$b(n) = -9.309 + 2.185 \log_{10}(14n - 12).$$

As in the case of previously considered components, in our analysis it is assumed that Approximation (51) with  $b(n)$ , defined by the above expression, is valid up to the critical temperatures; no low temperature limits for its validity were imposed.

### *Liquid heat capacity*

Following [59, 60], the temperature dependence of the heat capacity of liquid naphthalenes for  $10 \leq n \leq 20$  was approximated by Expression (61) with the coefficients defined as:

$$\begin{aligned} a_c &= 9.67805 + 2.7345 (n - 11), \\ b_c &= 5.982952 + 0.122732 (n - 11) \text{ K}^{-1}, \\ c_c &= 0.2688 + 0.123482 (n - 11) \text{ K}^{-2}. \end{aligned}$$

As in the case of previously considered components, the temperature range of applicability of these approximations is between melting and boiling temperatures.

### *Liquid thermal conductivity*

Following [46, 47], the temperature dependence of thermal conductivity of liquid naphthalenes for  $10 \leq n \leq 20$  can be approximated by Expression (62) with  $M_n = 14n - 12$ . As in the case of previously considered components, Expression (62) for naphthalenes is valid up to the boiling temperatures.

### *Saturated vapour pressure and enthalpy of evaporation*

Following [46, 47], the saturated vapour pressure for naphthalenes for  $10 \leq n \leq 20$  is approximated by the same Equation (65) as for bicycloalkanes and indanes & tetralines, but for

$$p_c \equiv p_{cn} = 10^5 (0.2009 n^2 - 8.443 n + 104.09) \text{ Pa},$$

$$\omega \equiv \omega_n = -0.0018 n^2 + 0.0997 n - 0.5082.$$

As in the case of previously considered components, Expression (65) is assumed to be valid up to the critical temperatures.

As in the case of alkanes, cycloalkanes, alkylbenzenes and indanes & tetralines, the values of  $L$  for naphthalenes were estimated by Expression (57). The values of  $A$  provided in [46] were approximated as

$$A = 0.2607 n^2 - 2.1791 n + 66.218 \quad \text{for } 10 \leq n \leq 16,$$

$$A = -0.1929 n^2 + 10.926 n - 37.384 \quad \text{for } n \geq 17.$$

The values of  $B$  provided by [46] were approximated as

$$B = -0.0003165 n^3 + 0.01545 n^2 - 0.2495 n + 1.722 \quad \text{for all } n.$$

As in the case of alkanes, cycloalkanes, alkylbenzenes, and indanes & tetralines, Expression (57) for naphthalenes is assumed to be valid up to the critical temperatures.

## **Appendix 7**

### **Transport and thermodynamic properties of tricycloalkanes, diaromatics and phenanthrenes**

The molar fractions of tricycloalkanes, diaromatics and phenanthrenes are 1.5647%, 1.2240% and 0.6577% respectively. Their range of  $n$  is rather narrow:  $14 \leq n \leq 20$  for tricycloalkanes,  $13 \leq n \leq 16$  for diaromatics and

$14 \leq n \leq 18$  for phenanthrenes. This allows us to ignore the dependence of the properties of these substances on  $n$  and consider the properties for just one  $n$  for which the properties are available. Thus, the analysis of these three groups will be reduced to the analysis of three representative components referred to as tricycloalkane, diaromatic and phenanthrene.

*Molecular structure, boiling and critical temperatures*

The chemical formula of tricycloalkanes is  $C_nH_{2n-4}$ . The properties presented in this appendix refer to  $n = 19$  ( $C_{19}H_{34}$ ). The chemical formula of diaromatics is  $C_nH_{2n-14}$ . The properties presented in this appendix refer to  $n = 13$  ( $C_{13}H_{12}$ ). The chemical formula of phenanthrenes is  $C_nH_{2n-18}$ . The properties presented in this appendix refer to  $n = 14$  ( $C_{14}H_{10}$ ). Typical chemical structures of diaromatics and phenanthrenes are shown in Fig. A1 (di(3-ethyl-phenyl)methane and ethylphenanthrene, respectively).

Using data provided in [68], the boiling and critical temperatures for tricycloalkane were estimated as:

$$T_{b(t)} = 692.33 \text{ K}, \quad T_{cr(t)} = T_{b(t)} \times 0.738686^{-1} = 937.25 \text{ K}.$$

Using data provided in [46], these temperatures for the remaining two substances were estimated as:

$$T_{b(d)} = 537.42 \text{ K}, \quad T_{cr(d)} = 760.00 \text{ K}$$

for diaromatics, and

$$T_{b(p)} = 610.00 \text{ K}, \quad T_{cr(p)} = 869.00 \text{ K}$$

for phenanthrenes. (t) stands for tricycloalkanes, (d) stands for diaromatics, and (p) stands for phenanthrenes.

*Liquid density*

Using data supplied in [67], the temperature dependence of the density of liquid tricycloalkane and phenanthrene was approximated as:

$$\rho_{l(t)}(T) = A_{\rho t} + B_{\rho t}T, \tag{80}$$

where

$$A_{\rho t} = 1151.17, \quad B_{\rho t} = -0.694690$$

for tricycloalkanes, and

$$A_{\rho t} = 1374.16, \quad B_{\rho t} = -0.819355$$

for phenanthrenes.

The approximation for tricycloalkane is valid in the range of temperatures (273.15 – 372.05) K, while the approximation for phenanthrenes is valid in the range of temperatures (490.70 – 557.80) K.

Using data supplied in [67], the temperature dependence of the density of liquid diaromatic was approximated as:

$$\rho_{l(t)}(T) = A_{\rho d} + B_{\rho d}T + C_{\rho d}T^2 + D_{\rho d}T^3, \quad (81)$$

where

$$\begin{aligned} A_{\rho d} &= 1.22498 \times 10^3, \quad B_{\rho d} = -7.21739 \times 10^{-1}, \\ C_{\rho d} &= -8.65342 \times 10^{-5}, \quad D_{\rho d} = 1.63332 \times 10^{-9}. \end{aligned}$$

This approximation is valid in the range of temperatures (284.15 – 523.15) K.

In contrast to the previously considered components, it was assumed that the values at  $T < T_{\min}$  are the same as the values at  $T = T_{\min}$ , and the values at  $T > T_{\max}$  are the same as the values at  $T = T_{\max}$ . This ‘cautious’ approach can be justified by the very small contribution of these components to the process of Diesel fuel droplet heating and evaporation.

#### *Liquid viscosity*

Following [68, 69], the temperature dependence of the liquid dynamic viscosity is approximated as:

$$\mu_l = M \exp \left\{ \frac{\eta_a - 597.82}{T} + \eta_b - 11.202 \right\}, \quad (82)$$

where  $M$  is molar mass,

$$M = 262.4733 \frac{\text{kg}}{\text{kmole}}, \quad \eta_a = 3107.93, \quad \eta_b = -9.936$$

for tricycloalkanes,

$$M = 168.23 \frac{\text{kg}}{\text{kmole}}, \quad \eta_a = 2199.18, \quad \eta_b = -5.395$$

for diaromatics, and

$$M = 178.23 \frac{\text{kg}}{\text{kmole}}, \quad \eta_a = 1613.54, \quad \eta_b = -3.372$$

for phenanthrenes.

Equation (82) is valid up to  $0.7 T_{\text{cr}}$ .

#### *Liquid heat capacity*

Following [59, 60], the temperature dependence of the heat capacity of liquid tricycloalkanes and polycyclic aromatics was approximated by Expression (61) with the coefficients defined as:

$$a_c = 32.9773, \quad b_c = 8.243707 \text{ K}^{-1}, \quad c_c = 0.93225 \text{ K}^{-2}$$

for tricycloalkanes,

$$a_c = 17.9997, \quad b_c = 3.230018 \text{ K}^{-1}, \quad c_c = 0.5203 \text{ K}^{-2}$$

for diaromatics, and

$$a_c = 2.43092, \quad b_c = 12.11225 \text{ K}^{-1}, \quad c_c = 0.80569 \text{ K}^{-2}$$

for phenanthrenes.

As in the case of previously considered components, the temperature range of applicability of these approximations is between melting and boiling points.

#### *Liquid thermal conductivity*

Following [47], the temperature dependence of thermal conductivity of liquid tricycloalkanes and polycyclic aromatics can be estimated based on Expression (62) with  $M_n = 14n - 4$  for tricycloalkanes,  $M_n = 14n - 14$  for diaromatics and  $M_n = 14n - 18$  for phenanthrenes. As in the case of previously considered components, Expression (62) for tricycloalkanes, diaromatics and phenanthrenes is assumed to be valid up to the critical temperatures.



*Saturated vapour pressure and enthalpy of evaporation*

Following [54], the saturated vapour pressures for tricycloalkane, diaromatic and phenanthrene are approximated by the Antoine equation (56) with

$$A(n) = 15.14702, \quad B(n) = 6103.355, \quad C(n) = 0$$

for tricycloalkane in the range of temperatures 301-321 K,

$$A(n) = 6.38684, \quad B(n) = 2334.129, \quad C(n) = -92.028$$

for tricycloalkane in the range of temperatures 333-464 K,

$$A(n) = 9.79557, \quad B(n) = 3740.286, \quad C(n) = 0$$

for diaromatic in the range of temperatures 273-298 K,

$$A(n) = 6.19796, \quad B(n) = 1885.888, \quad C(n) = -88.292$$

for diaromatic in the range of temperatures 333-647 K,

$$A(n) = 11.631, \quad B(n) = 4873.4, \quad C(n) = 0.05$$

for phenanthrene in the range of temperatures 306-321 K,

$$A(n) = 6.37081, \quad B(n) = 2329.54, \quad C(n) = -77.87$$

for phenanthrene in the range of temperatures 356-650 K.

The upper bounds of the temperatures mentioned above are very close to the critical temperatures of the components. In our analysis these bounds are identified with critical temperatures. At temperatures below  $T_{\min}$  and above  $T_{\max}$  it is assumed that  $p_v(T < T_{\min}) = p_v(T = T_{\min})$  and  $p_v(T > T_{\max}) = p_v(T = T_{\max})$ . At intermediate temperatures when  $p_v(T \leq T_1)$  and  $p_v(T \geq T_2)$  are known but  $p_v(T_1 < T < T_2)$  are not known, it is assumed that in the latter range of temperatures  $p_v$  can be approximated by interpolation as:

$$p_v(T) = p_v(T_1) + \frac{p_v(T_2) - p_v(T_1)}{T_2 - T_1}(T - T_1).$$

As in the case of density, this ‘cautious’ approach can be justified by the very small contribution of these components to the process of Diesel fuel droplet heating and evaporation.

Following [47, 33],  $L$  for tricycloalkane, diaromatic and phenanthrene was estimated by the equation, inferred from the Clausius-Clapeyron equation [12]:

$$L = -\frac{R_u}{M(n)} \frac{d \ln p^{\text{sat}}(n)}{d(1/T)}, \quad (83)$$

where  $R_u$  is the universal gas constant. Remembering (56), Formula (83) can be rewritten as:

$$L = \frac{R_u B(n) T^2}{M(n) (T + C(n))^2}. \quad (84)$$

where  $B(n)$  and  $C(n)$  are given earlier in this appendix.

Expression (84) is assumed to be valid up to the critical temperature.

## Appendix 8

### Thermal conductivity of liquid Diesel fuel

As mentioned in Section 3.7, Expression (46), widely used for the estimation of the thermal conductivity of mixtures (e.g. [23]), is not applicable for the estimation of the thermal conductivity of realistic Diesel fuels, including the one considered in this paper, as the maximal ratio of thermal conductivities of components for these is well above two. On the other hand, no experimental measurements of Diesel fuel, as considered in this paper, are available to the best of our knowledge. In these circumstances, the most sensible action would be to base the analysis on published experimental data referring to other types of Diesel fuel assuming that the difference between the values of thermal conductivities of various types of Diesel fuels is not large. This assumption will be implicitly supported by the results of our analysis. Note that liquid thermal conductivity depends both on temperature and ambient pressure in the general case (e.g. [70, 71, 72]). This is taken into account in our analysis.

Kolev [73] reported selective measurements of Diesel fuel thermal conductivities for a typical summer Diesel fuel at various ambient pressures, up to 240 MPa. The results of these measurements were approximated by the following formula [74]:

$$k_D(T, p) = \sum_{i=1}^3 \left( \sum_{j=1}^3 a_{ij} T^{j-1} \right) p^{i-1}, \quad (85)$$

where

$$a_{ij} = \begin{pmatrix} 0.13924 & 3.78253 \times 10^{-5} & -2.89732 \times 10^{-7} \\ -6.27425 \times 10^{-11} & 6.08052 \times 10^{-13} & 3.64777 \times 10^{-16} \\ -1.38756 \times 10^{-19} & -2.57608 \times 10^{-22} & -2.70893 \times 10^{-24} \end{pmatrix}, \quad (86)$$

$T$  is in K,  $p$  is in Pa and  $k_D$  is in SI units.

The plots of  $k_D$  versus  $T$  for  $p = 10^5$  Pa (1 bar) and  $p = 3 \times 10^6$  Pa (30 bars) are shown in Fig. A3. As can be seen from this figure, thermal conductivities predicted by Expression (85) for  $p = 1$  bar and  $p = 30$  bars almost coincide, which indicates that the dependence of Diesel fuel thermal conductivity on ambient pressure is weak.

Also, in Fig. A3 we have shown the result of the measurements of thermal conductivity at atmospheric pressure and temperature 24°C as reported in [75] (the value of temperature at which the measurements were performed were communicated to us by the lead author of [75]; this is not mentioned in the original paper). As one can see from Fig. A3, the difference between the results reported in [75] and predicted by Expression (85) is less than 10%. This indirectly supports our choice of Expression (85) for the estimation of the thermal conductivity of Diesel fuel. To be consistent with the choice of other parameters used for calculations, this thermal conductivity was estimated for  $p = 30$  bars.

In the same Fig. A3, we have shown the plots for thermal conductivity of n-dodecane, using the approximation recommended by [42]:

$$k_{nd}(T) = 0.1405 - 0.00022(T - 300). \quad (87)$$

As can be seen from Fig. A3, the values of thermal conductivity of n-dodecane are higher than those of Diesel fuel, and the difference between them is particularly noticeable at high temperatures. It is recommended that the thermal conductivity of Diesel fuel is estimated based on Formula (85) rather than Formula (87). As mentioned earlier, the approximation of Diesel fuel by n-dodecane is widely used in the literature.

Note that in all cases shown in Fig. A3 the thermal conductivity of Diesel fuel decreases with temperature. This trend does not capture the expected infinitely large values of thermal conductivity of components when the temperatures of these components reach critical temperatures [76]. The critical temperatures of Diesel fuel varies from one sample to another, but in all cases they were above 700 K [74]. Since no direct comparison of the predictions of

Expression (85) with experimental data for high temperatures was presented in [74], it was assumed that  $k_D(T > 700 \text{ K}) = k_D(T = 700 \text{ K})$ .

## Appendix 9

### Vapour molar heat capacity

In contrast to most transport and thermodynamic properties of the components of Diesel fuel, considered in Appendices 1–8, vapour molar heat capacities (in J/(mole K)) of all these components can be estimated by a single formula, derived from group-contributions [68]:

$$c_{pv} = a_{cpv} - 37.93 + [b_{cpv} + 0.210] T + [c_{cpv} - 3.91 \times 10^{-4}] T^2 + [d_{cpv} + 2.06 \times 10^{-7}] T^3, \quad (88)$$

where the values of coefficients for Diesel fuel components, calculated using the methodology described in [68], are given in Table A6.

#### Alkanes

| $n$ (number of carbon atoms) | $a_{cpv}$ | $b_{cpv}$ | $c_{cpv}$             | $d_{cpv}$             |
|------------------------------|-----------|-----------|-----------------------|-----------------------|
| 8                            | 33.546    | 0.55384   | $-2 \times 10^{-5}$   | $-1.2 \times 10^{-7}$ |
| 9                            | 32.637    | 0.64884   | $-7.5 \times 10^{-5}$ | $-1.1 \times 10^{-7}$ |
| 10                           | 31.728    | 0.74384   | $-0.00013$            | $-9.8 \times 10^{-8}$ |
| 11                           | 30.819    | 0.83884   | $-0.00018$            | $-8.6 \times 10^{-8}$ |
| 12                           | 29.91     | 0.93384   | $-0.00024$            | $-7.4 \times 10^{-8}$ |
| 13                           | 29.001    | 1.02884   | $-0.00029$            | $-6.3 \times 10^{-8}$ |
| 14                           | 28.092    | 1.12384   | $-0.00035$            | $-5.1 \times 10^{-8}$ |
| 15                           | 27.183    | 1.21884   | $-0.0004$             | $-3.9 \times 10^{-8}$ |
| 16                           | 26.274    | 1.31384   | $-0.00046$            | $-2.7 \times 10^{-8}$ |
| 17                           | 25.365    | 1.40884   | $-0.00051$            | $-1.5 \times 10^{-8}$ |
| 18                           | 24.456    | 1.50384   | $-0.00056$            | $-3 \times 10^{-9}$   |
| 19                           | 23.547    | 1.59884   | $-0.00062$            | $8.9 \times 10^{-9}$  |
| 20                           | 22.638    | 1.69384   | $-0.00067$            | $2.08 \times 10^{-8}$ |
| 21                           | 21.729    | 1.78884   | $-0.00073$            | $3.27 \times 10^{-8}$ |
| 22                           | 20.82     | 1.88384   | $-0.00078$            | $4.46 \times 10^{-8}$ |
| 23                           | 19.911    | 1.97884   | $-0.00084$            | $5.65 \times 10^{-8}$ |
| 24                           | 19.002    | 2.07384   | $-0.00089$            | $6.84 \times 10^{-8}$ |
| 25                           | 18.093    | 2.16884   | $-0.00095$            | $8.03 \times 10^{-8}$ |
| 26                           | 17.184    | 2.26384   | $-0.001$              | $9.22 \times 10^{-8}$ |
| 27                           | 16.275    | 2.35884   | $-0.00105$            | $1.04 \times 10^{-7}$ |

# Cycloalkanes

| $n$ (number of carbon atoms) | $a_{\text{cpv}}$ | $b_{\text{cpv}}$ | $c_{\text{cpv}}$ | $d_{\text{cpv}}$      |
|------------------------------|------------------|------------------|------------------|-----------------------|
| 10                           | -33.877          | 0.86592          | -0.00021         | $-8.9 \times 10^{-8}$ |
| 11                           | -34.786          | 0.96092          | -0.00026         | $-7.7 \times 10^{-8}$ |
| 12                           | -35.695          | 1.05592          | -0.00032         | $-6.5 \times 10^{-8}$ |
| 13                           | -36.604          | 1.15092          | -0.00037         | $-5.3 \times 10^{-8}$ |
| 14                           | -37.513          | 1.24592          | -0.00043         | $-4.1 \times 10^{-8}$ |
| 15                           | -38.422          | 1.34092          | -0.00048         | $-2.9 \times 10^{-8}$ |
| 16                           | -39.331          | 1.43592          | -0.00054         | $-1.7 \times 10^{-8}$ |
| 17                           | -40.24           | 1.53092          | -0.00059         | $-5.3 \times 10^{-9}$ |
| 18                           | -41.149          | 1.62592          | -0.00065         | $6.6 \times 10^{-9}$  |
| 19                           | -42.058          | 1.72092          | -0.0007          | $1.85 \times 10^{-8}$ |
| 20                           | -42.967          | 1.81592          | -0.00075         | $3.04 \times 10^{-8}$ |
| 21                           | -43.876          | 1.91092          | -0.00081         | $4.23 \times 10^{-8}$ |
| 22                           | -44.785          | 2.00592          | -0.00086         | $5.42 \times 10^{-8}$ |
| 23                           | -45.694          | 2.10092          | -0.00092         | $6.61 \times 10^{-8}$ |
| 24                           | -46.603          | 2.19592          | -0.00097         | $7.8 \times 10^{-8}$  |
| 25                           | -47.512          | 2.29092          | -0.00103         | $8.99 \times 10^{-8}$ |
| 26                           | -48.421          | 2.38592          | -0.00108         | $1.02 \times 10^{-7}$ |
| 27                           | -49.33           | 2.48092          | -0.00114         | $1.14 \times 10^{-7}$ |

# Bicycloalkanes

| $n$ (number of carbon atoms) | $a_{\text{cpv}}$ | $b_{\text{cpv}}$ | $c_{\text{cpv}}$ | $d_{\text{cpv}}$      |
|------------------------------|------------------|------------------|------------------|-----------------------|
| 10                           | -84.21           | 1.07572          | -0.00038         | $-3.6 \times 10^{-8}$ |
| 11                           | -85.119          | 1.17072          | -0.00044         | $-2.4 \times 10^{-8}$ |
| 12                           | -86.028          | 1.26572          | -0.00049         | $-1.2 \times 10^{-8}$ |
| 13                           | -86.937          | 1.36072          | -0.00055         | $2 \times 10^{-10}$   |
| 14                           | -87.846          | 1.45572          | -0.0006          | $1.21 \times 10^{-8}$ |
| 15                           | -88.755          | 1.55072          | -0.00066         | $2.4 \times 10^{-8}$  |
| 16                           | -89.664          | 1.64572          | -0.00071         | $3.59 \times 10^{-8}$ |
| 17                           | -90.573          | 1.74072          | -0.00076         | $4.78 \times 10^{-8}$ |
| 18                           | -91.482          | 1.83572          | -0.00082         | $5.97 \times 10^{-8}$ |
| 19                           | -92.391          | 1.93072          | -0.00087         | $7.16 \times 10^{-8}$ |
| 20                           | -93.3            | 2.02572          | -0.00093         | $8.35 \times 10^{-8}$ |
| 21                           | -94.209          | 2.12072          | -0.00098         | $9.54 \times 10^{-8}$ |
| 22                           | -95.118          | 2.21572          | -0.00104         | $1.07 \times 10^{-7}$ |
| 23                           | -96.027          | 2.31072          | -0.00109         | $1.19 \times 10^{-7}$ |
| 24                           | -96.936          | 2.40572          | -0.00114         | $1.31 \times 10^{-7}$ |
| 25                           | -97.845          | 2.50072          | -0.0012          | $1.43 \times 10^{-7}$ |

# Alkylbenzene

| $n$ (number of carbon atoms) | $a_{\text{cpv}}$ | $b_{\text{cpv}}$ | $c_{\text{cpv}}$      | $d_{\text{cpv}}$      |
|------------------------------|------------------|------------------|-----------------------|-----------------------|
| 8                            | -0.359           | 0.47492          | $-5.2 \times 10^{-5}$ | $-9.7 \times 10^{-8}$ |
| 9                            | -1.268           | 0.56992          | -0.00011              | $-8.5 \times 10^{-8}$ |
| 10                           | -2.177           | 0.66492          | -0.00016              | $-7.3 \times 10^{-8}$ |
| 11                           | -3.086           | 0.75992          | -0.00021              | $-6.1 \times 10^{-8}$ |
| 12                           | -3.995           | 0.85492          | -0.00027              | $-4.9 \times 10^{-8}$ |
| 13                           | -4.904           | 0.94992          | -0.00032              | $-3.7 \times 10^{-8}$ |
| 14                           | -5.813           | 1.04492          | -0.00038              | $-2.5 \times 10^{-8}$ |
| 15                           | -6.722           | 1.13992          | -0.00043              | $-1.3 \times 10^{-8}$ |
| 16                           | -7.631           | 1.23492          | -0.00049              | $-1.3 \times 10^{-9}$ |
| 17                           | -8.54            | 1.32992          | -0.00054              | $1.06 \times 10^{-8}$ |
| 18                           | -9.449           | 1.42492          | -0.0006               | $2.25 \times 10^{-8}$ |
| 19                           | -10.358          | 1.51992          | -0.00065              | $3.44 \times 10^{-8}$ |
| 20                           | -11.267          | 1.61492          | -0.0007               | $4.63 \times 10^{-8}$ |
| 21                           | -12.176          | 1.70992          | -0.00076              | $5.82 \times 10^{-8}$ |
| 22                           | -13.085          | 1.80492          | -0.00081              | $7.01 \times 10^{-8}$ |
| 23                           | -13.994          | 1.89992          | -0.00087              | $8.2 \times 10^{-8}$  |
| 24                           | -14.903          | 1.99492          | -0.00092              | $9.39 \times 10^{-8}$ |

# Indanes & tetraline

| $n$ (number of carbon atoms) | $a_{\text{cpv}}$ | $b_{\text{cpv}}$ | $c_{\text{cpv}}$ | $d_{\text{cpv}}$      |
|------------------------------|------------------|------------------|------------------|-----------------------|
| 10                           | -38.12           | 0.75632          | -0.00031         | $1.7 \times 10^{-9}$  |
| 11                           | -39.029          | 0.85132          | -0.00037         | $1.36 \times 10^{-8}$ |
| 12                           | -39.938          | 0.94632          | -0.00042         | $2.55 \times 10^{-8}$ |
| 13                           | -40.847          | 1.04132          | -0.00048         | $3.74 \times 10^{-8}$ |
| 14                           | -41.756          | 1.13632          | -0.00053         | $4.93 \times 10^{-8}$ |
| 15                           | -42.665          | 1.23132          | -0.00059         | $6.12 \times 10^{-8}$ |
| 16                           | -43.574          | 1.32632          | -0.00064         | $7.31 \times 10^{-8}$ |
| 17                           | -44.483          | 1.42132          | -0.00069         | $8.5 \times 10^{-8}$  |
| 18                           | -45.392          | 1.51632          | -0.00075         | $9.69 \times 10^{-8}$ |
| 19                           | -46.301          | 1.61132          | -0.0008          | $1.09 \times 10^{-7}$ |
| 20                           | -47.21           | 1.70632          | -0.00086         | $1.21 \times 10^{-7}$ |
| 21                           | -48.119          | 1.80132          | -0.00091         | $1.33 \times 10^{-7}$ |
| 22                           | -49.028          | 1.89632          | -0.00097         | $1.45 \times 10^{-7}$ |

## Naphthalenes

| $n$ (number of carbon atoms) | $a_{\text{cpv}}$ | $b_{\text{cpv}}$ | $c_{\text{cpv}}$ | $d_{\text{cpv}}$      |
|------------------------------|------------------|------------------|------------------|-----------------------|
| 10                           | -39.73           | 0.7048           | -0.00044         | $9.21 \times 10^{-8}$ |
| 11                           | -20.23           | 0.69672          | -0.00028         | $-4.6 \times 10^{-9}$ |
| 12                           | -21.139          | 0.79172          | -0.00034         | $7.3 \times 10^{-9}$  |
| 13                           | -22.048          | 0.88672          | -0.00039         | $1.92 \times 10^{-8}$ |
| 14                           | -22.957          | 0.98172          | -0.00045         | $3.11 \times 10^{-8}$ |
| 15                           | -23.866          | 1.07672          | -0.0005          | $4.3 \times 10^{-8}$  |
| 16                           | -24.775          | 1.17172          | -0.00056         | $5.49 \times 10^{-8}$ |
| 17                           | -25.684          | 1.26672          | -0.00061         | $6.68 \times 10^{-8}$ |
| 18                           | -26.593          | 1.36172          | -0.00067         | $7.87 \times 10^{-8}$ |
| 19                           | -27.502          | 1.45672          | -0.00072         | $9.06 \times 10^{-8}$ |
| 20                           | -28.411          | 1.55172          | -0.00077         | $1.03 \times 10^{-7}$ |

## Tricycloalkanes, diaromatics and phenanthrenes

| Component       | $a_{\text{cpv}}$ | $b_{\text{cpv}}$ | $c_{\text{cpv}}$ | $d_{\text{cpv}}$       |
|-----------------|------------------|------------------|------------------|------------------------|
| Tricycloalkanes | -140.906         | 1.95052          | -0.00094         | $1.009 \times 10^{-7}$ |
| Diaromatics     | -25.419          | 0.90652          | -0.00034         | $-2.45 \times 10^{-8}$ |
| Phenanthrenes   | -54.4            | 0.978            | -0.00058         | $1.122 \times 10^{-7}$ |

Table A6

## References

- [1] Flynn PF, Durrett RP, Hunter GL, zur Loye AO, Akinyemi OC, Dec JE, Westbrook CK. Diesel combustion: an integrated view combining laser diagnostics, chemical kinetics, and empirical validation, SAE report 1999-01-0509; 1999.
- [2] Sazhina EM, Sazhin SS, Heikal MR, Babushok VI, Johns R. A detailed modelling of the spray ignition process in diesel engines. Combustion Science and Technology 2000;160:317-44.
- [3] Sazhin SS. Advanced models of fuel droplet heating and evaporation. Progress in Energy and Combustion Science 2006;32:162-214.
- [4] Sazhin SS, Krutitskii PA, Gusev IG, Heikal MR. Transient heating of an evaporating droplet. International Journal of Heat and Mass Transfer 2010;53:2826-36.

- [5] Sazhin SS, Krutitskii PA, Gusev IG, Heikal MR. Transient heating of an evaporating droplet with presumed time evolution of its radius. *International Journal of Heat and Mass Transfer* 2011;54:1278-88.
- [6] Sazhin SS, Xie J.-F., Shishkova IN, Elwardany AE, Heikal MR. A kinetic model of droplet heating and evaporation: effects of inelastic collisions and a non-unity evaporation coefficient. *International Journal of Heat and Mass Transfer* 2013;56:525-37.
- [7] Sazhin SS, Elwardany AE, Sazhina EM, Heikal MR. A quasi-discrete model for heating and evaporation of complex multicomponent hydrocarbon fuel droplets. *International Journal of Heat and Mass Transfer* 2011;54:4325-32.
- [8] Elwardany AE, Sazhin SS. A quasi-discrete model for droplet heating and evaporation: application to Diesel and gasoline fuels. *Fuel* 2012;97:685-94.
- [9] Elwardany AE, Sazhin SS, Farooq A. Modelling of heating and evaporation of gasoline fuel droplets: a comparative analysis of approximations. *Fuel* 2013;111:643-47.
- [10] Sazhin SS, Elwardany AE, Krutitskii PA, Castanet G, Lemoine F, Sazhina EM, Heikal MR. A simplified model for bi-component droplet heating and evaporation. *International Journal of Heat and Mass Transfer* 2010;53:4495-505.
- [11] Sazhin SS, Elwardany AE, Krutitskii PA, Deprédurand V, Castanet G, Lemoine F, Sazhina EM, Heikal MR. Multi-component droplet heating and evaporation: numerical simulation versus experimental data. *International Journal of Thermal Science* 2011;50:1164-80.
- [12] Arias-Zugasti M, Rosner DF. Multicomponent fuel droplet vaporization and combustion using spectral theory for a continuous mixture. *Combustion and Flame* 2003;135:271-284.
- [13] Abdel-Qader Z, Hallett WLH. The role of liquid mixing in evaporation of complex multicomponent mixtures: modelling using continuous thermodynamics. *Chemical Engineering Science* 2005;60:1629-40.



- [14] Rivard E, Brüggemann D. Numerical investigation of semi-continuous mixture droplet vaporization. *Chemical Engineering Science* 2010;65:5137-45.
- [15] Burger M, Schmehl R, Prommersberger K, Schäfer O, Koch R, Wittig S. Droplet evaporation modelling by the distillation curve model: accounting for kerosene fuel and elevated pressures. *International Journal of Heat and Mass Transfer* 2003;46:4403-12.
- [16] Zhang L, Kong S-C. Vaporization modeling of petroleum-biofuel drops using a hybrid multi-component approach. *Combustion and Flame* 2010;157:2165-74.
- [17] Laurent C, Lavergne G, Villedieu P. Continuous thermodynamics for droplet vaporization: Comparison between Gamma-PDF model and QMoM. *C.R. Mechanique* 2009;337:449-57.
- [18] Teng ST, Williams AD, Urdal K. Detailed hydrocarbon analysis of gasoline by GC-MS (SI-PI0NA). *Journal of High Resolution Chromatography* 1994;17:469-75.
- [19] Venkatramani CJ, Philips JB. Comprehensive 2-dimensional gas chromatography applied to the analysis of complex mixtures. *Journal of Microcolumn Separations* 1993;5:511-6.
- [20] Adam F, Bertoncini F, Thiebaut D, Esnault S, Espinat D, Hennion MC. Towards comprehensive hydrocarbon analysis of middle distillates by LC-GCxGC. *Journal of Chromatographic Science* 2007;45:643-9.
- [21] Seeley JV, Seeley SK, Libby EK, McCurry JD. Analysis of biodiesel/petroleum Diesel blends with comprehensive two-dimensional gas chromatography. *Journal of Chromatographic Science* 2007;45:650-9.
- [22] Ledier C, Orain M, Grisch F, Kashdan J, Bruneaux G. Vapour concentration measurements in biofuel sprays using innovative Planar Laser-Induced Fluorescence strategies. *Proceedings of ILASS Europe 2011, 24th European Conference on Liquid Atomization and Spray Systems, Estoril, Portugal, September 2011 (Book of Abstracts, page 100; full paper is on the conference CD) 2011.*

- [23] Sazhin SS, Al Qubeissi M, Kolodnytska R, Elwardany A, Nasiri R, Heikal MR. Modelling of biodiesel fuel droplet heating and evaporation, *Fuel* 2014;115:559-72.
- [24] Carslaw HS, Jaeger JC. *Conduction of Heat in Solids*. Second Edition. Oxford: Clarendon Press, 1986.
- [25] Kartashov EM. *Analytical Methods in Heat Transfer Theory in Solids*. Moscow: Vysshaya Shkola; 2001 (in Russian).
- [26] Abramzon B, Sirignano WA. Droplet vaporization model for spray combustion calculations. *International Journal of Heat and Mass Transfer* 1989;32:1605-18.
- [27] Sazhin SS, Krutitskii PA, Abdelghaffar WA, Mikhlovsky SV, Meikle ST, Heikal MR. Transient heating of diesel fuel droplets. *International Journal of Heat and Mass Transfer* 2004;47:3327-40.
- [28] Sazhin SS, Krutitskii PA. A conduction model for transient heating of fuel droplets. In Begehr HGW, Gilbert RP, Wong MW, editors. *Progress in Analysis Vol. II. Proceedings of the 3rd International ISAAC (International Society for Analysis, Applications and Computations) Congress (August 20 - 25, 2001, Berlin)*, Singapore: World Scientific; pp. 1231-9; 2003.
- [29] Maqua C, Castanet G, Grisch F, Lemoine F, Kristyadi T, Sazhin SS. Monodisperse droplet heating and evaporation: experimental study and modelling. *International Journal of Heat and Mass Transfer* 2008;51:3932-45.
- [30] Elwardany AE, Gusev IG, Castanet G, Lemoine F, Sazhin SS. Mono- and multi-component droplet cooling/heating and evaporation: comparative analysis of numerical models. *Atomization and Sprays* 2011;21:907-31.
- [31] Tonini S, Cossali GE. An analytical model of liquid drop evaporation in gaseous environment. *International Journal of Thermal Sciences* 2012;57:45-53.

- [32] Tonini S, Cossali GE. A novel vaporisation model for a single-component drop in high temperature air streams. *International Journal of Thermal Sciences* 2014;75:194-203.
- [33] Poling BE, Prausnitz JM, O'Connell J. *The Properties of Gases and Liquids*. 5th Edition. New York: McGraw-Hill; 2001.
- [34] Vignes A. Diffusion in binary solutions. *Industrial & Engineering Chemistry Fundamentals* 1966;5:189-99.
- [35] Kneer R. *Grundlegende Untersuchungen zur Sprühstrahlausbreitung in hochbelasteten Brennräumen: Tropfenverdunstung und Sprühstrahlcharakterisierung*. Dissertation Doktors der Ingenieurwissenschaften, Karlsruhe; 1993.
- [36] Bird RB, Stewart EW, Lightfoot EN. *Transport Phenomena*. Second Edition. New York, Chichester: Wiley & Sons; 2002.
- [37] Silva CM, Li H, Macedo EA. Models for self-diffusion coefficients of dense fluids, including hydrogen-bonding substances. *Chemical Engineering Science* 1998;53:2423-29.
- [38] Hirschfelder JO, Curtiss CF, Bird RB. *Molecular Theory of Gases and Liquids*. 4th Edition. New York: Wiley; 1967.
- [39] Dooley S, Uddi M, Won SH, Dryer FL, Ju Y. Methyl butanoate inhibition of n-heptane diffusion flames through an evaluation of transport and chemical kinetics. *Combustion and Flame* 2012;159:1371-84.
- [40] Magalhães AL, Da Silva FA, Silva CM. New models for tracer diffusion coefficients of hard spheres and real systems: application to gases, liquids and supercritical fluids. *Journal of Supercritical Fluids* 2011;55:898-923.
- [41] Sazhin SS, Kristyadi T, Abdelghaffar WA, Heikal MR. Models for fuel droplet heating and evaporation: comparative analysis. *Fuel* 2006;85:1613-30.
- [42] Abramzon B, Sazhin SS. (2006) Convective vaporization of fuel droplets with thermal radiation absorption. *Fuel* 2006;85:32-46.

- [43] Bykov V, Goldfarb I, Gol'dshtein V, Sazhin SS, Sazhina EM. System decomposition technique for spray modelling in CFD codes. *Computers & Fluids* 2007;36:601-10.
- [44] Goldfarb I, Gol'dshtein V, Kuzmenko G, Sazhin SS. Thermal radiation effect on thermal explosion in gas containing fuel droplets. *Combustion Theory and Modelling* 1999;3:769-87.
- [45] Sazhin SS, Feng G, Heikal MR, Goldfarb I, Gol'dshtein V, Kuzmenko G. Thermal ignition analysis of a monodisperse spray with radiation. *Combustion and Flame* 2001;124:684-701.
- [46] Yaws CL. (Editor). *Thermophysical properties of chemicals and hydrocarbons*. William Andrew Inc; 2008.
- [47] Reid RC, Prausnitz JM, Poling BE. *The Properties of Gases and Liquids*. 4th Edition. New York: McGraw-Hill, p. 550; 1987.
- [48] Ejim CE, Fleck BA, Amirfazli A. Analytical study for atomization of biodiesels and their blends in a typical injector: Surface tension and viscosity effects. *Fuel* 2007;86:1534-44.
- [49] Kolodnytska RV. Analytical study for atomization of hemp oil biodiesel. *Visnik East-Ukrainian National University* 2010;6(148):41-6. (In Ukrainian).
- [50] Mehrotra AK. Correlation and prediction of the viscosity of pure hydrocarbon. *The Canadian Journal of Chemical Engineering* 1994;72:554-7.
- [51] NIST Chemistry WebBook, Thermophysical Properties of Fluid Systems. <http://webbook.nist.gov/chemistry/> Last online-access on 29th October 2013.
- [52] Van Miltenburg JC. Fitting the heat capacity of liquid n-alkanes: new measurements of n-heptadecane and n-octadecane. *Thermochimica Acta* 2000;343:57-62.
- [53] Yaws CL. (Editor). *Handbook of Thermal Conductivity*. Vol. 2 (Organic compounds, C<sub>5</sub> to C<sub>7</sub>) and Vol. 3 (Organic compounds, C<sub>8</sub> to C<sub>28</sub>). Gulf Publishing Company. Houston, London, Paris, Zurich, Tokyo; 1995.

- [54] Dykyj J, Svoboda J, Wilhoit RC, Frenkel M, Hall KR. LANDOLT-BORNSTEIN: Numerical Data and Functional Relationships in Science and Technology. Vol. 20, Vapor Pressure of Chemicals. Subvolume A: Vapor Pressure and Antoine Constants for Hydrocarbons. Springer; 1999.
- [55] Hopfe D. Thermophysical Data of Pure Substances, Data Compilation of FIZ CHEMIE Germany, 1; 1990.
- [56] Liessmann G, Schmidt W, Reiffarth S. Recommended Thermophysical Data, Data compilation of the Saechsische Olefinwerke Boehlen Germany, 1; 1995.
- [57] Daridon JL, Lagrabette A, Lagourette B. Speed of sound, density, and compressibilities of heavy synthetic cuts from ultrasonic measurements under pressure. *Journal of Chemical Thermodynamics* 1998;30:607-23.
- [58] Mehrotra AK. A generalized viscosity equation for pure heavy hydrocarbons. *Industrial & Engineering Chemistry Research* 1991;30:420-7.
- [59] Ruzicka JR V, Domalski ES. Estimation of the heat capacities of organic liquids as a function of temperature using group additivity. I. hydrocarbon compounds. *Journal of Physical and Chemical Reference Data* 1993;22:597-618; <http://dx.doi.org/10.1063/1.555923>.
- [60] Ruzicka Jr V, Domalski ES. Estimation of the heat capacities of organic liquids as a function of temperature using group additivity: an amendment. *Journal of Physical and Chemical Reference Data* 2005;33:1071-81; <http://dx.doi.org/10.1063/1.1797811>.
- [61] Bagga OP, Rattan VK, Singh S, Sethi BPS, Raju KSN. Isobaric vapour-liquid equilibria for binary mixtures of ethylbenzene and p-xylene with dimethylformamide. *Journal of Physical and Chemical Reference Data* 1987;32:198-201.
- [62] Nesterova TN, Nesterov IA, Pimerzin AA. The thermodynamics of the sorption and evaporation of alkylbenzene. II. Critical temperatures. *Izvestia Vysshikh Uchebnykh Zavedeniy. Khimia i Khicheskaya Tekhnologia* (Reports of Higher Education Establishments, Chemistry and Chemical Technology) 2000;43:14-22.

- [63] Ambrose D, Broderick BE, Townsend R. The Vapour pressures above the normal boiling point and the critical pressures of some aromatic hydrocarbons. *Journal of the Chemical Society A* 1967;633-41. DOI: 10.1039/J19670000633
- [64] Simmrock KH, Janowsky R, Ohnsorge A. Critical Data Of Pure Substances, In 'Dechema Chemistry Data Series', Volume II. Frankfurt; 1986.
- [65] Nikitin ED, Popov AP, Bogatishcheva NS. Vapour-liquid critical properties of n-alkylbenzenes from toluene to 1-phenyltridecane. *Journal of Chemical and Engineering Data* 2002;47:1012-6.
- [66] Wilhoit RC, Hong X, Frenkel M, Hall KR. Edited by K.R. Hall and K.N. Marsh, LANDOLT-BORNSTEIN: Numerical Data and Functional Relationships in Science and Technology. Vol. 8. Thermodynamic Properties of Organic Compounds and their Mixtures. Subvolume E: Densities of Aromatic Hydrocarbons. Springer; 1998.
- [67] Wilhoit RC, Hong X, Frenkel M, Hall KR. Edited by K.R. Hall and K.N. Marsh, LANDOLT-BORNSTEIN: Numerical Data and Functional Relationships in Science and Technology. Vol. 8. Thermodynamic Properties of Organic Compounds and their Mixtures. Subvolume F: Densities of Polycyclic Hydrocarbons. Springer; 1998.
- [68] Joback KG, Reid RC. Estimation of pure-component properties from group-contributions. *Chemical Engineering Communications* 1987;57:233-43.
- [69] Constantinou L, Gani R. New group contribution method for estimating properties of pure compounds. *American Institute of Chemical Engineers (AIChE) Journal* 1994;40:1697-710.
- [70] Ross RG, Andersson P, Sundqvist B, Backstrom G. Thermal conductivity of solids and liquids under pressure. *Reports on Progress in Physics* 1984;47:1347-402.
- [71] Marsh KN. (Editor) Recommended Reference Materials for Realization of Physicochemical Properties. Blackwell Science, Oxford; 1987.

- [72] Fareleira JMNA, Li SFY, Wakeham WA. The Thermal conductivity of liquid mixtures at elevated pressures. *International Journal of Thermophysics* 1989;10:1041-51.
- [73] Kolev NI. *Multiphase Flow Dynamics 3: Turbulence, Gas Absorption and Release, Diesel Fuel Properties*. ISBN 978-3-540-71443-9, Springer, Berlin; 2007.
- [74] Lin R, Tavlarides LL. Thermophysical properties needed for the development of the supercritical Diesel combustion technology: Evaluation of Diesel fuel surrogate models. *Journal of Supercritical Fluids* 2012;71:136-46.
- [75] Guimarães AO, Machado FAL, da Silva EC, Mansanares AM. Investigating thermal properties of biodiesel/diesel mixtures using photopyroelectric technique. *Thermochimica Acta* 2012;527:125-30.
- [76] Bellan J. Supercritical (and subcritical) fluid behavior and modeling: drops, streams, shear and mixing layers, jets and sprays. *Progress in Energy and Combustion Science* 2000;26:329-66

## Figure Captions

**Fig. 1** The plots of the droplet surface temperatures  $T_s$  and radii  $R_d$  versus time for four approximations of Diesel fuel composition: the contributions of all 98 components are taken into account (indicated as (98)); the contributions of only 20 alkane components shown in Table 2 are taken into account (indicated as (20A)); the contribution of all 98 components are approximated by 6 quasi-components (corresponding to 6 groups shown in Table 2) and 3 components (tricycloalkane, diaromatic and phenanthrene) without taking into account the diffusion between them so that their mass fractions remain equal to the initial mass fractions and they behave like a single component (indicated as (S)); the contributions of only 20 alkane components shown in Table 2 are taken into account and these are treated as a single component with the average value of the carbon number ( $C_{14.763}H_{31.526}$ ; indicated as (SA)). **Ambient gas pressure and temperature are assumed to be equal to 30 bar and 880 K respectively; the ETC/ED model was**

used for the analysis.

**Fig. 2** The plots of the droplet surface temperatures  $T_s$  and radii  $R_d$  versus time for five approximations of Diesel fuel composition: 98 components (indicated as (98)); 85 quasi-components/components (indicated as (85)); 58 quasi-components/components (indicated as (58)); 40 quasi-components/components (indicated as (40)); the contribution of all 98 components is taken into account as that of a single component as in the case shown in Fig. 1 (indicated as (S)) (see the details in the text of the paper). **The same ambient conditions and model as in the case shown in Fig. 1 were used for the analysis.**

**Fig. 3** Zoomed part of Fig. 2 referring to the droplet surface temperatures  $T_s$ .

**Fig. 4** Zoomed part of Fig. 2 referring to the droplet surface radii  $R_d$ .

**Fig. 5** The plots of the droplet surface temperatures  $T_s$  versus time for ten approximations of Diesel fuel composition: 98 components (indicated as (98)); 23, 21, 17, 15, 12, 9 and 7 quasi-components/components (indicated as (23), (21), (17), (15), (12), (9) and (7) respectively); the contributions of all groups shown in Table 2 are approximated by single quasi-components, to which the contribution of tricycloalkane is added, leading to 7 quasi-components/components (indicated as (S7)); the contribution of all 98 components is taken into account as that of a single component as in the case shown in Figs. 1 and 2 (indicated as (S)) (see the details in the text of the paper); **the contributions of only 20 alkane components, shown in Table 2, are taken into account and these are treated as a single component, with the average value of the carbon number ( $C_{14.763}H_{31.526}$ ; indicated as (SA)). The same ambient conditions and model as in the case shown in Figs. 1-4 were used for the analysis.**

**Fig. 6** Zoomed part of Fig. 5.

**Fig. 7** The same as Fig. 5 but for the droplet radii  $R_d$ .

**Fig. 8** Zoomed part of Fig. 7.



**Fig. 9** The plots of the surface mass fractions  $Y_{lis}$  of 9 characteristic and/or dominant components, predicted based on the model, taking into account the contributions of all 98 components, for the same conditions as in Figs. 1-8: alkanes  $C_{18}H_{38}$  (1),  $C_{25}H_{52}$  (2),  $C_{27}H_{56}$  (3), cycloalkanes  $C_{20}H_{40}$  (4),  $C_{24}H_{48}$  (5),  $C_{26}H_{52}$  (6),  $C_{27}H_{54}$  (7), alkylbenzene  $C_{10}H_{14}$  (8) and tricycloalkane  $C_{19}H_{34}$  (9).

**Fig. 10** The same as Fig. 9 but for alkane  $C_{10}H_{22}$  (1), bicycloalkanes  $C_{11}H_{20}$  (2) and  $C_{25}H_{48}$  (3), alkylbenzenes  $C_{23}H_{40}$  (4) and  $C_{24}H_{42}$  (5), indane or tetraline  $C_{13}H_{18}$  (6), naphthalenes  $C_{10}H_8$  (7),  $C_{11}H_{10}$  (8), and  $C_{19}H_{26}$  (9).

**Fig. 11** The same as Figs. 9 and 10 but for the surface mass fractions  $Y_{lis}$  of 8 characteristic and/or dominant quasi-components/components, predicted based on the model, taking into account the contributions of 21 quasi-components/components; these are the quasi-components/components: alkane  $C_{17.622}H_{37.244}$  (range  $C_{16}H_{34} - C_{19}H_{40}$ ) (1), alkane  $C_{20.869}H_{43.737}$  (range  $C_{20}H_{42} - C_{23}H_{48}$ ) (2), cycloalkane  $C_{25.644}H_{51.287}$  (range  $C_{25}H_{50} - C_{27}H_{54}$ ) (3), bicycloalkane  $C_{21.243}H_{40.485}$  (range  $C_{20}H_{38} - C_{25}H_{48}$ ) (4), alkylbenzene  $C_{10.207}H_{14.413}$  (range  $C_8H_{10} - C_{13}H_{20}$ ) (5), indane or tetraline  $C_{11.407}H_{14.814}$  (range  $C_{10}H_{12} - C_{13}H_{18}$ ) (6), naphthalene  $C_{11.533}H_{11.067}$  (range  $C_{10}H_8 - C_{15}H_{18}$ ) (7), tricycloalkane  $C_{19}H_{34}$  (8).

**Fig. 12** The same as Fig. 11 but for the surface mass fractions  $Y_{lis}$  of 11 characteristic and/or dominant quasi-components/components, predicted based on the model, taking into account the contributions of 15 quasi-components/components; these are the quasi-components/components: alkane  $C_{10.335}H_{22.670}$  (range  $C_8H_{18} - C_{12}H_{26}$ ) (1), alkane  $C_{19.380}H_{40.760}$  (range  $C_{18}H_{38} - C_{22}H_{46}$ ) (2), cycloalkane  $C_{12.562}H_{25.125}$  (range  $C_{10}H_{20} - C_{15}H_{30}$ ) (3), cycloalkane  $C_{18.297}H_{36.595}$  (range  $C_{16}H_{32} - C_{21}H_{42}$ ) (4), cycloalkane  $C_{22.977}H_{45.953}$  (range  $C_{22}H_{44} - C_{27}H_{54}$ ) (5), bicycloalkane  $C_{14.743}H_{27.487}$  (range  $C_{10}H_{18} - C_{25}H_{48}$ ) (6), alkylbenzene  $C_{10.207}H_{14.413}$  (range  $C_8H_{10} - C_{13}H_{20}$ ) (7), indane or tetraline  $C_{12.495}H_{16.990}$  (range  $C_{10}H_{12} - C_{16}H_{24}$ ) (8), indane or tetraline  $C_{18.615}H_{29.229}$  (range  $C_{17}H_{26} - C_{22}H_{36}$ ) (9), naphthalene  $C_{12.392}H_{12.783}$  (range  $C_{10}H_8 - C_{20}H_{28}$ ) (10), tricycloalkane  $C_{19}H_{34}$  (11).

**Fig. 13** The plots of the mass fractions of alkylbenzene  $C_{10}H_{14}$  (indicated as A) and tricycloalkane  $C_{19}H_{34}$  (indicated as T) versus normalised distance from the droplet centre ( $R/R_d$ ) at four instants of time 0.02 ms, 0.3 ms, 0.5

ms and 1 ms (indicated near the plots) as predicted by the model, taking into account the contributions of all 98 components. **The same ambient conditions and model as in the case shown in Figs. 1-12 were used for the analysis.**

**Fig. 14** The plots of temperature versus normalised distance from the droplet centre ( $R/R_d$ ) at four instants of time 0.02 ms, 0.3 ms, 0.5 ms and 1 ms (indicated near the plots) as predicted by the model, taking into account the contributions of all 98 components. **The same ambient conditions and model as in the case shown in Figs. 1-13 were used for the analysis.**

**Fig. 15** The plots of the mass fractions of alkylbenzene quasi-component  $C_{10.207}H_{14.413}$  (range  $C_8H_{10} - C_{13}H_{20}$ ) and tricycloalkane  $C_{19}H_{34}$ , versus normalised distance from the droplet centre ( $R/R_d$ ) at four instants of time 0.02 ms, 0.3 ms, 0.5 ms and 1 ms (indicated near the plots) as predicted by the model based on the approximation of Diesel fuel by 15 quasi-components/components. **The same ambient conditions and model as in the case shown in Figs. 1-14 were used for the analysis.**

**Fig. 16** The same as Fig. 14, but predicted by the model based on the approximation of Diesel fuel by 15 quasi-components/components.

**Fig. 17** The values of droplet surface temperatures (a) and radii (b) versus the number of quasi-components/components used for the approximation of Diesel fuel for the time instant 0.02 ms for the same conditions as in Figs. 1-16.

**Fig. 18** The same as Fig. 17 but for the time instant 0.5 ms.

**Fig. 19** The same as Figs. 17 and 18 but for the time instant 1 ms.

**Fig. 20** The same as Figs. 17-19 but for the time instant 2 ms.

**Fig. 21** The same as Figs. 17-20 but for the time instant 2.5 ms.

**Fig. 22** The plots of the droplet surface temperatures  $T_s$  versus time for 3 approximations of Diesel fuel composition: the contributions of all 98 compo-

nents is taken into account (indicated as (98)); 15 quasi-components/components (indicated as (15)); the contributions of all 98 components are taken into account as that of a single component as in the case shown in Figs. 1, 2 and 5 (indicated as (S)) for the same conditions as in Figs. 1-16 except that the droplet is assumed to be moving with a velocity equal to 10 m/s and using both the Effective Thermal Conductivity/Effective Diffusivity model (indicated as E) and the Infinite Thermal Conductivity/ Infinite Diffusivity model (indicated as I).

**Fig. 23** The same as Fig. 22 but for the droplet radii  $R_d$ .

**Fig. 24** The plot of CPU time, required for calculations of stationary droplet heating and evaporation for the same parameters as in Figs. 1-21, versus the number of quasi-components/components used in the model.

**Fig. A1** The structures of some organic components of Diesel fuel.

**Fig. A2** The values of  $A$  used in Formula (57), as inferred from the data provided by [46], and their approximations by  $A_L$  and  $A_H$ .

**Fig. A3** The plots of thermal conductivity of Diesel fuel as predicted by Formula (85), recommended by Lin and Tavlarides [74], for 1 and 30 bars, the result of the measurements of thermal conductivity at atmospheric pressure and temperature 24°C as reported by Guimarães et al. [75], and the values of thermal conductivity of n-dodecane estimated based on Formula (87) by Abramzon and Sazhin [42].

## Table Captions

**Table 1** The composition (molar fractions) of a realistic Diesel fuel sample (gas chromatography data) used in the analysis.

**Table 2** The simplified composition (molar fractions) of the same Diesel fuel sample as in Table 1.

**Table 3** The relation between parameter  $m$  and groups ( $m = 1 - 6$ ) and components ( $m = 7 - 9$ ).

**Table A1** Numerical values of the coefficients used in Expressions (47) and (48).

**Table A2** Numerical values of the coefficients used in Expressions (58) and (59).

**Table A3** Numerical values of the coefficients used in Expressions (67) and (68).

**Table A4** Numerical values of the coefficients used in Expressions (72) and (73).

**Table A5** Numerical values of the coefficients used in Expressions (76) and (77).

**Table A6** Numerical values of the coefficients used in Expression (88).

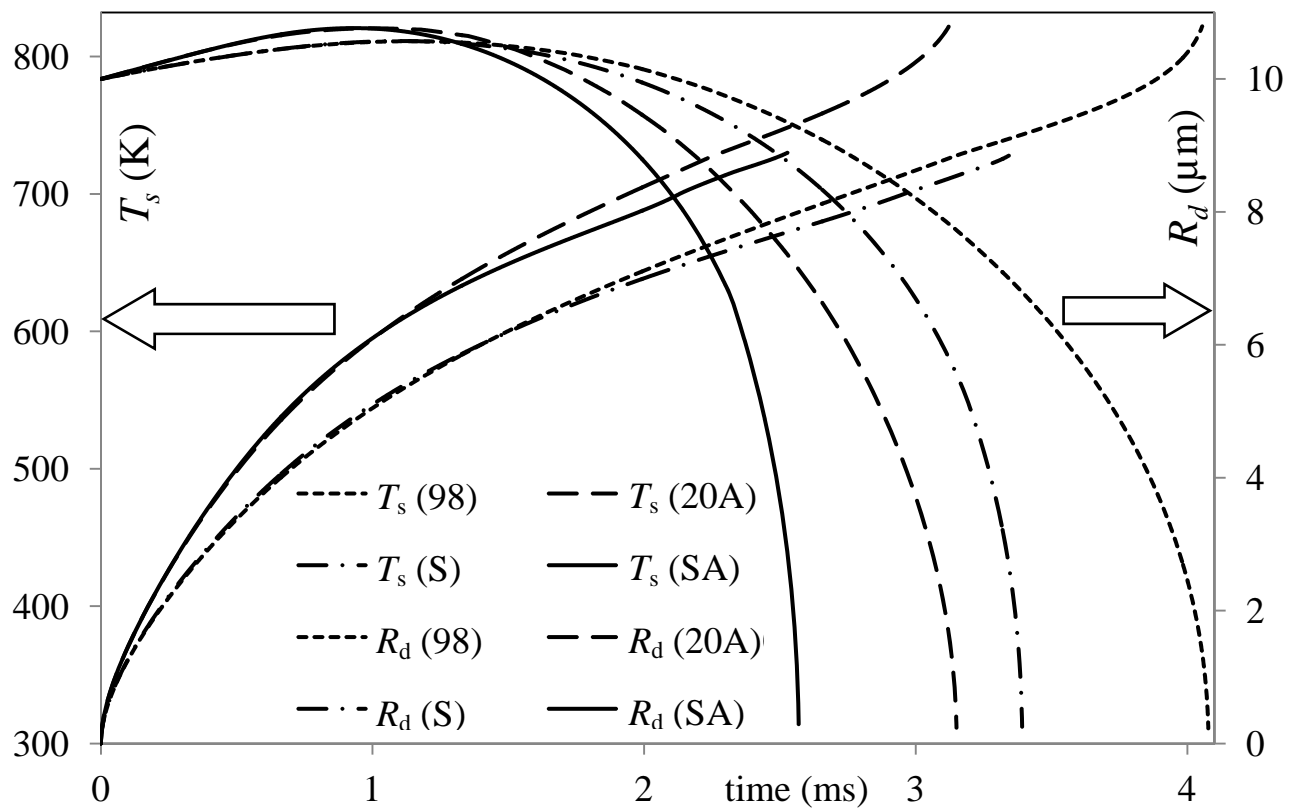


Fig. 1

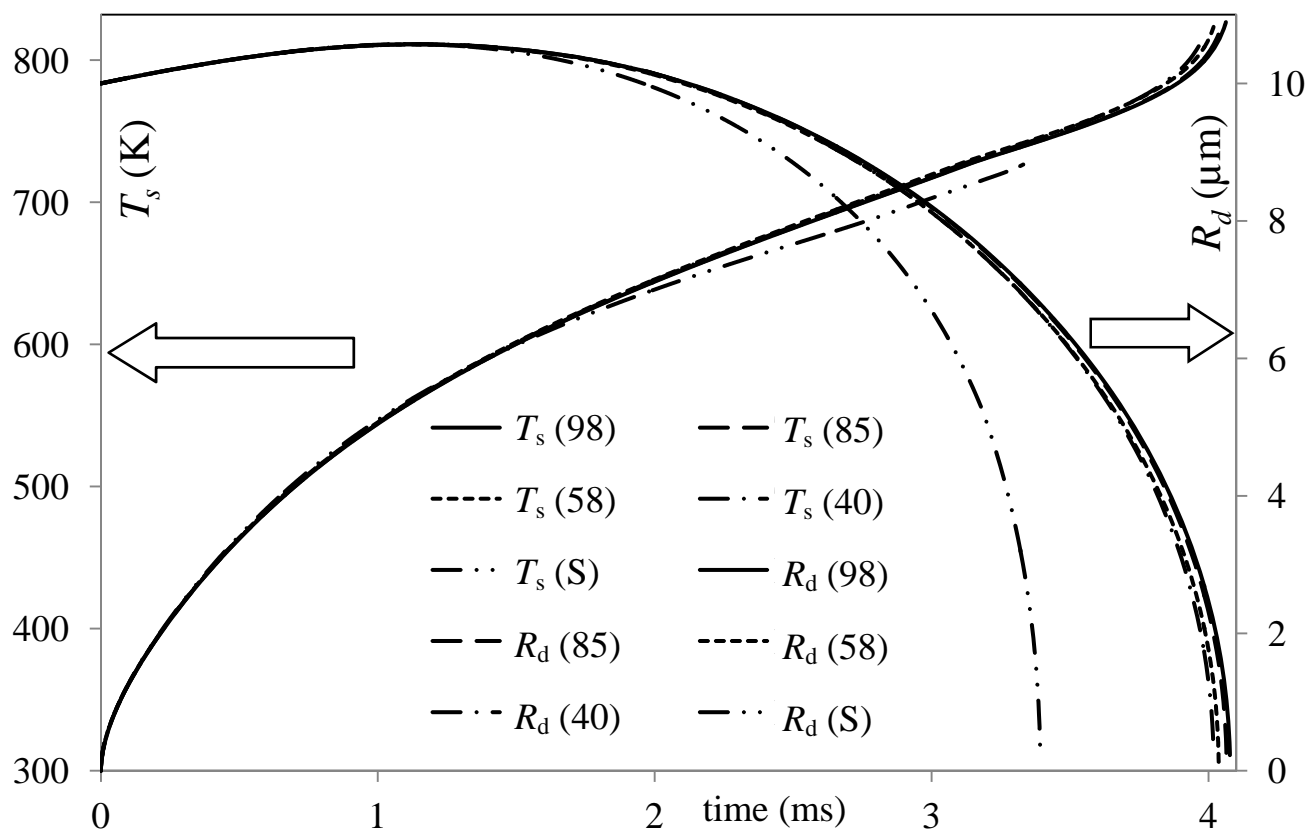


Fig. 2

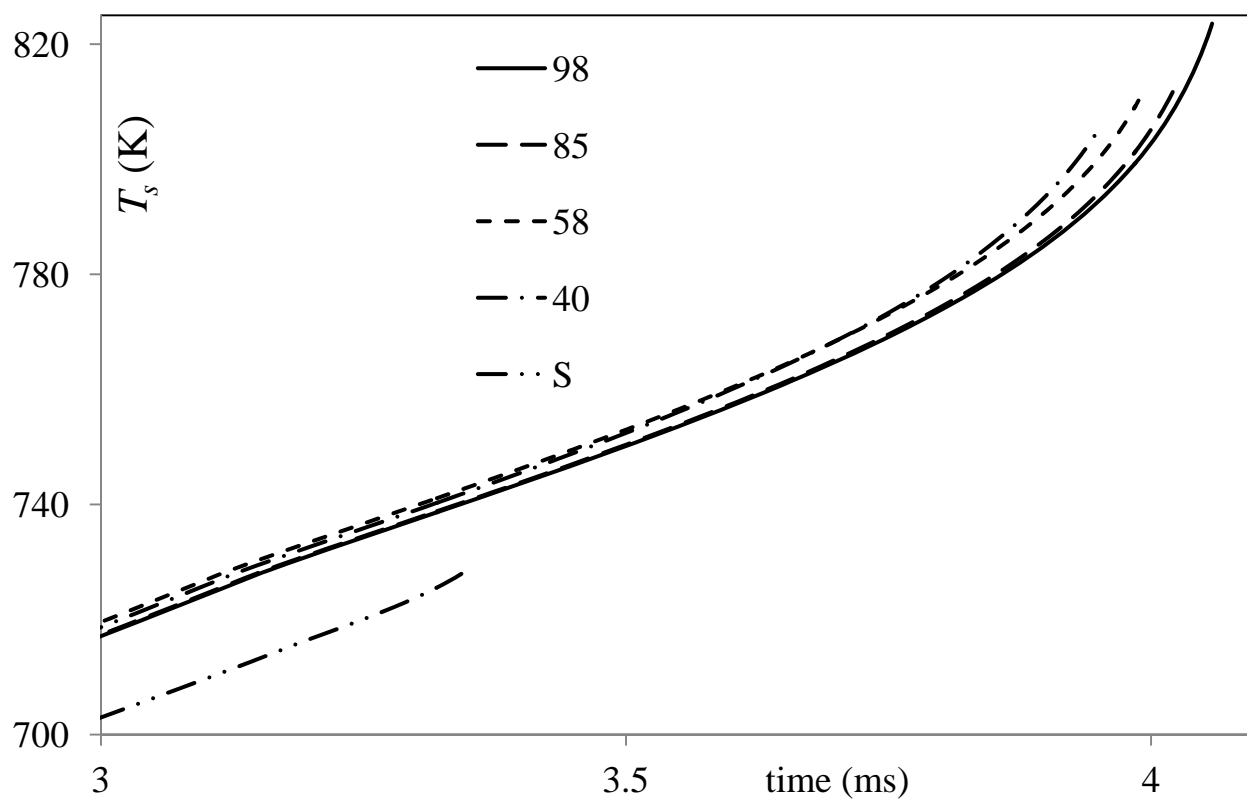


Fig. 3

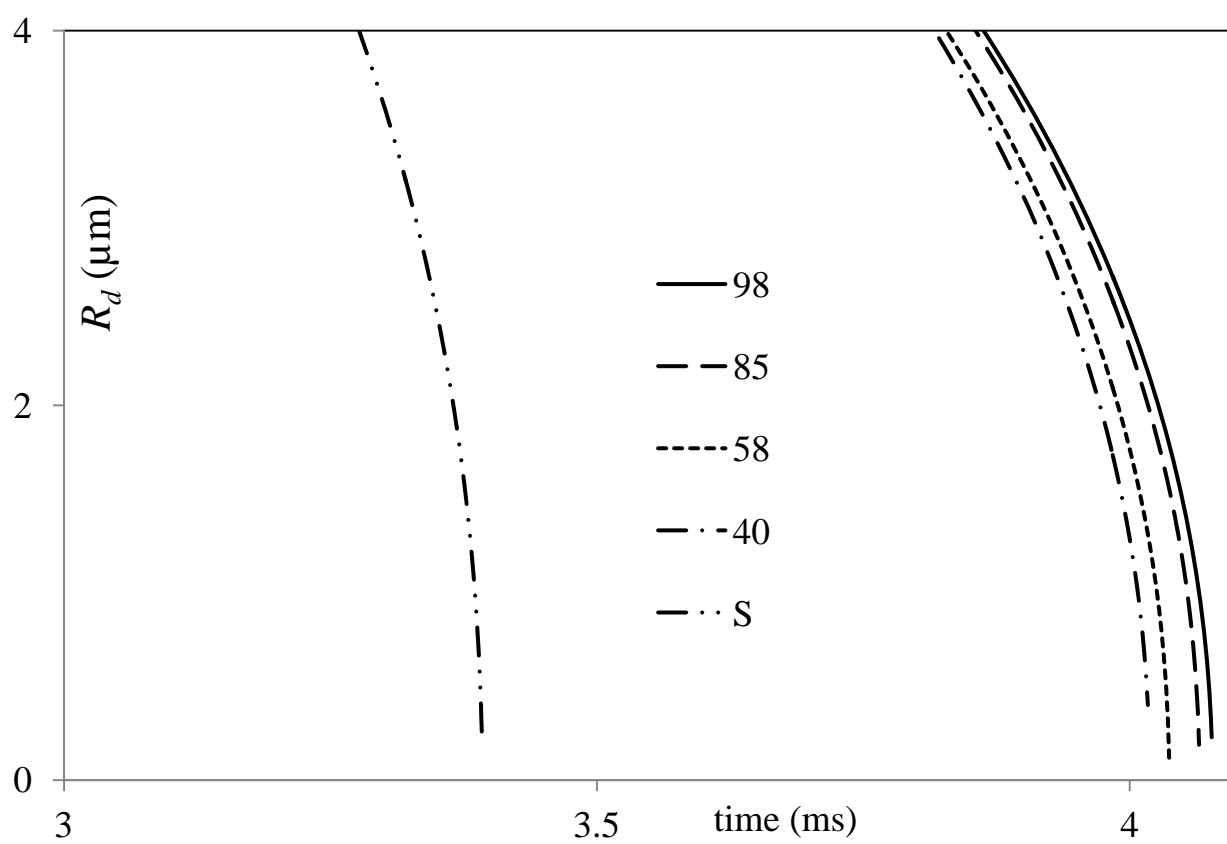


Fig. 4

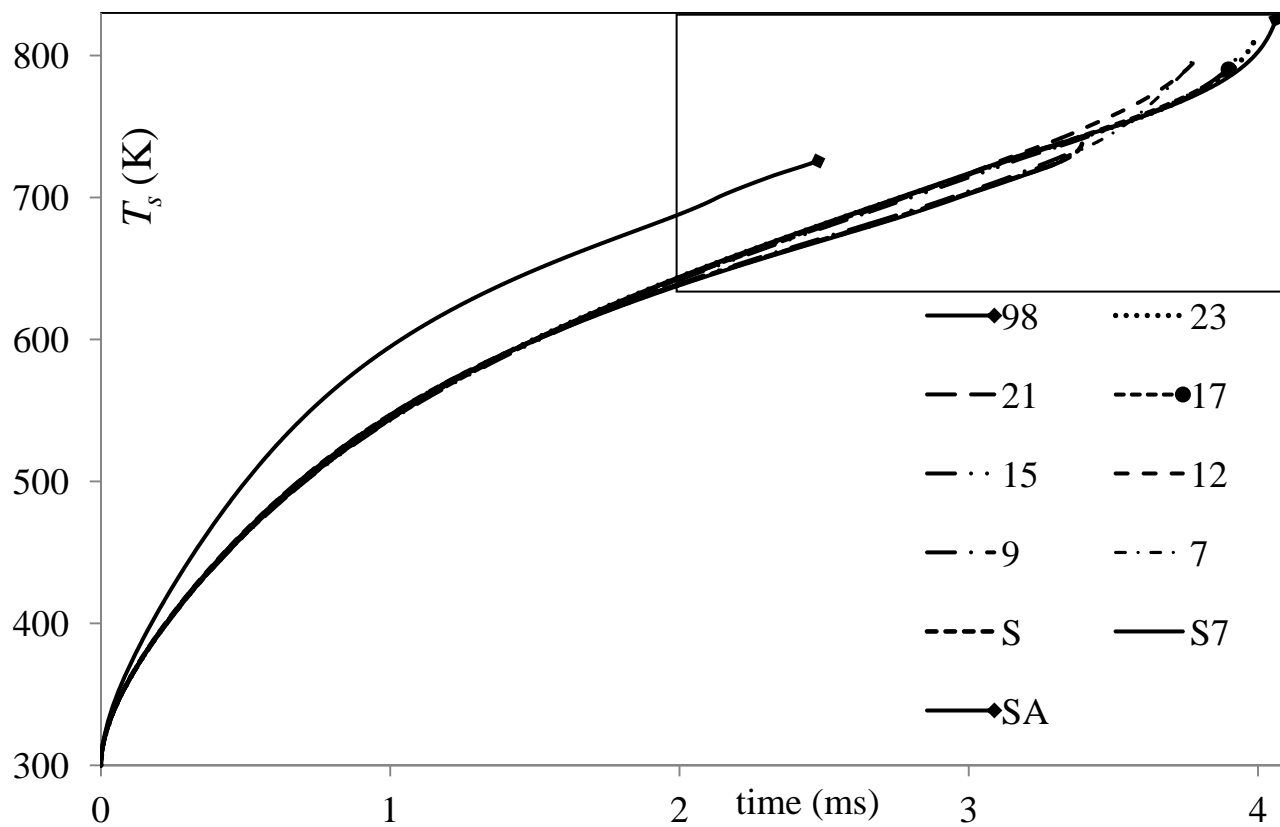


Fig. 5

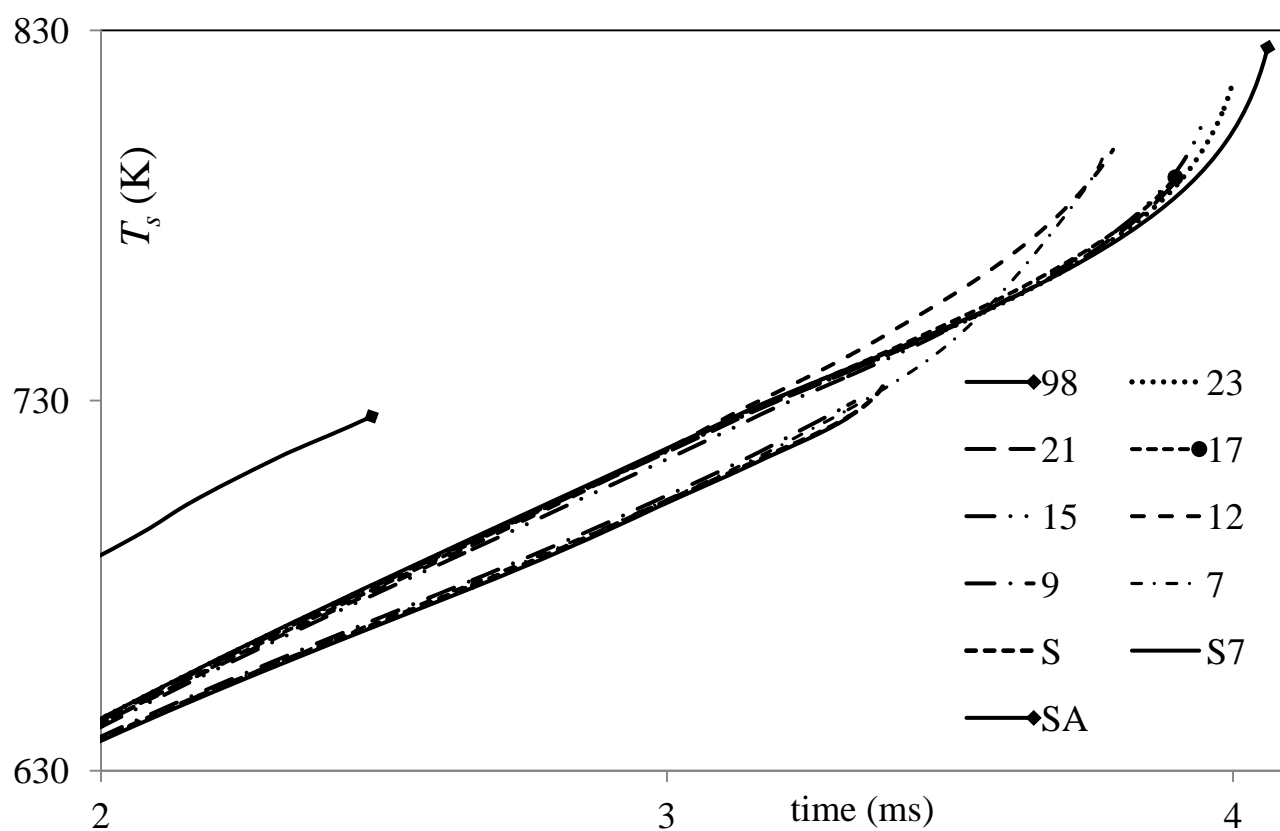


Fig. 6

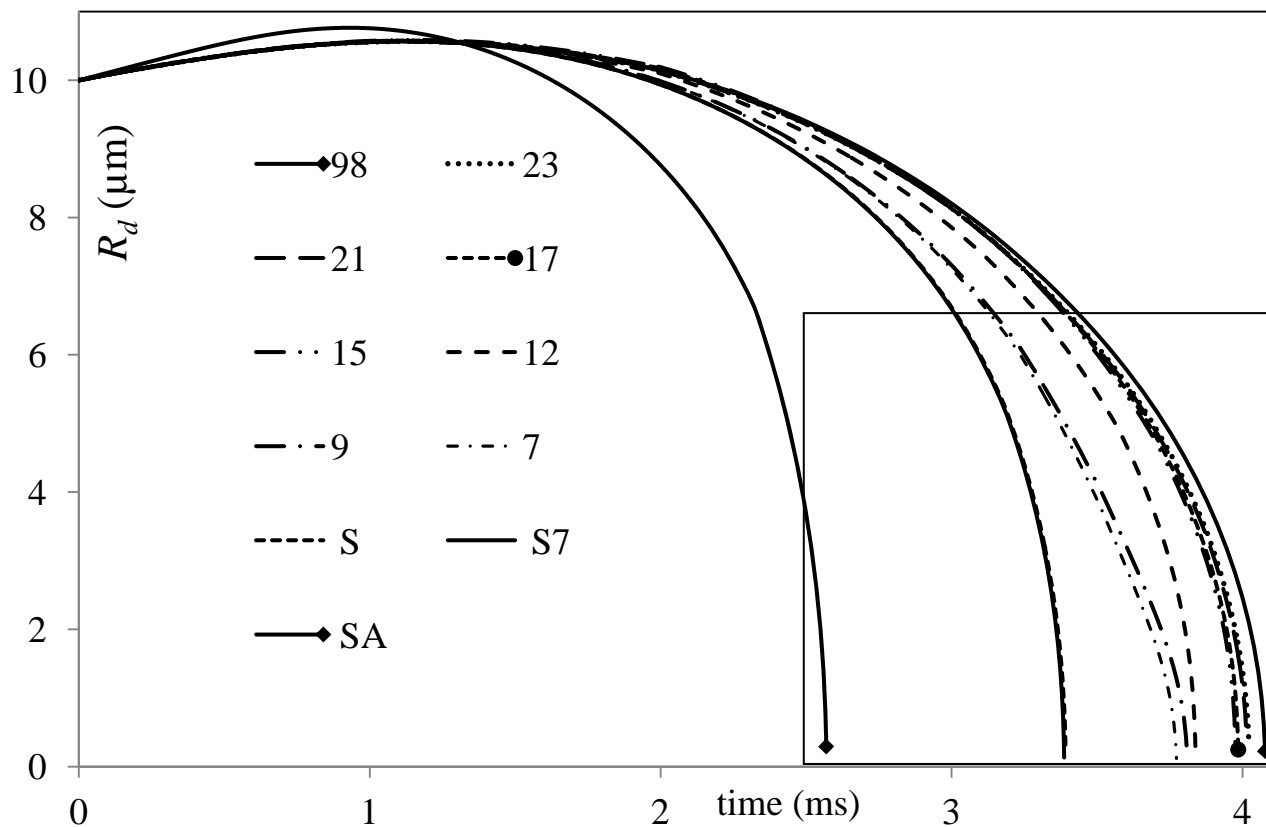


Fig. 7

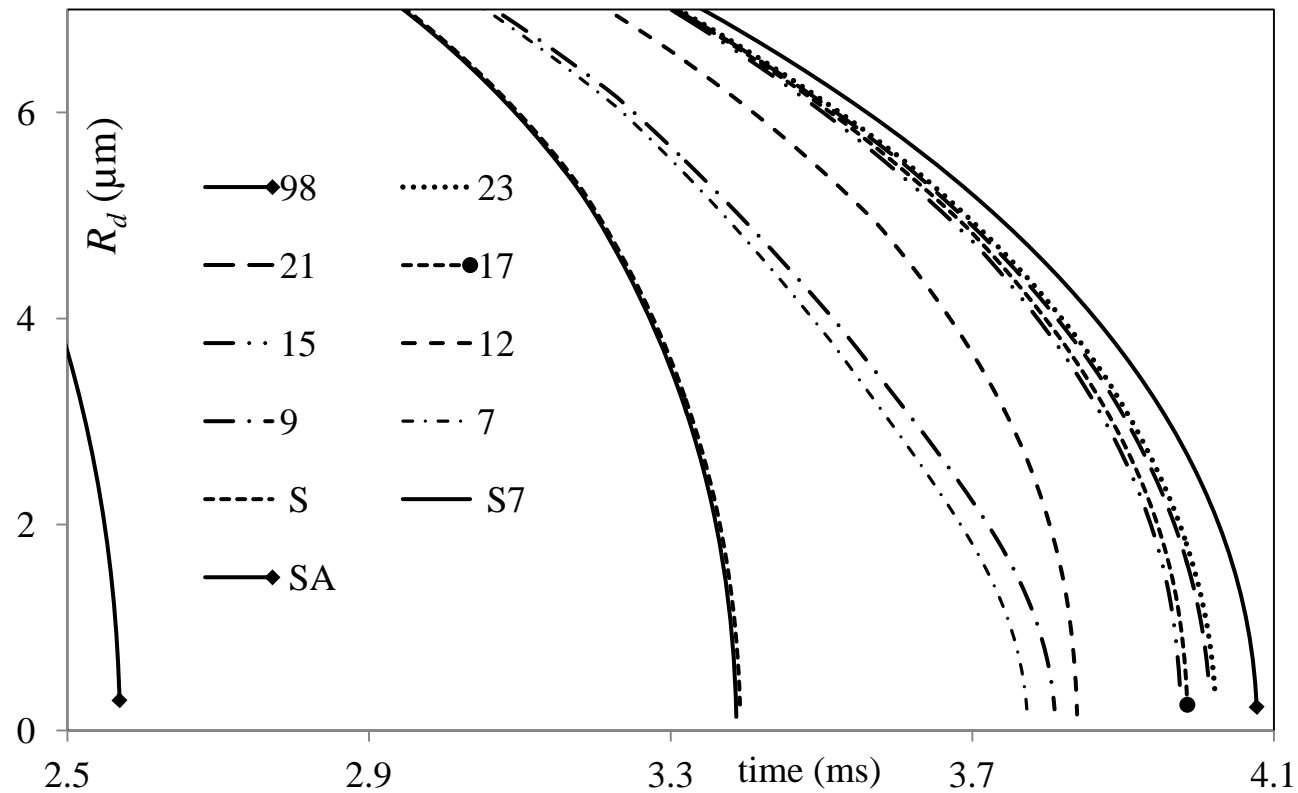


Fig. 8



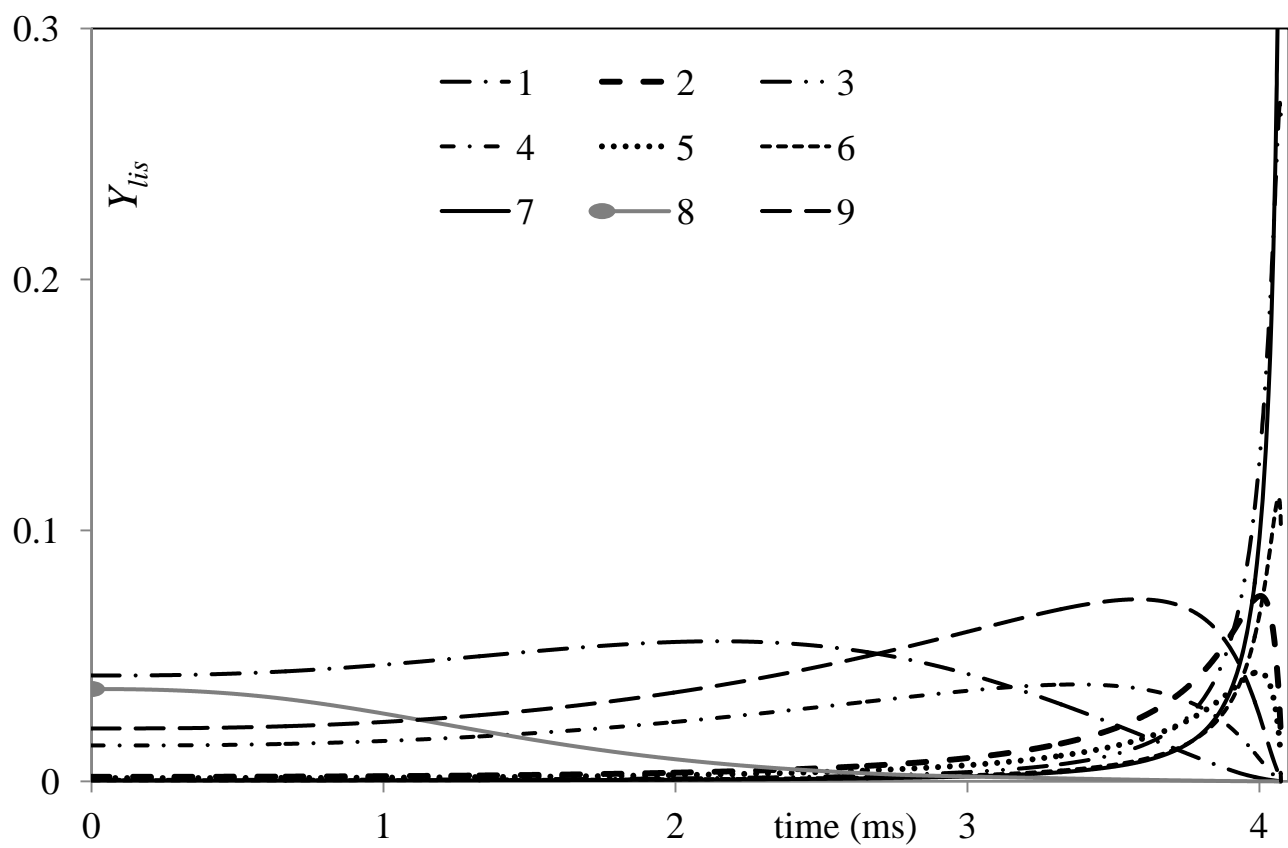


Fig. 9

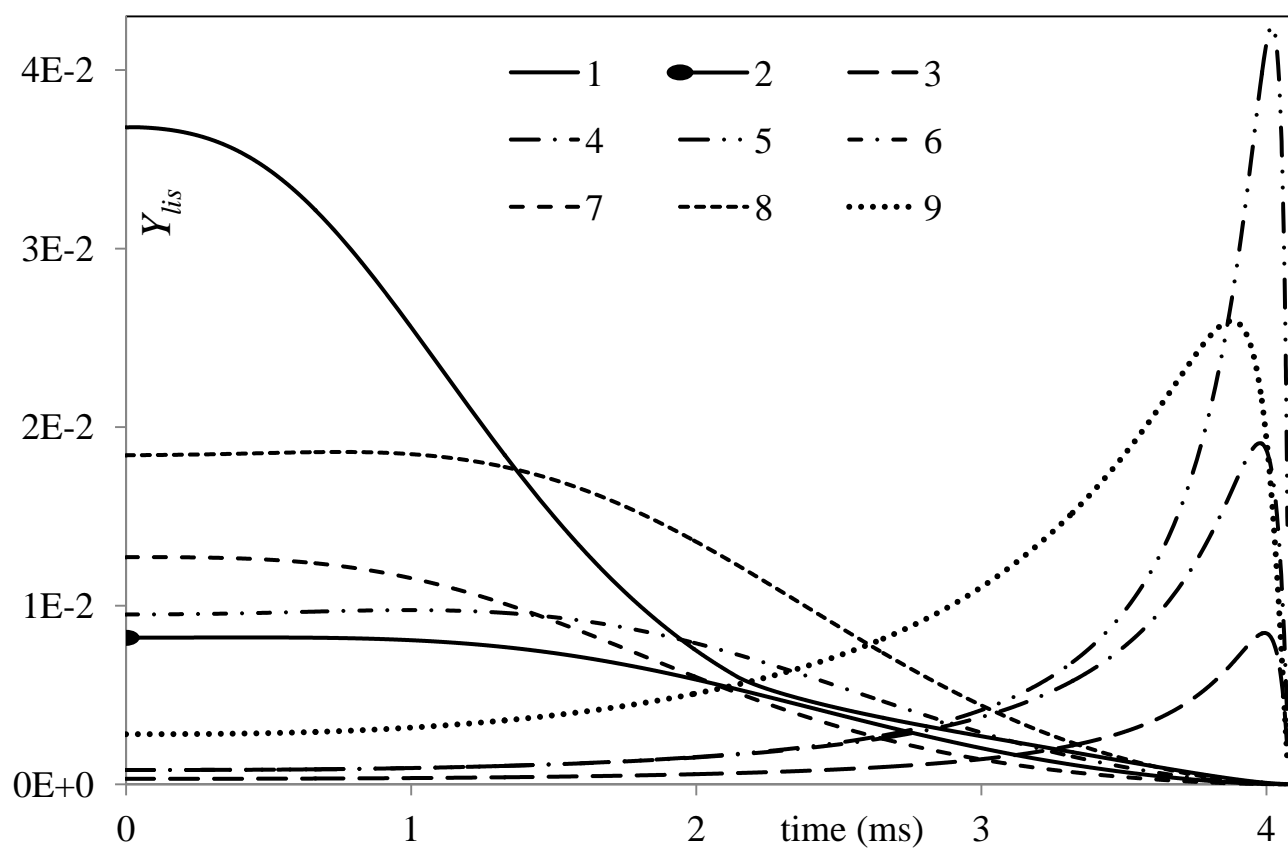


Fig. 10

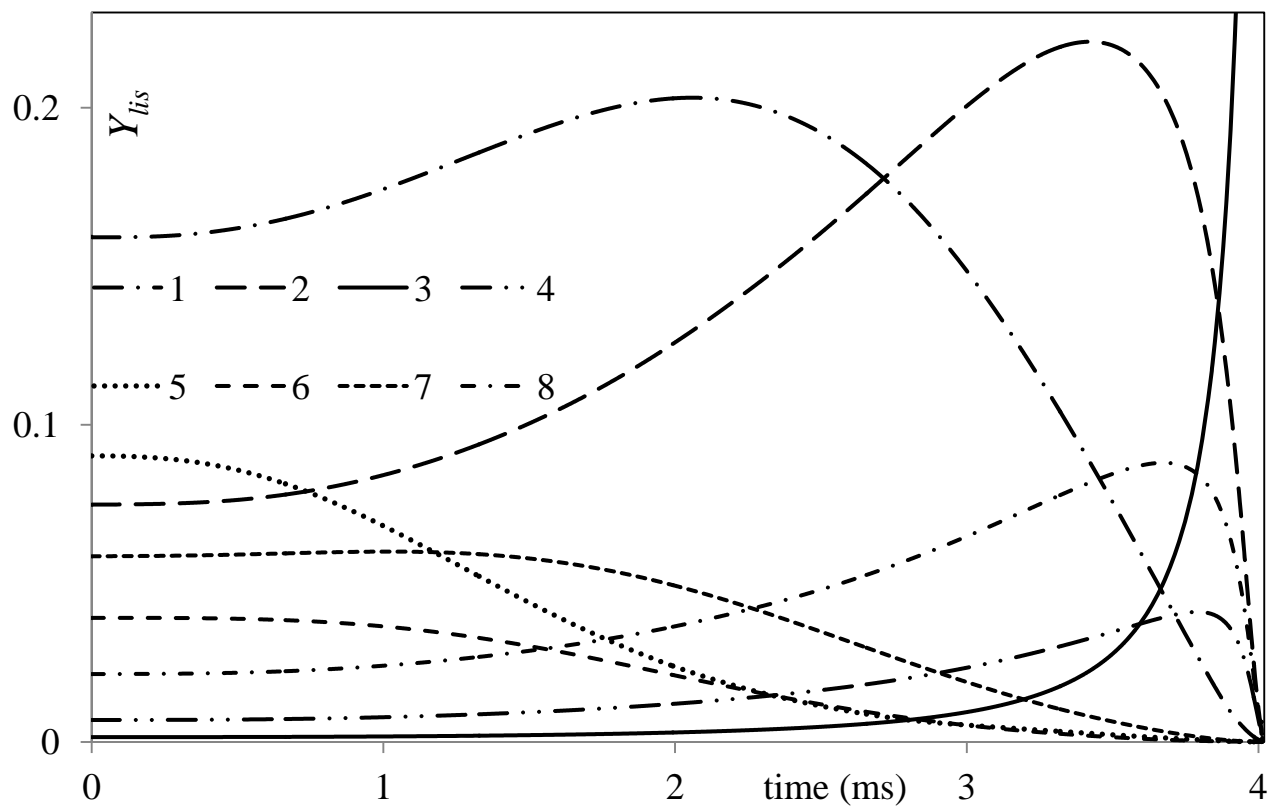


Fig. 11

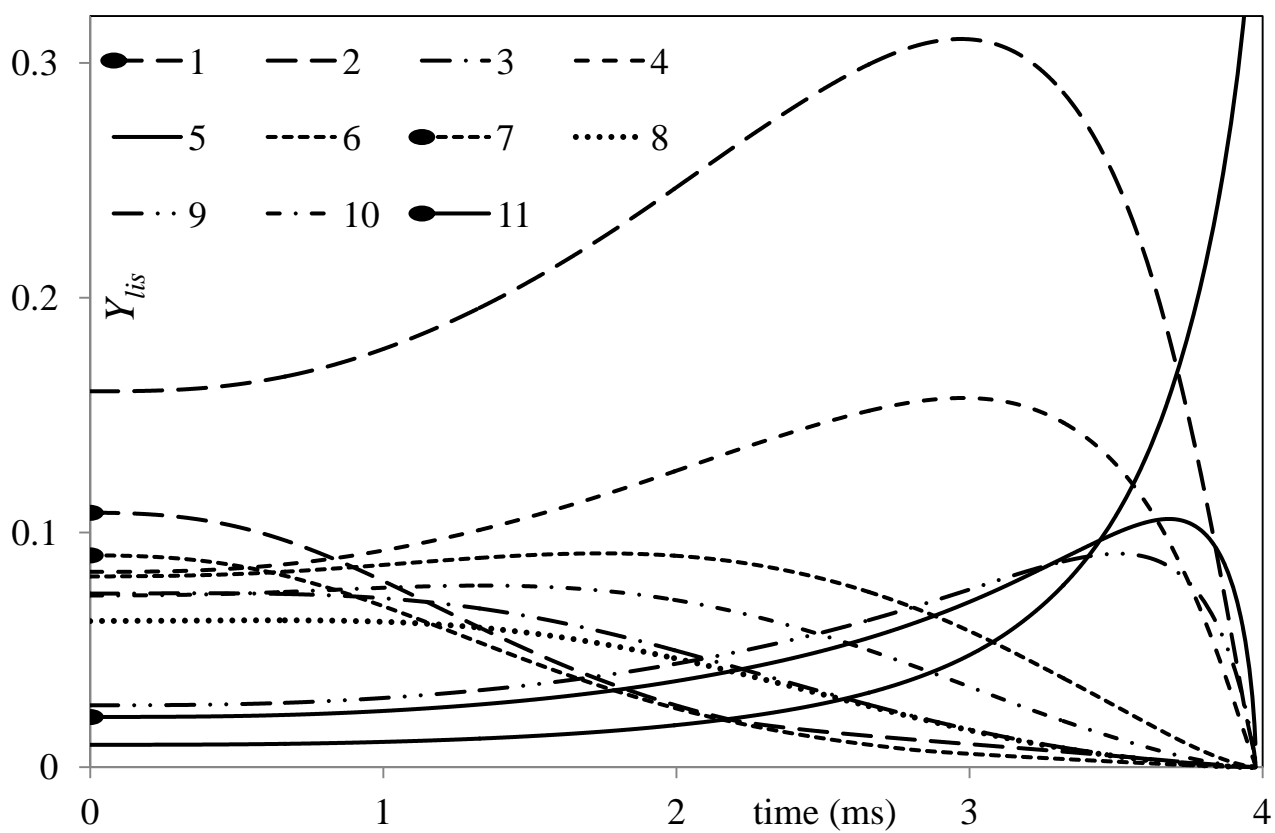


Fig. 12

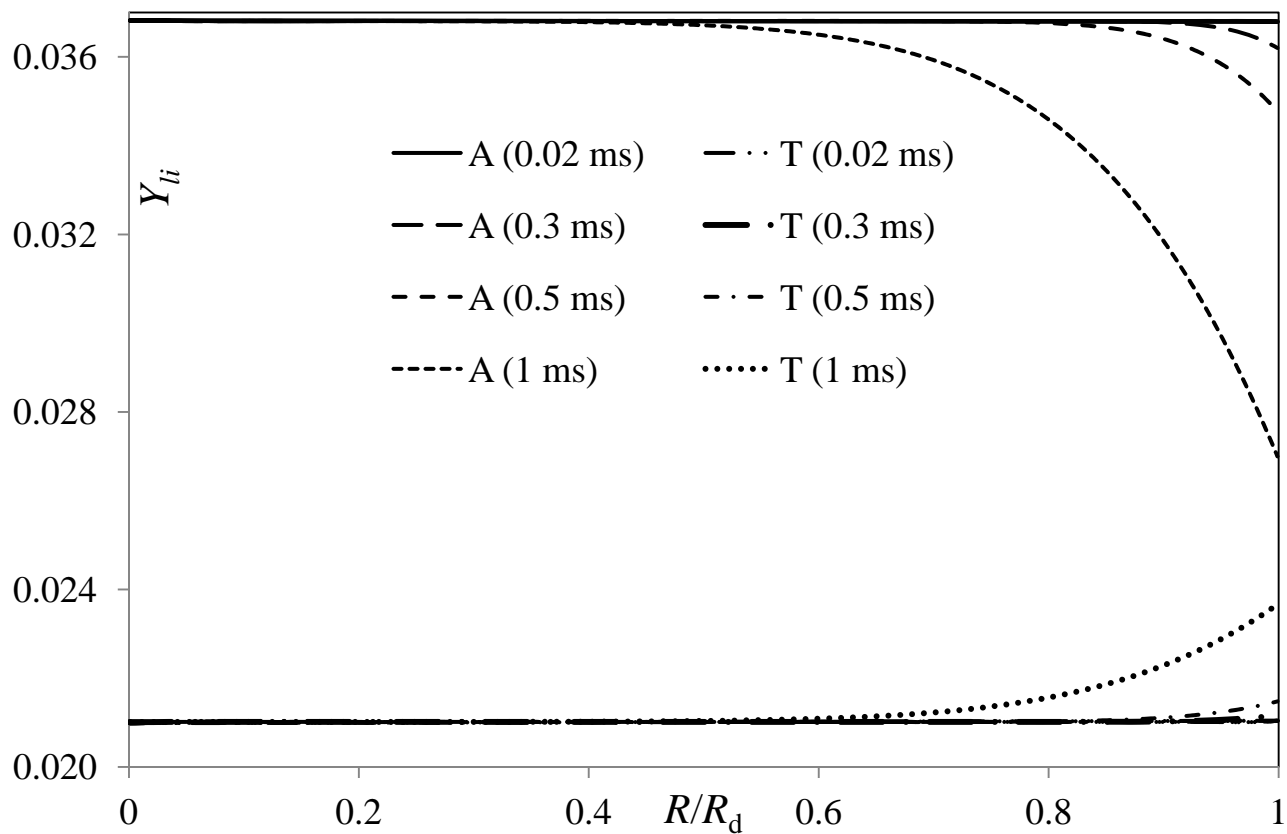


Fig. 13

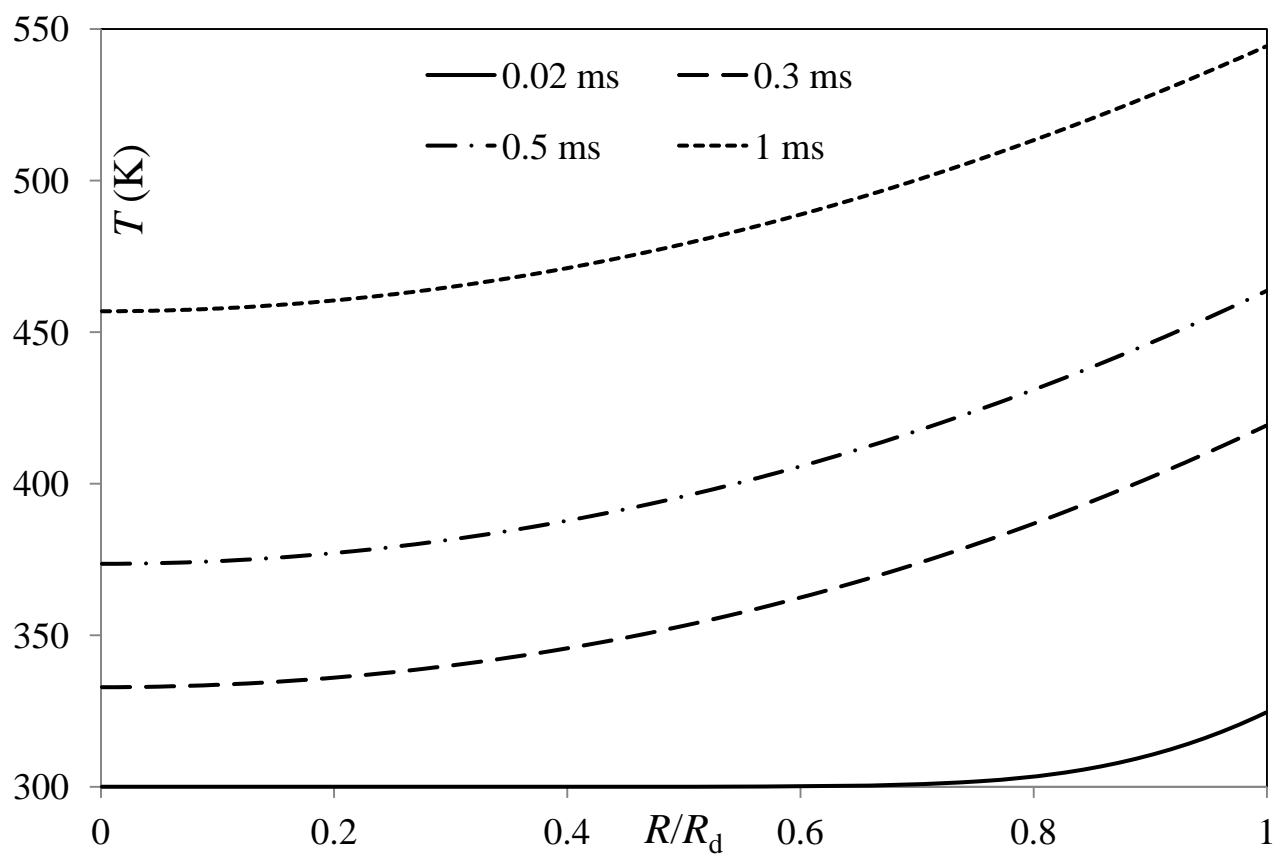


Fig. 14

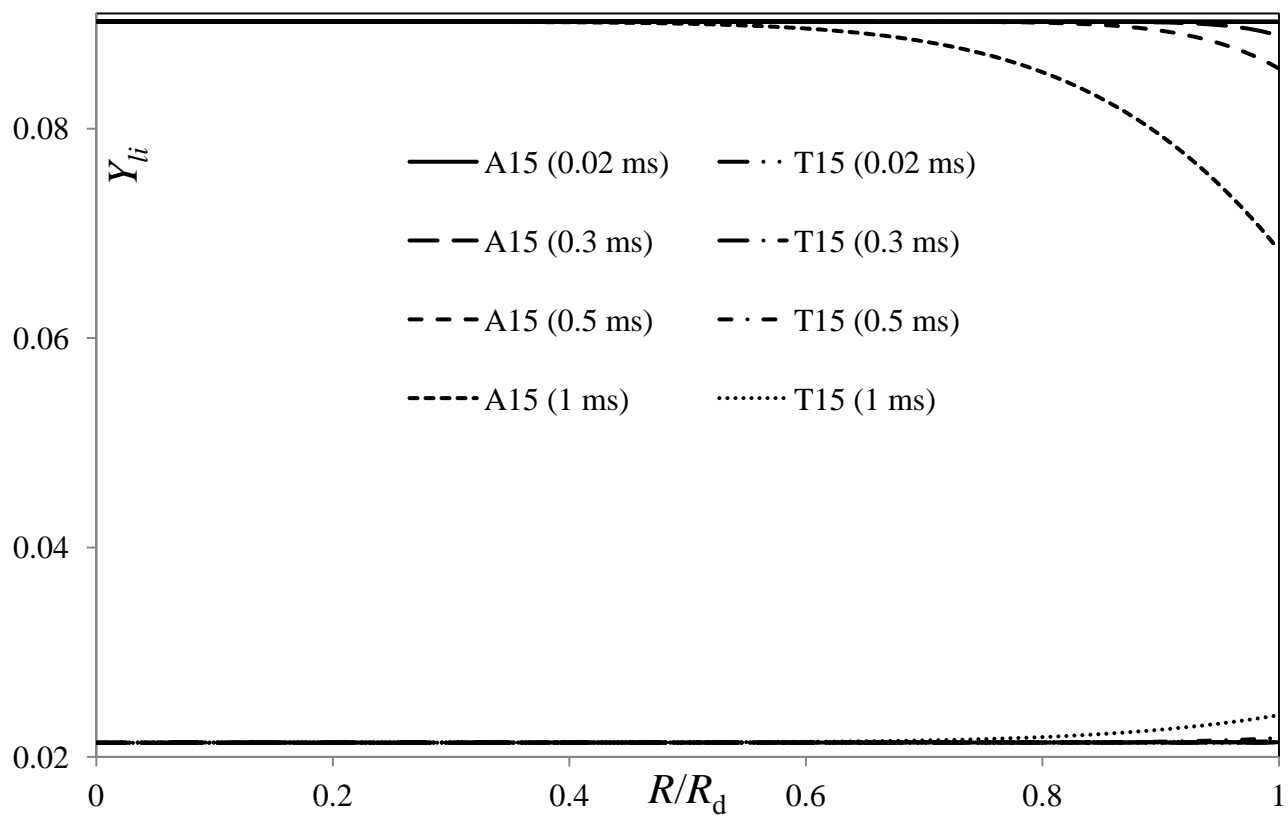


Fig. 15

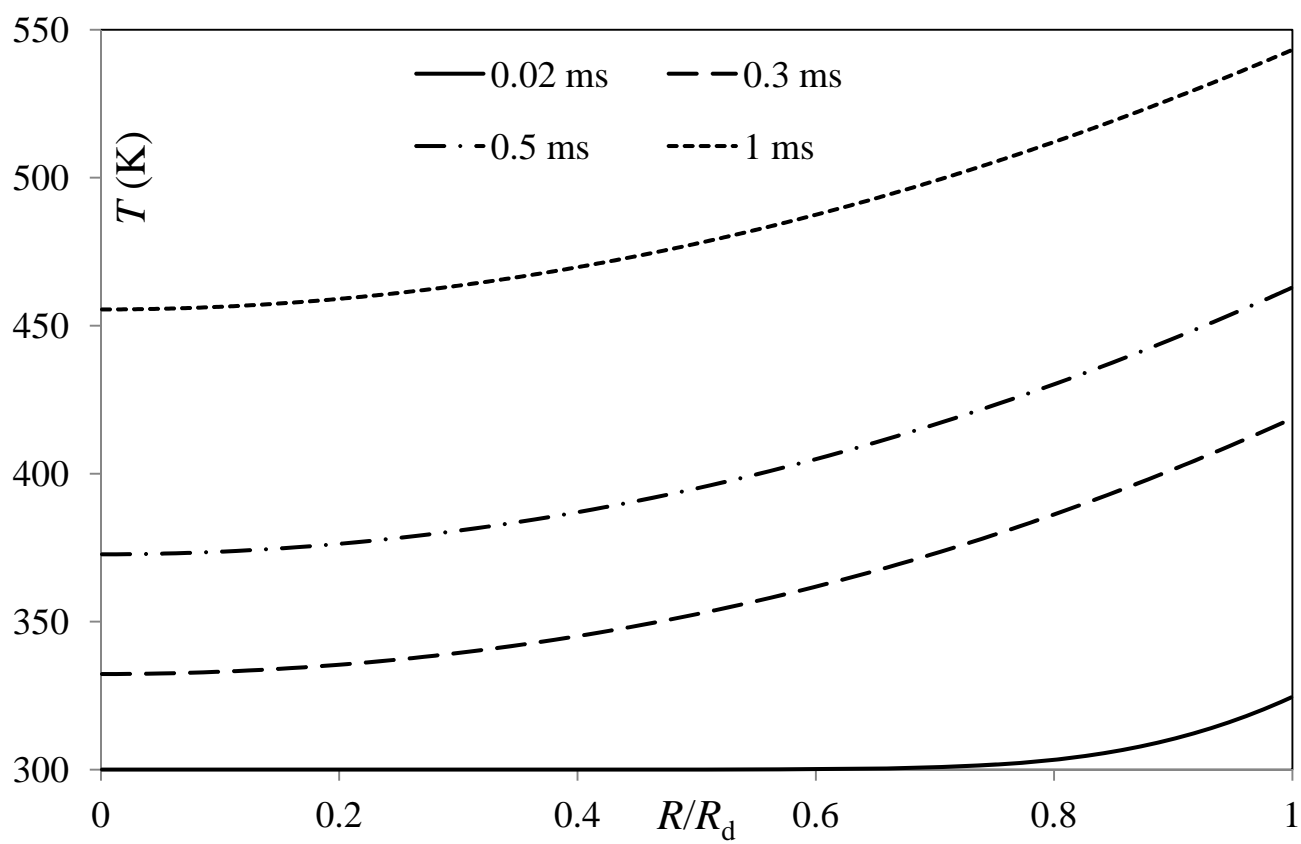


Fig. 16

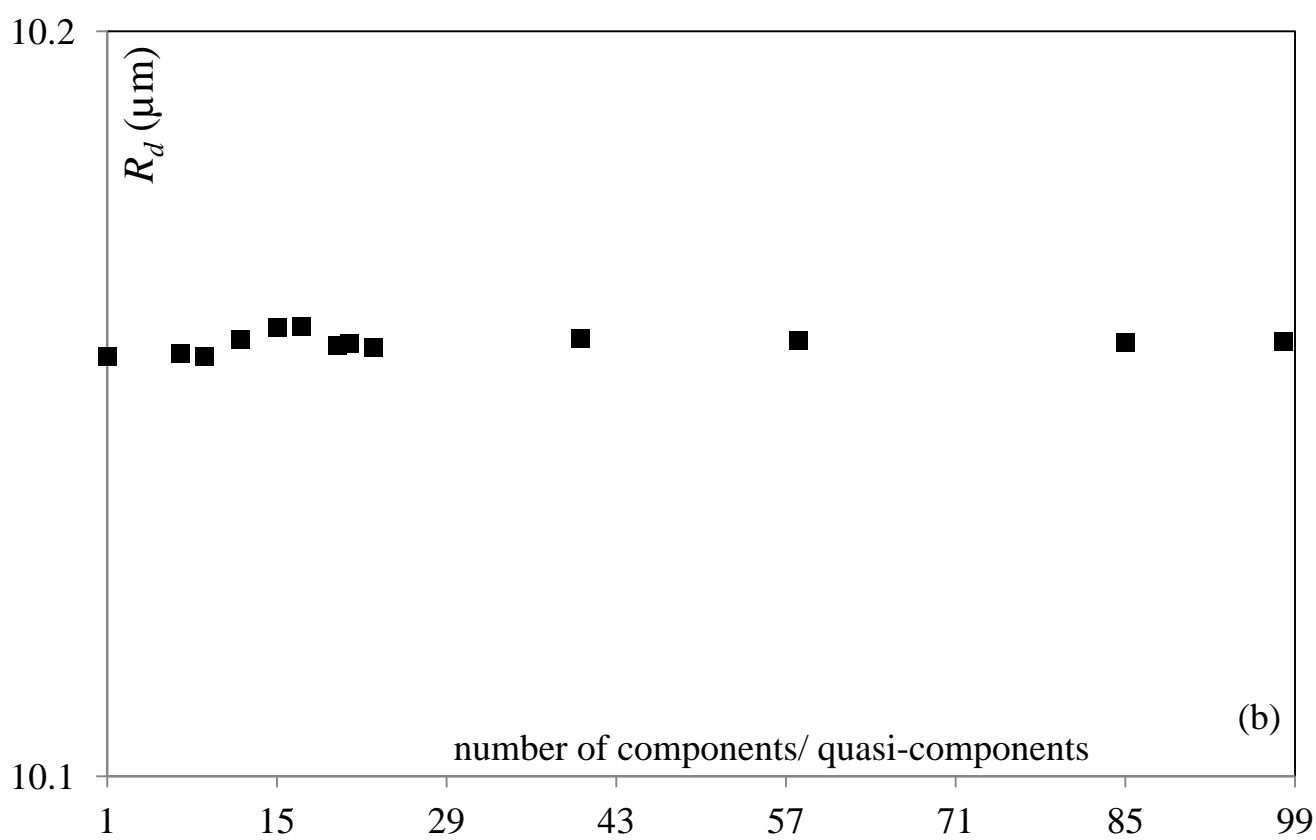
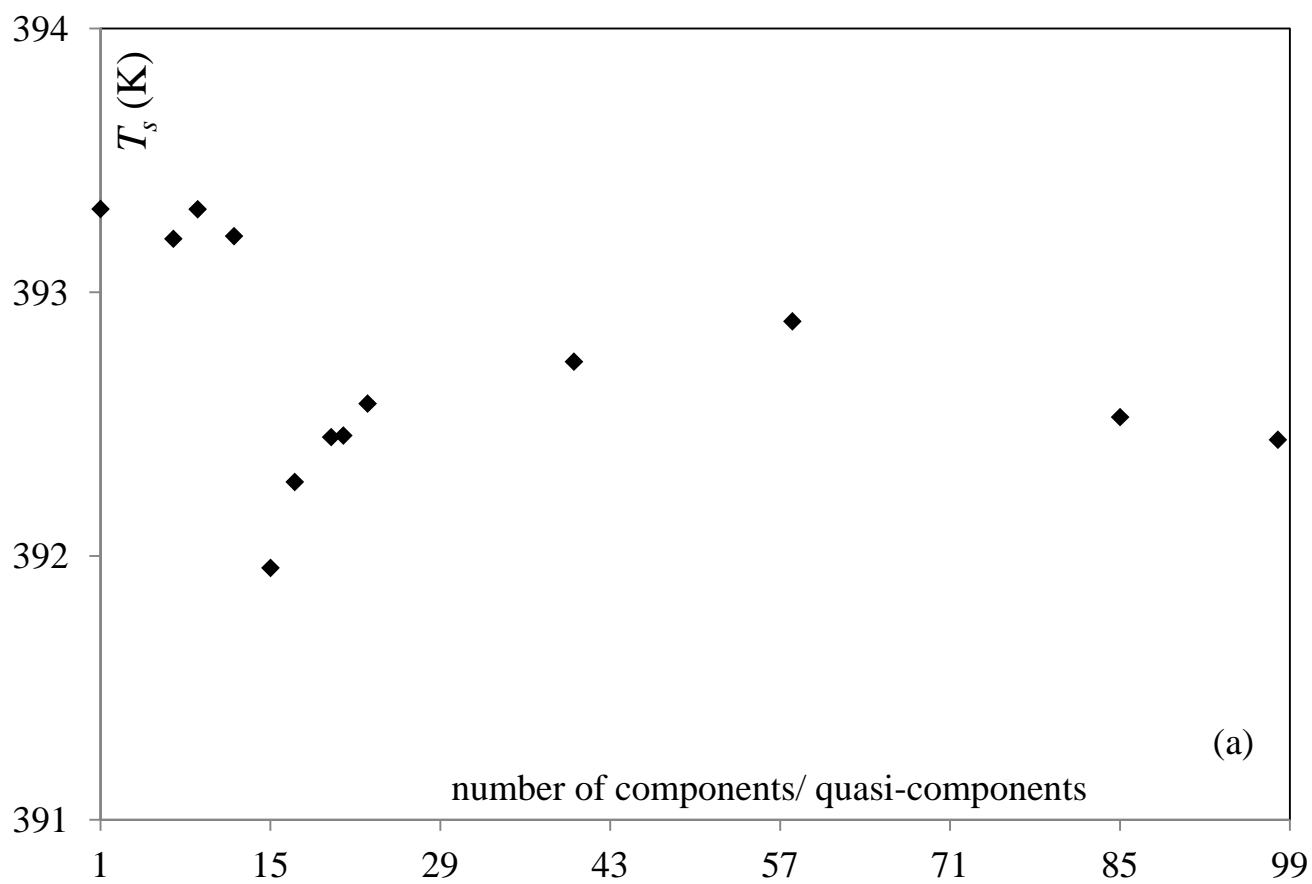


Fig. 17

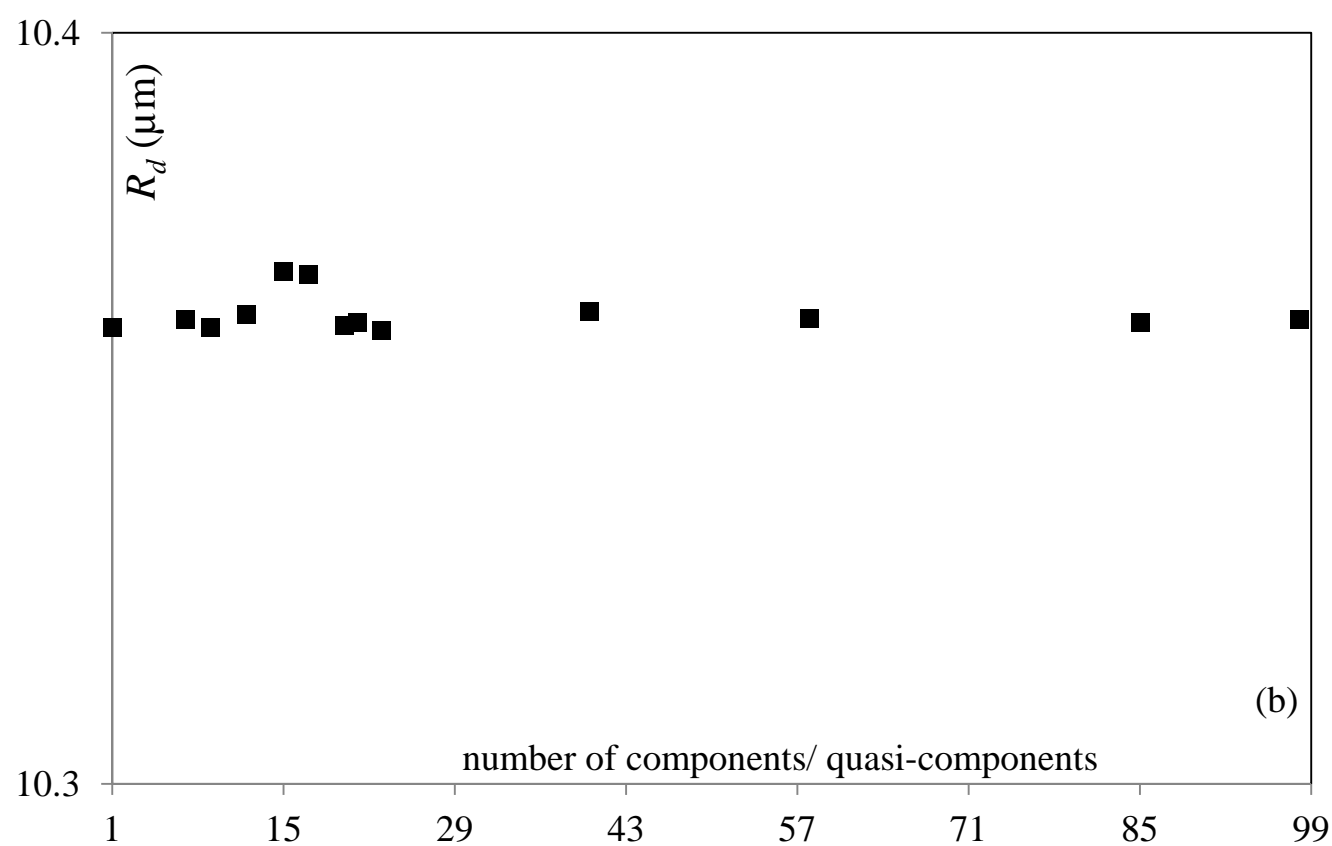
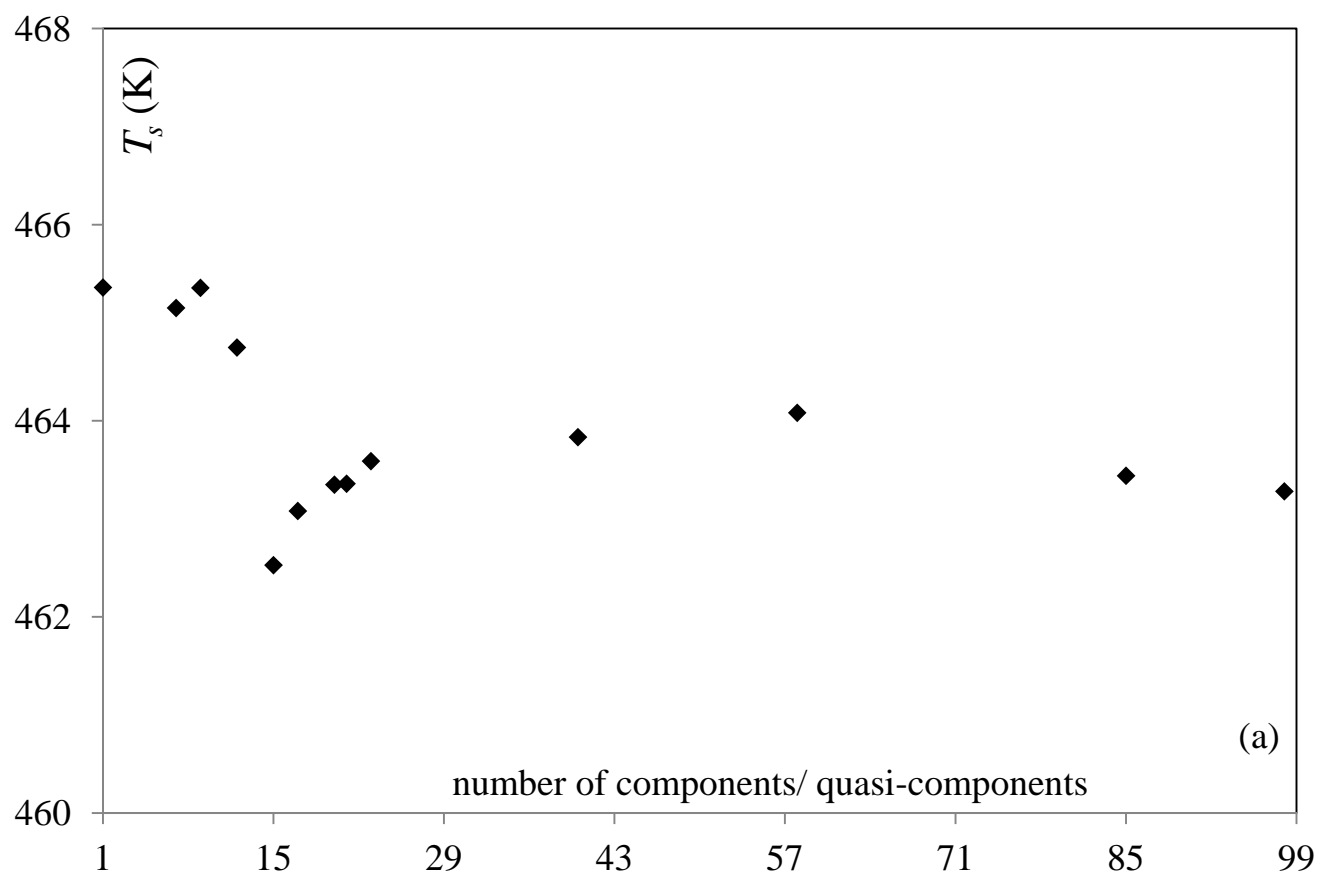


Fig. 18

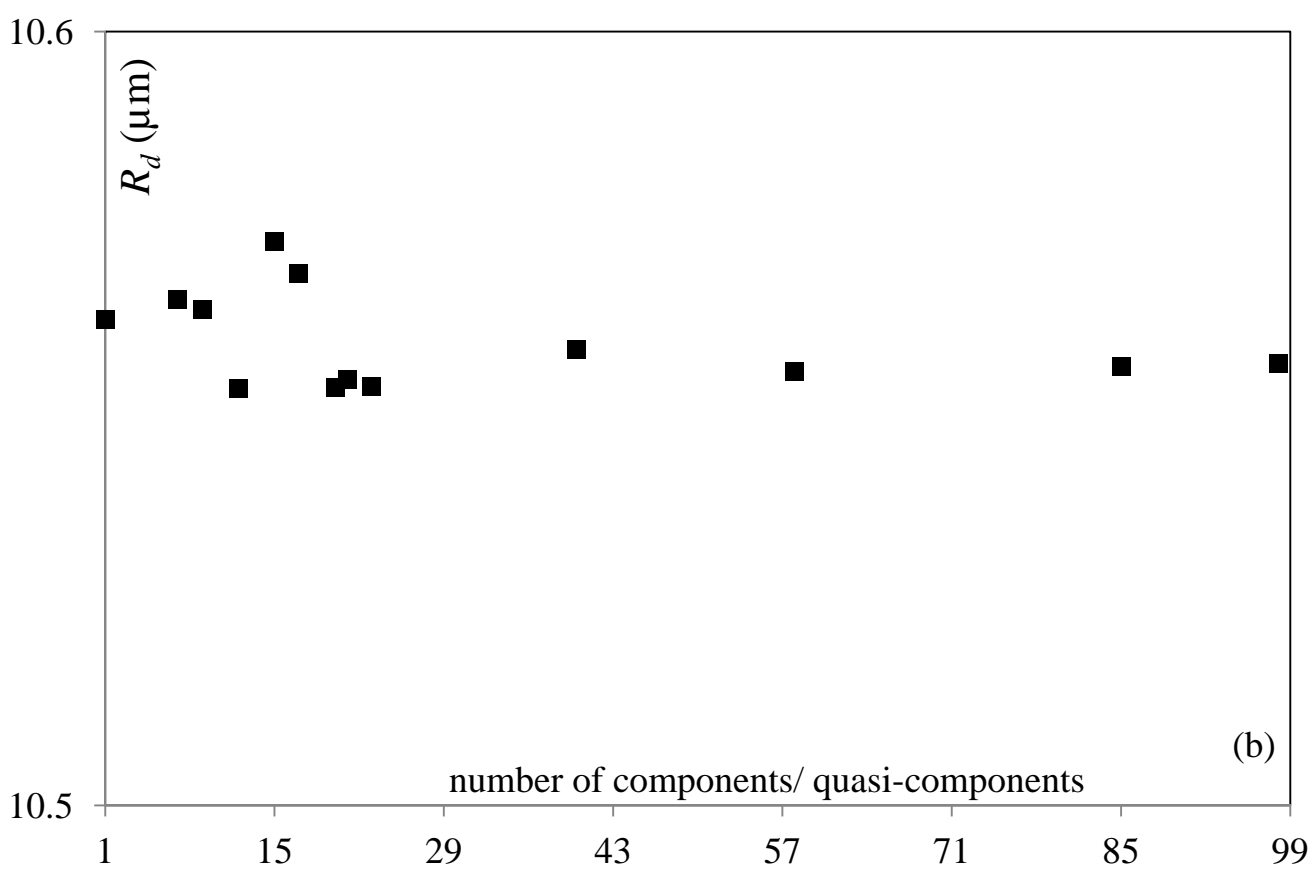
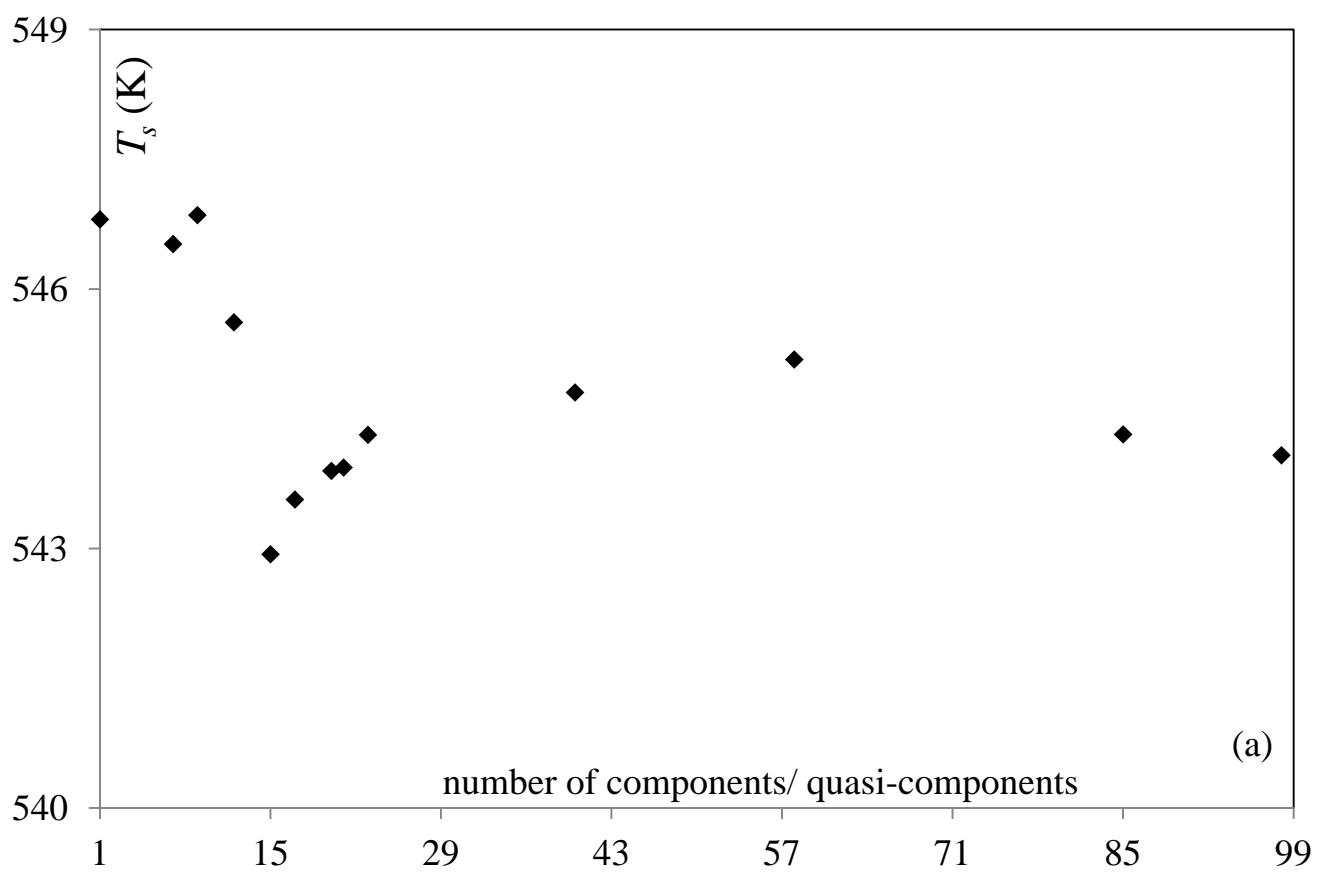


Fig. 19

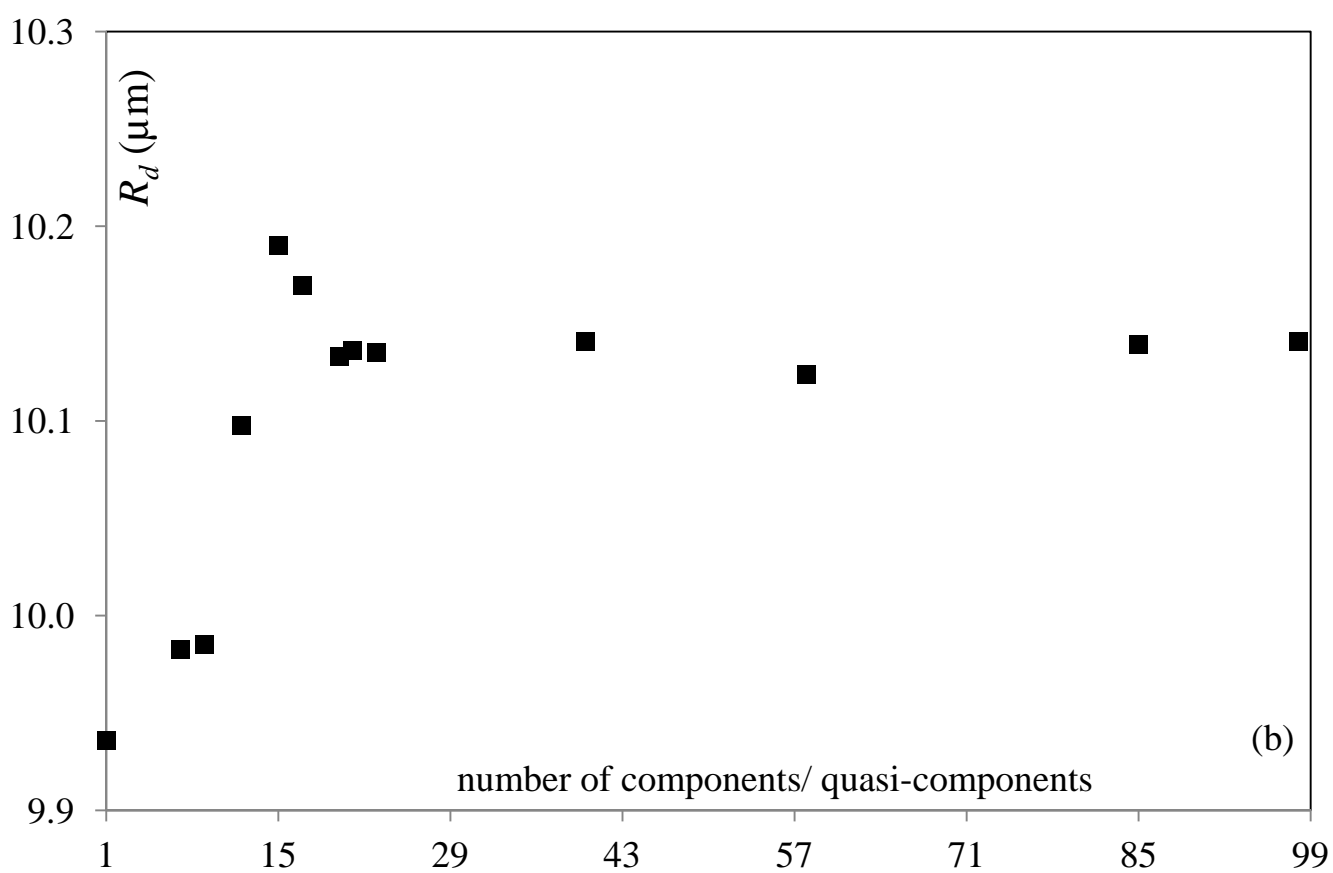
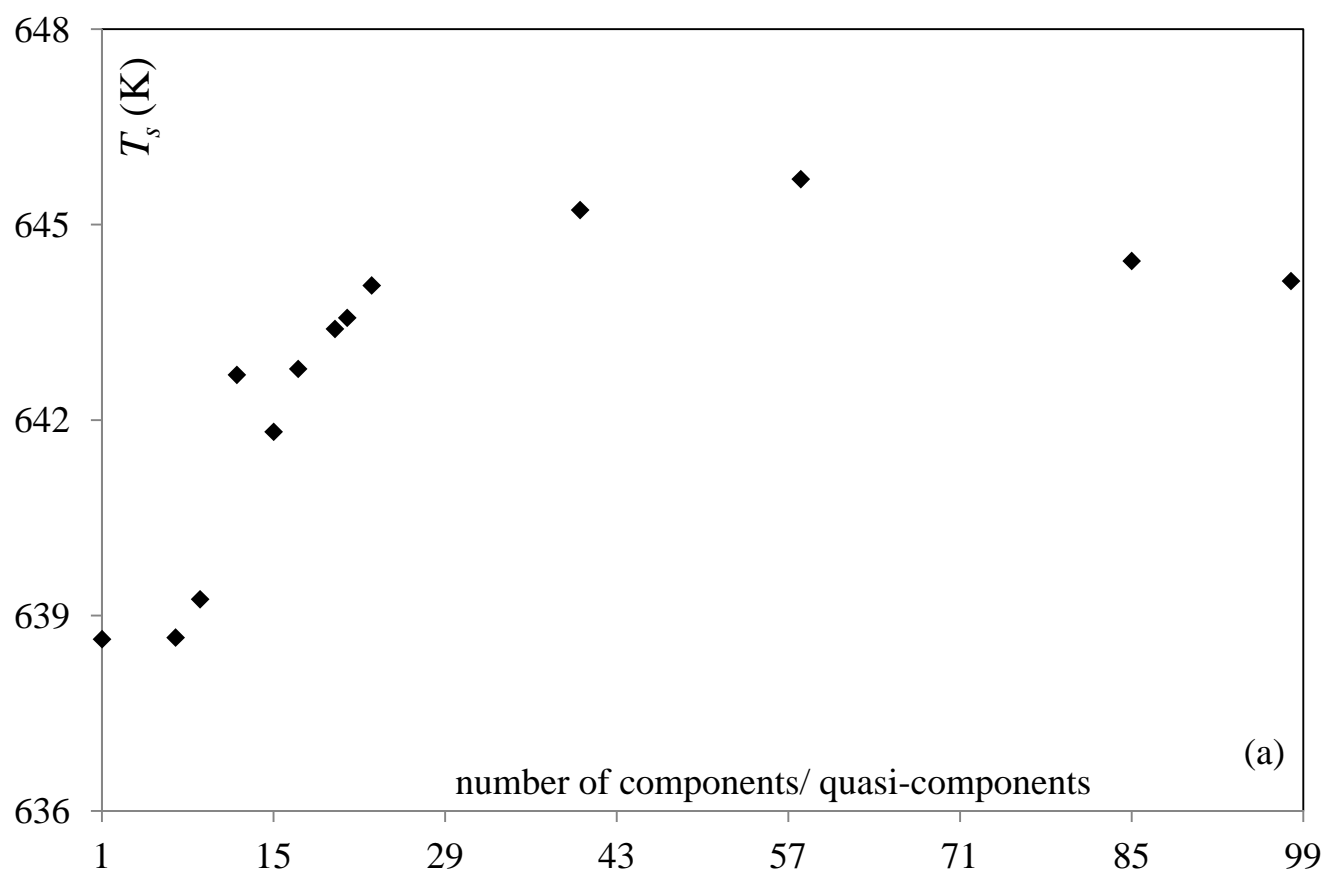


Fig. 20



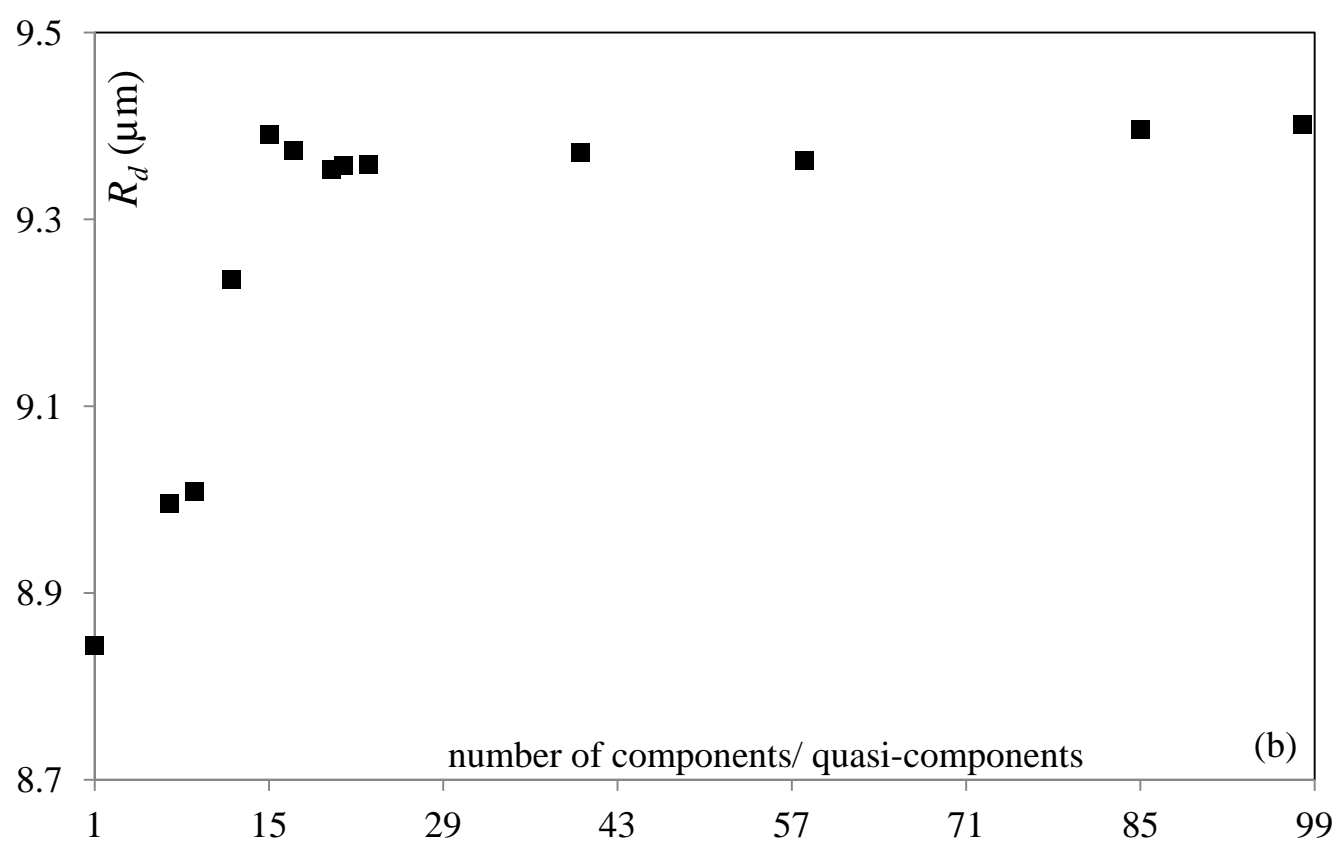
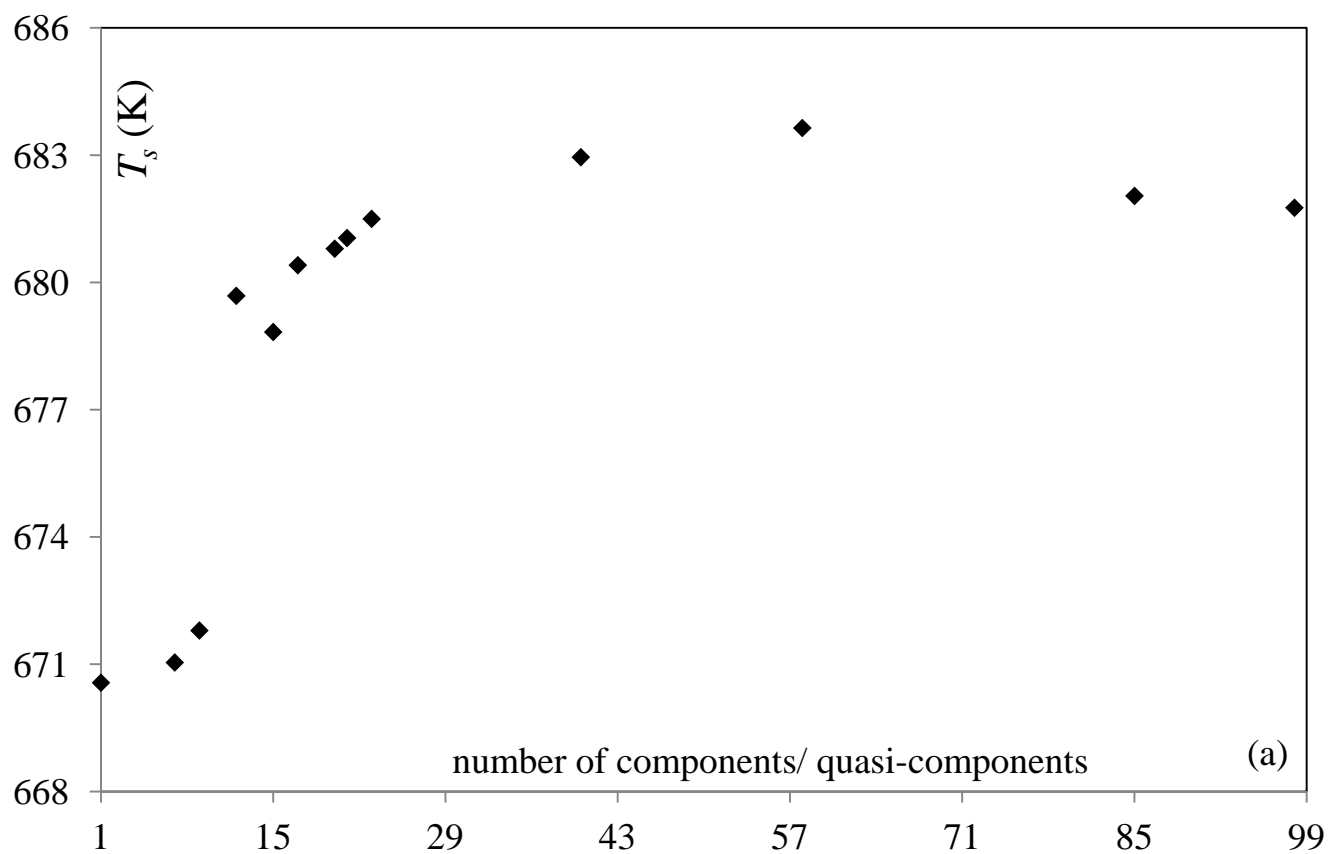


Fig. 21

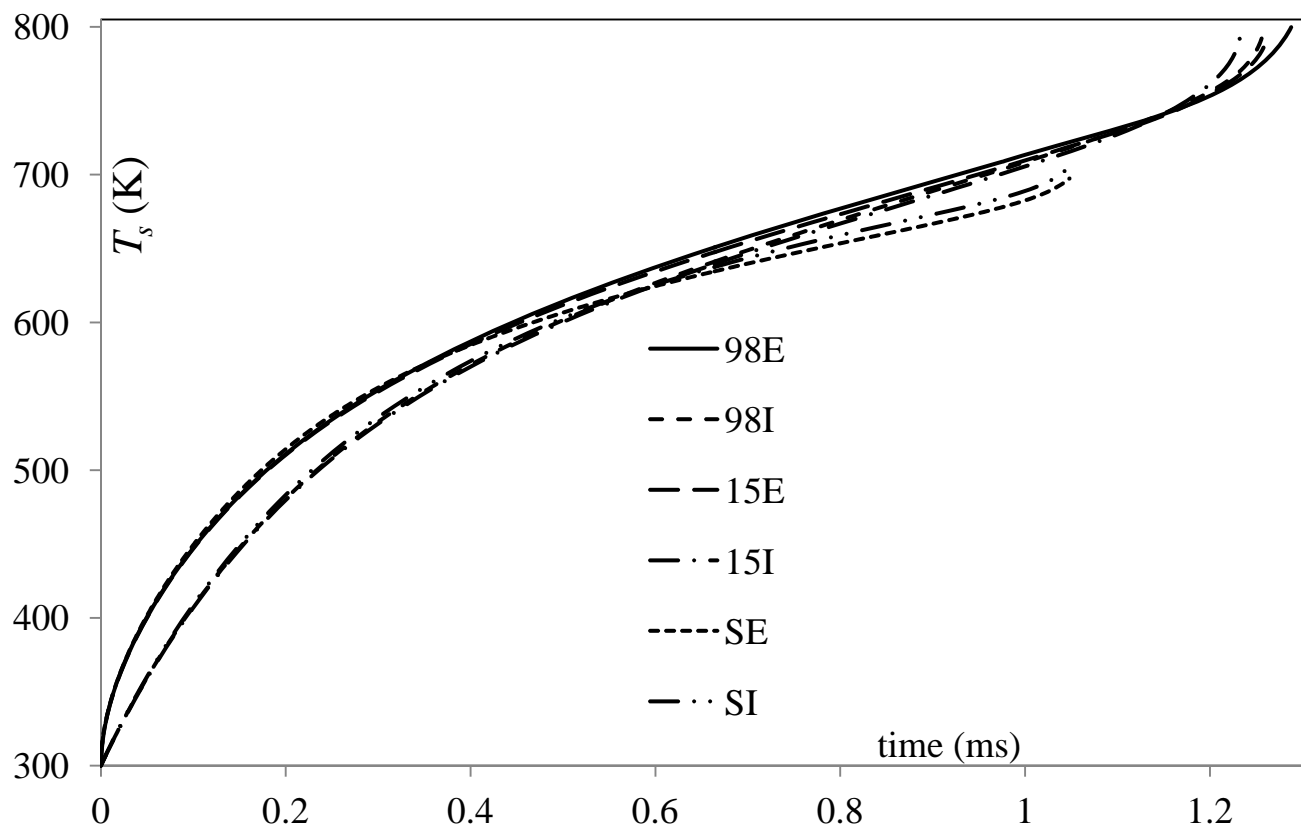


Fig. 22

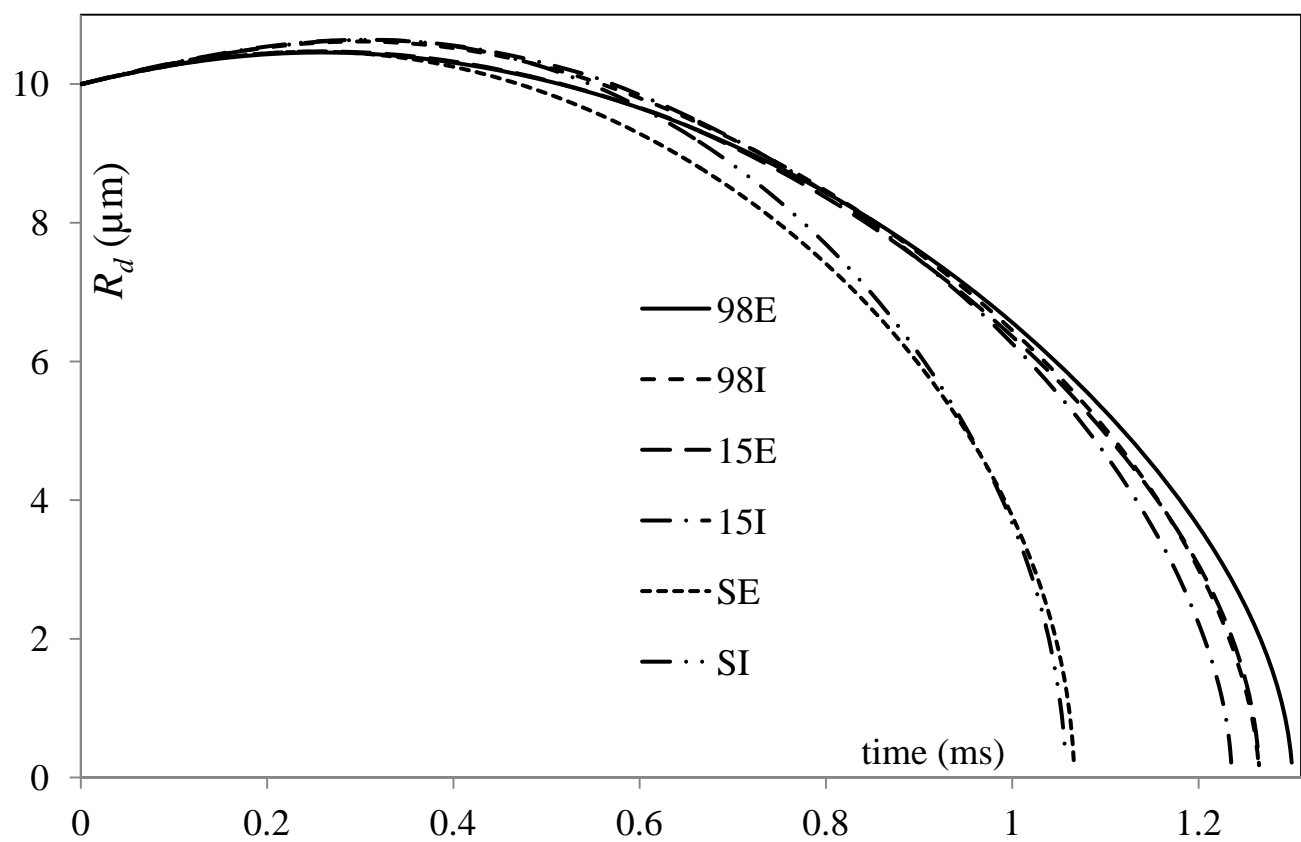


Fig. 23

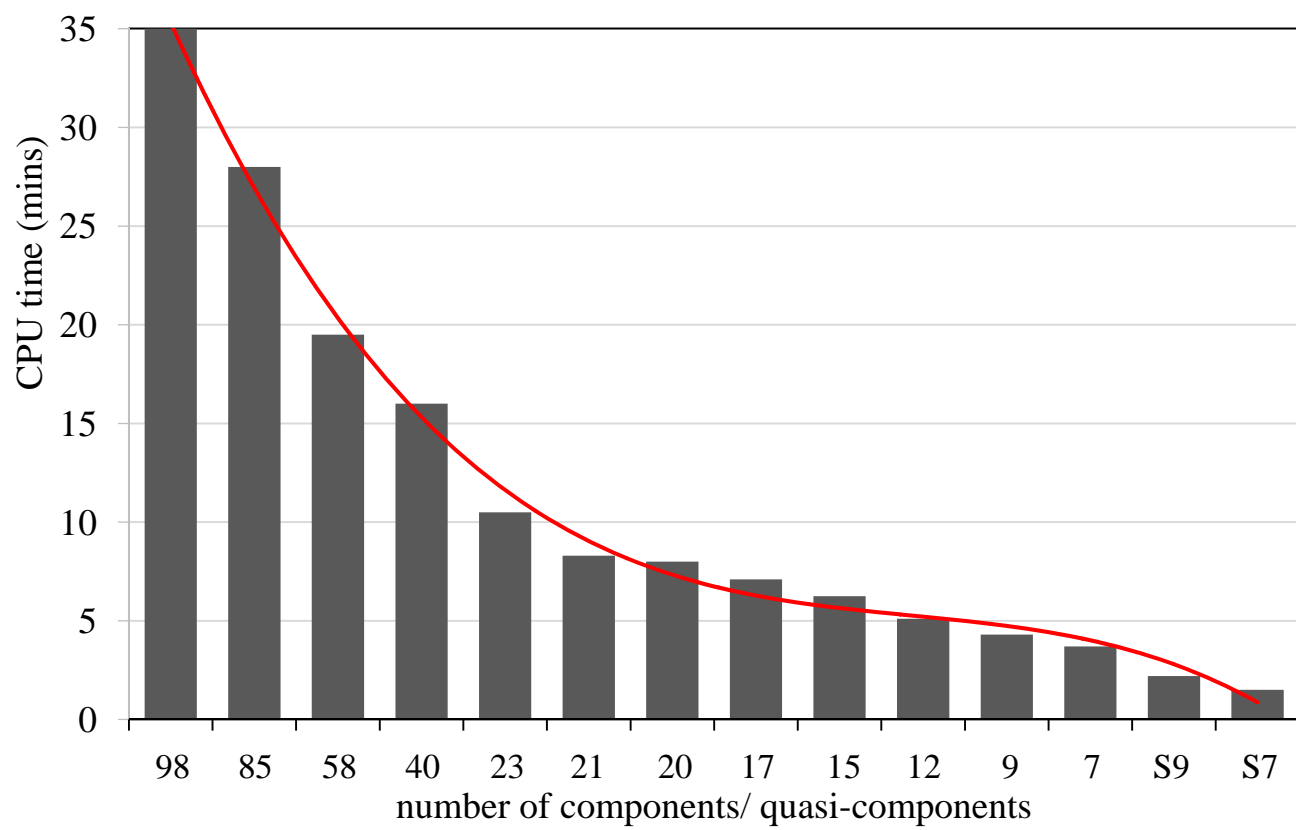
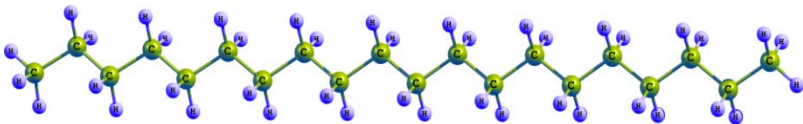
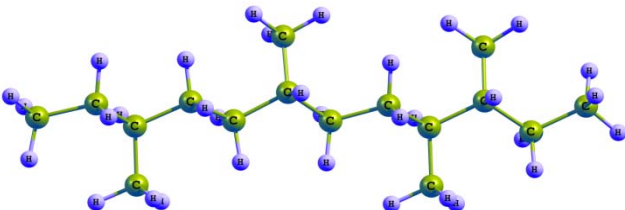
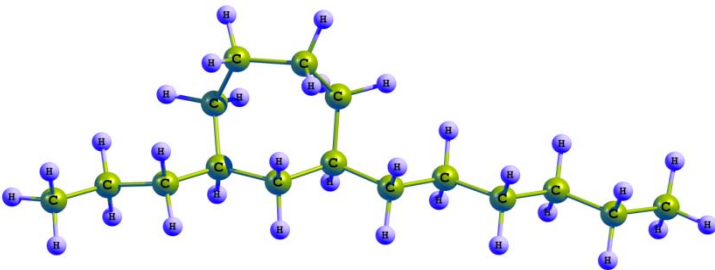
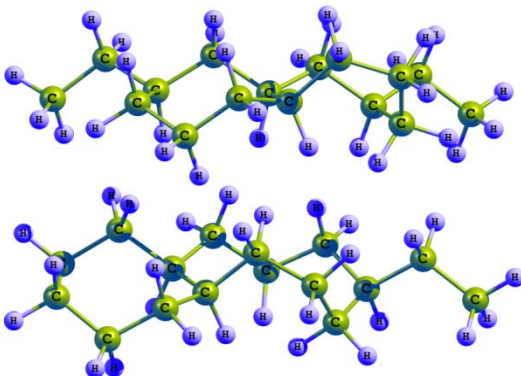
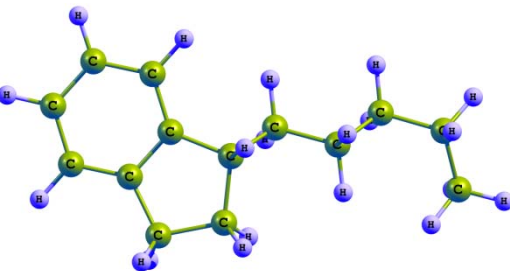
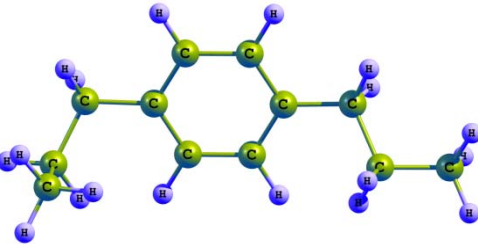


Fig. 24

|   |  |
|---|--|
| n-didecyl, $C_{20}H_{42}$   |    |
| 3,6,9,10-methyl-dodecane, $C_{16}H_{34}$  |    |
| 1-propyl-3-hexyl-cycloheptan, $C_{16}H_{32}$  |    |
| Diethylbicycloheptan, $C_{16}H_{30}$ + ethylcycloheptan-cyclononane, $C_{16}H_{30}$ |  |
| pentylindane, $C_{14}H_{20}$  |  |
| 1,4-dipropylbenzene, $C_{12}H_{18}$   |  |

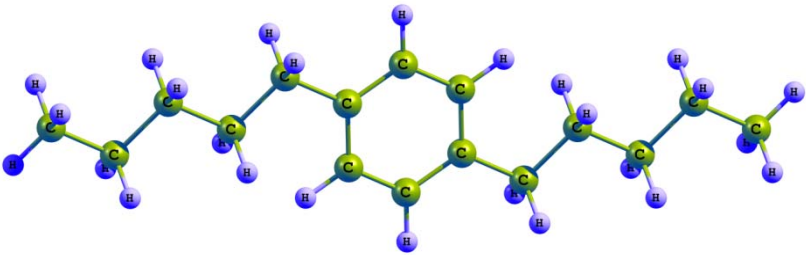
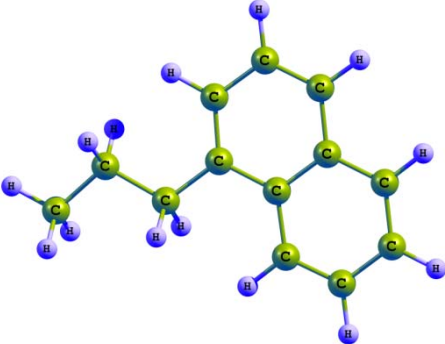
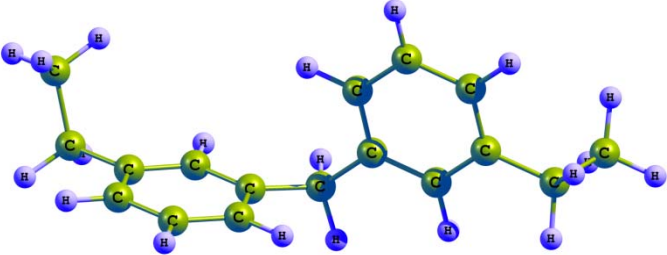
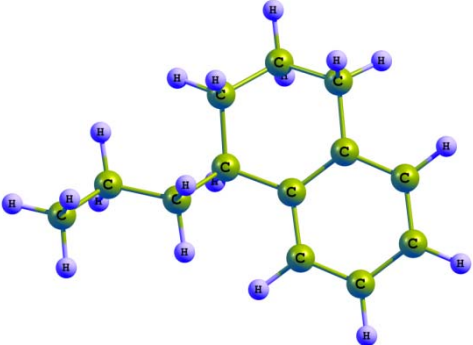
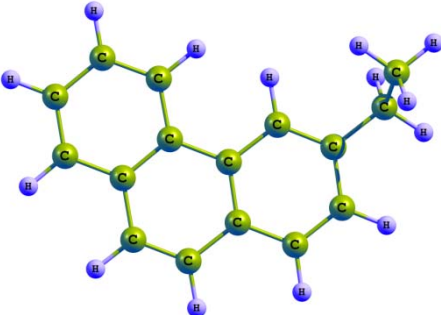
|  |  |
|--|--|
| 1,4-dipentylbenzene, $C_{16}H_{26}$                      |    |
| 1-propylnaphthalene, $C_{13}H_{14}$                      |    |
| di(3-ethyl-phenyl)methane, $C_{19}H_{20}$                |   |
| 1-propyl-(1,2,3,4-tetrahydronaphthalene), $C_{13}H_{18}$ |  |
| ethylphenanthrene, $C_{16}H_{14}$                        |  |

Fig. A1

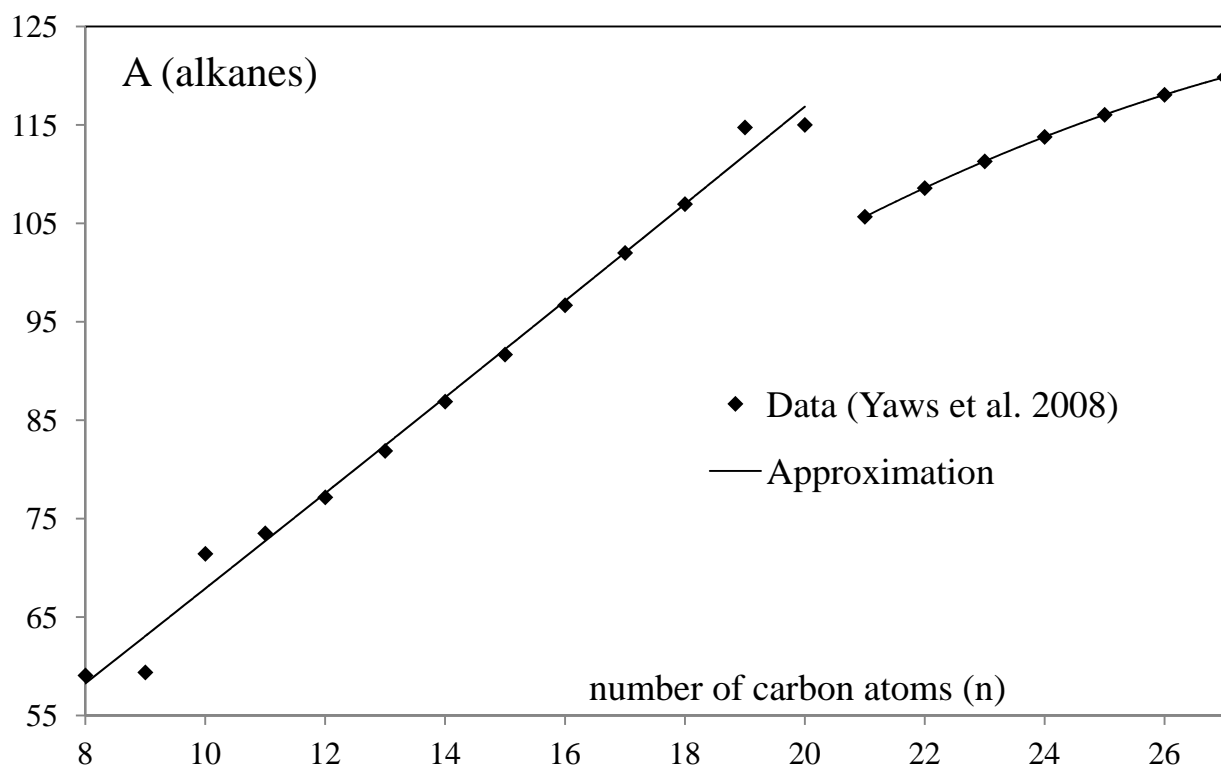


Fig. A2

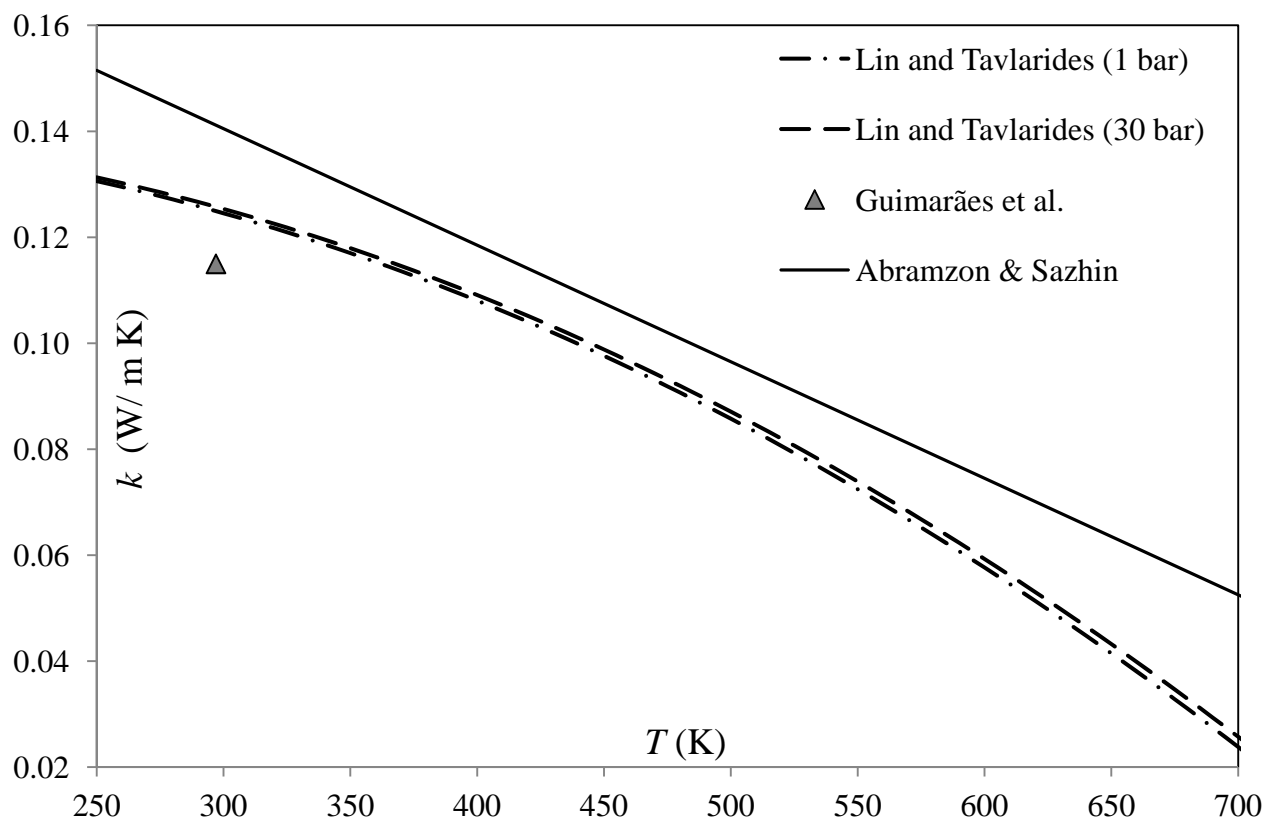


Fig. A3

| Number<br>C atoms | n-alkanes | iso-alkanes | cycloalkanes | bicycloalkanes | tricycloalkanes | alkylbenzenes | indanes&tetralines | naphthalenes | diaromatics | phenanthrenes |
|-------------------|-----------|-------------|--------------|----------------|-----------------|---------------|--------------------|--------------|-------------|---------------|
| C8                | 0.3080    | 0           | 0            | 0              | 0               | 0.4970        | 0                  | 0            | 0           | 0             |
| C9                | 1.0513    | 1.9807      | 0            | 0              | 0               | 3.2357        | 0                  | 0            | 0           | 0             |
| C10               | 1.2635    | 3.7906      | 0.6408       | 0.6926         | 0               | 5.3584        | 1.3157             | 1.9366       | 0           | 0             |
| C11               | 1.1002    | 2.0628      | 1.8745       | 1.0524         | 0               | 0.9492        | 1.3632             | 2.5290       | 0           | 0             |
| C12               | 0.9866    | 1.6290      | 1.6951       | 0.9753         | 0               | 1.9149        | 1.1951             | 1.4012       | 0           | 0             |
| C13               | 0.9646    | 1.5793      | 1.2646       | 0.6611         | 0               | 0.6873        | 1.0652             | 0.7692       | 0.3834      | 0             |
| C14               | 1.0146    | 1.6351      | 1.3633       | 0.5631         | 0.0914          | 0.6469        | 0.8406             | 0.4879       | 0.3217      | 0.0768        |
| C15               | 1.2051    | 1.9595      | 1.2353       | 0.4314         | 0.1799          | 0.4782        | 0.7051             | 0.3843       | 0.2589      | 0.2033        |
| C16               | 1.0442    | 1.6137      | 1.0449       | 0.4921         | 0.1773          | 0.4564        | 0.6684             | 0.2854       | 0.2602      | 0.1705        |
| C17               | 1.0564    | 1.8041      | 1.0162       | 0.6529         | 0.4001          | 0.4204        | 0.5598             | 0.2072       | 0           | 0.1154        |
| C18               | 1.0596    | 2.1807      | 1.2848       | 0.6554         | 0.3304          | 0.5234        | 0.5357             | 0.2358       | 0           | 0.0917        |
| C19               | 1.0916    | 2.4380      | 1.3566       | 0.9901         | 0.2159          | 0.3226        | 0.3403             | 0.2151       | 0           | 0             |
| C20               | 0.7054    | 1.5284      | 0.9961       | 0.1965         | 0.1696          | 0.2848        | 0.3227             | 0.2256       | 0           | 0             |
| C21               | 0.3756    | 1.0674      | 0.5374       | 0.0935         | 0               | 0.2032        | 0.1638             | 0            | 0           | 0             |
| C22               | 0.2328    | 0.5662      | 0.3040       | 0.0701         | 0               | 0.0969        | 0.0781             | 0            | 0           | 0             |
| C23               | 0.1083    | 0.2889      | 0.1090       | 0.0488         | 0               | 0.0494        | 0                  | 0            | 0           | 0             |
| C24               | 0.0461    | 0.1442      | 0.0755       | 0.0234         | 0               | 0.0473        | 0                  | 0            | 0           | 0             |
| C25               | 0.0221    | 0.0776      | 0.0445       | 0.0169         | 0               | 0             | 0                  | 0            | 0           | 0             |
| C26               | 0.0106    | 0.0319      | 0.0214       | 0              | 0               | 0             | 0                  | 0            | 0           | 0             |
| C27               | 0.0052    | 0.0257      | 0.0155       | 0              | 0               | 0             | 0                  | 0            | 0           | 0             |
| mol%              | 13.6518   | 26.4039     | 14.8795      | 7.6154         | 1.5647          | 16.1719       | 9.1537             | 8.6773       | 1.2240      | 0.6577        |

Table 1

| Number<br>C atoms | alkanes | cycloalkanes | bicycloalkanes | alkylbenzenes | indanes&tetralines | naphthalenes |
|-------------------|---------|--------------|----------------|---------------|--------------------|--------------|
| C8                | 0.308   | 0            | 0              | 0.4970        | 0                  | 0            |
| C9                | 3.032   | 0            | 0              | 3.2357        | 0                  | 0            |
| C10               | 5.0541  | 0.6408       | 0.6926         | 5.3584        | 1.3157             | 1.9366       |
| C11               | 3.163   | 1.8745       | 1.0524         | 0.9492        | 1.3632             | 2.5290       |
| C12               | 2.6156  | 1.6951       | 0.9753         | 1.9149        | 1.1951             | 1.4012       |
| C13               | 2.5439  | 1.2646       | 0.6611         | 0.6873        | 1.0652             | 0.7692       |
| C14               | 2.6497  | 1.3633       | 0.5631         | 0.6469        | 0.8406             | 0.4879       |
| C15               | 3.1646  | 1.2353       | 0.4314         | 0.4782        | 0.7051             | 0.3843       |
| C16               | 2.6579  | 1.0449       | 0.4921         | 0.4564        | 0.6684             | 0.2854       |
| C17               | 2.8605  | 1.0162       | 0.6529         | 0.4204        | 0.5598             | 0.2072       |
| C18               | 3.2403  | 1.2848       | 0.6554         | 0.5234        | 0.5357             | 0.2358       |
| C19               | 3.5296  | 1.3566       | 0.9901         | 0.3226        | 0.3403             | 0.2151       |
| C20               | 2.2338  | 0.9961       | 0.1965         | 0.2848        | 0.3227             | 0.2256       |
| C21               | 1.443   | 0.5374       | 0.0935         | 0.2032        | 0.1638             | 0            |
| C22               | 0.799   | 0.3040       | 0.0701         | 0.0969        | 0.0781             | 0            |
| C23               | 0.3972  | 0.1090       | 0.0488         | 0.0494        | 0                  | 0            |
| C24               | 0.1903  | 0.0755       | 0.0234         | 0.0473        | 0                  | 0            |
| C25               | 0.0997  | 0.0445       | 0.0169         | 0             | 0                  | 0            |
| C26               | 0.0425  | 0.0214       | 0              | 0             | 0                  | 0            |
| C27               | 0.0309  | 0.0155       | 0              | 0             | 0                  | 0            |
| mol%              | 40.0556 | 14.8795      | 7.6154         | 16.1719       | 9.1537             | 8.6773       |

Table 2